Jørgen Bauck Jensen

Optimal Operation of Refrigeration Cycles

Doctoral thesis
for the degree of philosophiae doctor

Trondheim, May 2008

Norwegian University of Science and Technology
Faculty of Natural Sciences and Technology
Department of chemical engineering

NTNU
Innovation and Creativity

NTNU

Norwegian University of Science and Technology

Doctoral thesis
for the degree of philosophiae doctor

Faculty of Natural Sciences and Technology
Department of chemical engineering

ISBN 978-82-471-7801-0 (printed version)
ISBN 978-82-471-7815-7 (electronic version)
ISSN 1503-8181

Doctoral theses at NTNU, 2008:91

Printed by tapir uttrykk

Abstract

The theme of this thesis is optimal operation of refrigeration cycles, but the results also applies to the reverse process generating heat.

A simple refrigeration cycle has five steady-state degrees of freedom related to; compressor, choke valve, heat transfer in condenser, heat transfer in evaporator and "active charge". One degree of freedom is used to control the load of the cycle, e.g. the compressor. It is usually optimal to maximize the heat transfer in the condenser and in the evaporator (e.g. by maximizing the fan speeds). The two remaining degrees of freedom may be used to control the degree of super-heating and the degree of sub-cooling. It is found that super-heating should be minimized, whereas some sub-cooling is optimal in terms of cycle efficiency. The degree of freedom related to active charge is often lost by specifying no sub-cooling by the design. This gives a loss in the order of 2%. Different designs for affecting the active charge are discussed.

By allowing for sub-cooling in the condenser of a sub-critical refrigerant cycle there are no fundamental differences between a trans-critical cycle (e.g. with CO_2 as working fluid) and a sub-critical cycle (e.g. with ammonia as working fluid). However, the practical operation is quite different. For a sub-critical ammonia cycle several simple control structures gives close to optimal operation. For the trans-critical CO_2 cycle on the other hand, a combination of measurements is necessary.

Refrigeration processes are often designed by specifying a minimum approach temperature ($\Delta T_{\min}$) in the evaporator and in the condenser. With this approach, the optimality of sub-cooling in the condenser will not be found. In addition, specifying the areas found by designing with the $\Delta T_{\min}$-method and re-optimizing without the constraints on $\Delta T_{\min}$ leads to a different operating point. These two deficiencies shows that the $\Delta T_{\min}$-method is not sufficient. An alternative method (simplified TAC) is proposed and compared with the $\Delta T_{\min}$-method.

Considering the large amount of work that goes into the design of LNG processes, there is surprisingly little attention to their subsequent operation. This partly comes from the assumption that optimal design and optimal operation is the same, but this is generally not true.

The PRICO LNG process is used as an example for optimal design and optimal operation of LNG processes. In the design phase there are a number of constraints that must be satisfied to get a feasible design. The limitations imposed by the constraints are discussed. It is found that constraints related to the compressor per-

formance is important to consider. In operation the objective function is much simpler than in design where also the equipment is part of the optimization. Two main modes of operation are studied; i) minimize compressor shaft work for given production and ii) maximum production (e.g. for maximum compressor shaft work).

An important issue for optimal operation and plantwide control is to find the degrees of freedom available for optimization. A previously published systematic approach to determine the steady-state degrees of freedom is extended to take into account the active charge and the refrigerant composition as possible degrees of freedom. A number of case studies are used to illustrate the findings.

Acknowledgement

Most of all I would like to thank my supervisor Sigurd Skogestad for giving me the chance to work on this thesis. His support and guidance has helped me through these four years. I would also like to thank people at Statoil and Linde for arranging my stay and work at the offices of Linde Engineering in Munich. The key persons responsible for providing this opportunity are Jostein Pettersen and Heinz Bauer.

The Process Systems Engineering Group has been may daily colleagues and I would like to thank the people that has been working there for a nice working environment and a lot of interesting discussions.

Finally, I would like to thank my girlfriend Christina for her support and understanding.

Jørgen Bauck Jensen

Contents

List of Figures

List of Tables

Chapter 1

Introduction

1.1 Motivation

The demand for energy is increasing rapidly and it is expected to increase even faster in the years to come. At the same time the amount of oil is decreasing so alternative transportable energy sources has gained more attention. One of these alternatives is liquefied natural gas (LNG) which is natural gas (mainly methane) in liquid state at atmospheric pressure and about $-160\,^{\circ}\mathrm{C}$. The process of liquefying natural gas requires large amounts of energy so a lot of work has been done on design of LNG processes. However, it seems that the subsequent operation is less studied, at least in the open literature. This is a bit surprising considering that even small improvements will give large savings due to high throughput.

An important issue for optimal operation is to find the steady-state degrees of freedom available for optimization (N_{opt}). This number is important for several reasons. First, it determines the degrees of freedom available for solving the optimization problem. However, more importantly in terms of operation it determines the number of steady-state controlled variables that need to be selected. Optimal operation is normally implemented by keeping those variables at constant setpoints. The selection of controlled variables is therefor also an important issue. The objective is to achieve "self-optimizing" control where a constant setpoint for the selected variable indirectly leads to near-optimal operation. Note that the selection of a good controlled variable is equally important in an "advanced" control scheme like MPC which also is based on keeping the controlled variables close to given setpoints.

Our goal was to study optimal operation of refrigeration cycles used for liquefac-

tion of LNG, but as a start we needed to understand operation of simpler refrigeration cycles. We therefore started out by studying basic refrigeration cycles and moved in the direction of refrigeration processes used for liquefaction of natural gas.

1.2 Thesis overview

We discuss degrees of freedom for simple refrigeration cycles in Chapter 3. A simple ammonia refrigerator model is used for numerical results. The main focus is to show that allowing for sub-cooling in the condenser gives one extra steady-state degree of freedom related to "active charge". This shows that there are no fundamental differences between a sub-critical cycle and a trans-critical cycle (e.g. the CO_2 cycle presented in Chapter 4). We also show that some sub-cooling is beneficial in terms of cycle efficiency.

Chapter 4 is dedicated to selection of controlled variables for simple refrigeration cycles. We present two different case studies; a conventional sub-critical ammonia cycle and a trans-critical CO_2 cycle. We find that the ammonia cycle has several control structures that will give close to optimal operation. For the CO_2 cycle however, a combination of controlled variables is necessary to give acceptable performance.

We address the problem of specifying the minimum approach temperature ($\Delta T_{\min}$) as a method of designing processes with heat exchangers in Chapter 5. A simple design method for preliminary designs are presented and compared with the $\Delta T_{\min}$ method.

In Chapter 6 we discuss design optimization of a simple LNG process, the PRICO process. Nine cases are presented to show the effect of different constraints on the optimum. The PRICO process is studied further in Chapter 7 where the theme is optimal operation and selection of controlled variables. We present different modes of operation and find a self-optimizing control structure.

Chapter 8 discuss operational degrees of freedom for refrigeration cycles and summarize some of the important results for degree of freedom analysis. Several illustrative process examples are presented to illustrate our findings. These cases are including heat integrated distillation and two complex processes for liquefaction of natural gas, the mixed fluid cascade (MFC) process from Statoil-Linde LNG Technology Alliance and the propane pre-cooled mixed refrigerant (C3MR) process from Air Products.

Appendix A presents some results from optimization on the MFC process. We assumed that the degree of super-heating was controlled at 10 °C and optimized the remaining 13 unconstrained degrees of freedom (including 9 compositions). The paper only presents the nominal operating point so it still remains to find a self-optimizing control structure.

In Appendix B we consider a refrigerator that is used to refrigerate food cabinet inside a store. Optimal operation of this refrigerator is studied with respect to both food quality and energy consumption by using a simple model for the food quality and a simple model for the refrigerator performance. We compare the traditional way of controlling such refrigerators with different improved schemes. The main savings are from letting the condenser pressure vary with the ambient temperature. However, there are also some savings related to reducing the temperature in the food cabinet during the night when the refrigerator has higher efficiency.

1.3 Publication list

Journal papers

Chapter 3

J. B. Jensen and S. Skogestad (2007), "Optimal operation of simple refrigeration cycles. Part I: Degrees of freedom and optimality of sub-cooling", Comput. Chem. Eng. 31, 712-721.

Chapter 4

J. B. Jensen and S. Skogestad (2007), "Optimal operation of simple refrigeration cycles. Part II: Selection of controlled variables", Comput. Chem. Eng. 31, 1590-1601.

Chapter 5

J. B. Jensen and S. Skogestad, "Problems with specifying $\Delta T_{\min}$ in design of processes with heat exchangers", *Accepted for publication in Ind. Eng. Chem. Research.*

Chapter 8

J. B. Jensen and S. Skogestad, “Degrees of freedom for refrigeration cycles”, *Submitted to Ind. Eng. Chem. Research*.

Conferences

Chapter 4

J. B. Jensen and S. Skogestad, “Control and optimal operation of simple heat pump cycles”, *European Symposium on Computer Aided Process Engineering - 15*, Barcelona, Spain, 2005, Published by Elsevier; ISBN 0-444-51987-4. p. 1429-1434

Chapter 7

J. B. Jensen and S. Skogestad, “Optimal operation of a simple LNG process”, *International Symposium on Advanced Control of Chemical Processes*, Gramado, Brazil, 2006

Appendix A

J. B. Jensen and S. Skogestad, “Optimal operation of a mixed fluid cascade LNG plant”, *16th European Symposium on Computer Aided Process Engineering (ESCAPE) and 9th International Symposium on Process Systems Engineering (PSE)*, Garmisch-Partenkirchen, Germany, 2006, Published by Elsevier; ISBN 0-444-52969-1. p. 1568-1574

Co-authored papers

Appendix B

J. Cai and J. B. Jensen and S. Skogestad and J. Stoustrup, “Balance Energy Consumption and Food Quality Loss in Supermarket Refrigeration System”, *Submitted for publication in the proceedings of the 2008 American Control Conference*, Seattle, USA

Chapter 2

Introduction to vapour compression cycles

2.1 Introduction

In this chapter, it is given an overview of some basic vapour compression cycle designs. The goal is not to cover all designs, but we wish to introduce the features used later in the thesis.

The vapour compression cycle is the most common process used in both refrigeration systems and heat pumps. The two processes operate in the same manner. A simple flowsheet and pressure enthalpy diagram with the nomenclature is given in Figure 2.1. For refrigeration it is the cooling duty Q_C that is of interest, whereas it is the heating duty Q_H that is of interest for a heating cycle. When a heat pump is used in heat integration, both the heating and cooling duty is utilized.

Some typical areas of usage are:

Household: Refrigerators, air-conditioners and heat pumps.

Automotive: Air-conditioners and refrigerators.

Industry: Refrigeration of process streams, heat pumps for heat integration.

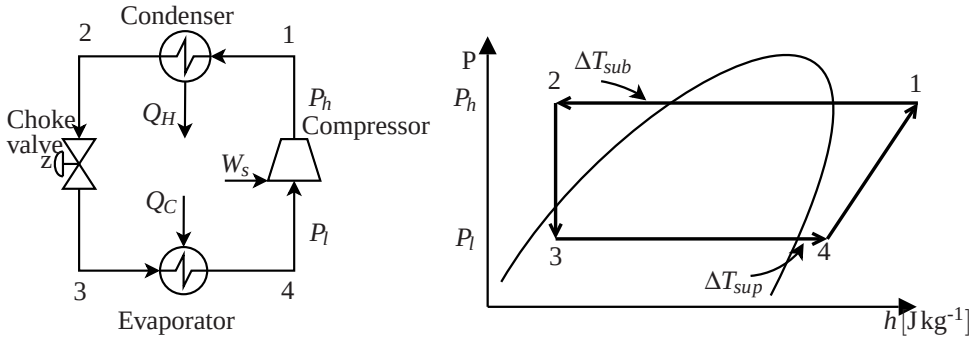

(a) Flowsheet (b) Pressure enthalpy diagram

Figure 2.1: A simple refrigeration or heat pump cycle with a corresponding typical pressure-enthalpy diagram indicating both sub-cooling and super-heating

2.1.1 Fundamentals

The basic refrigeration (or heating) cycle has four states (denoted 1,2,3,4 in Figure 2.1) and operates in the following manner:

The working fluid is evaporated and possibly super-heated ($3 \rightarrow 4$) by heat exchange with the cold source (e.g. air inside the refrigerator). Energy is added in a compressor (e.g. as electricity) to increase the pressure of the working fluid ($4 \rightarrow 1$). The high pressure vapour is de-super-heated, condensed and possibly sub-cooled ($1 \rightarrow 2$) by heat exchange with the hot source (e.g. air in the room). The liquid is then expanded through an expansion device (choke valve) ($2 \rightarrow 3$) to give a low temperature two-phase mixture at the evaporator inlet.

The efficiency of a vapour compression cycle is often reported in terms of "coefficient of performance" (COP). The COP for for a heating and cooling process is given by

$$\mathrm{COP}_h = \frac{h_1 - h_2}{h_1 - h_4} = \frac{\dot{m}(h_1 - h_2)}{\dot{m}(h_1 - h_4)} = \frac{Q_H}{W_s} \tag{2.1}$$

and

$$\mathrm{COP}_c = \frac{h_4 - h_3}{h_1 - h_4} = \frac{\dot{m}(h_4 - h_3)}{\dot{m}(h_1 - h_4)} = \frac{Q_C}{W_s} \tag{2.2}$$

respectively.

The vapour compression cycle for heating or cooling has some similarities with cyclic processes for generating mechanical work from heat, e.g. steam turbine cycles. These work generating cycles were studied extensively during the 1800 and

Nicolas Leonard Sadi Carnot studied the theoretical cycle later called the Carnot cycle. He found that the maximum work that may be extracted from a given hot source is only depending on the hot source temperature T_H and the cold sink temperature T_C. This may be derived using the 2nd law of thermodynamics, $\Delta S_{\text{total}} \geq 0$, where the equality holds for an ideal reversible process.

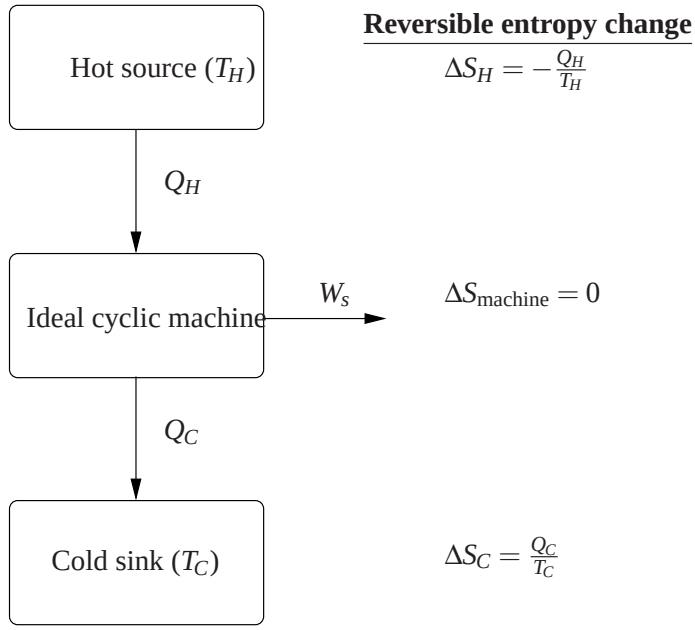

Figure 2.2: Schematic illustration of a Carnot machine generating mechanical work from a hot source

The Carnot machine is illustrated in Figure 2.2. The cyclic machine will have no net change in entropy, so $\Delta S_{\text{machine}} = 0$. If we assume reversible heat transfer and that the hot source and cold sink has constant temperature we get $\Delta S_H = \frac{-Q_H}{T_H}$ and $\Delta S_C = \frac{Q_C}{T_C}$. Thus, for the reversible case we get:

$$\frac{Q_H}{T_H} = \frac{Q_C}{T_C} \tag{2.3}$$

Taking an energy balance around the machine, $W = Q_H - Q_C$, we may express the above as follows:

$$W = \left(1 - \frac{T_C}{T_H}\right) Q_H \tag{2.4}$$

Here, $1 - \frac{T_C}{T_H} = \eta_{\text{Carnot}}$ is named the Carnot efficiency. This is the theoretical maximum fraction of the heat Q_H that may be converted to mechanical work W_s for an

ideal reversible process. Correspondingly, $\frac{T_H}{T_C} - 1$ is the minimum fraction of the cooling duty Q_C that must be added as mechanical work W_s. Thus, for a work generating process a large difference between T_C and T_H is beneficial. For a cooling process however, the opposite is true.

2.1.2 Expansion device

In household refrigerators a fixed expansion device called capillary tube is often used. This is a thin long pipe that gives the necessary pressure drop from the condenser to the evaporator. The operational characteristics of systems with capillary tubes is discussed Dossat (2002, page 356).

For larger systems with more variations in operating conditions it is desirable to have a variable expansion device. The most common is a choke valve, where the pressure is reduced without doing any work (isenthalpic expansion).

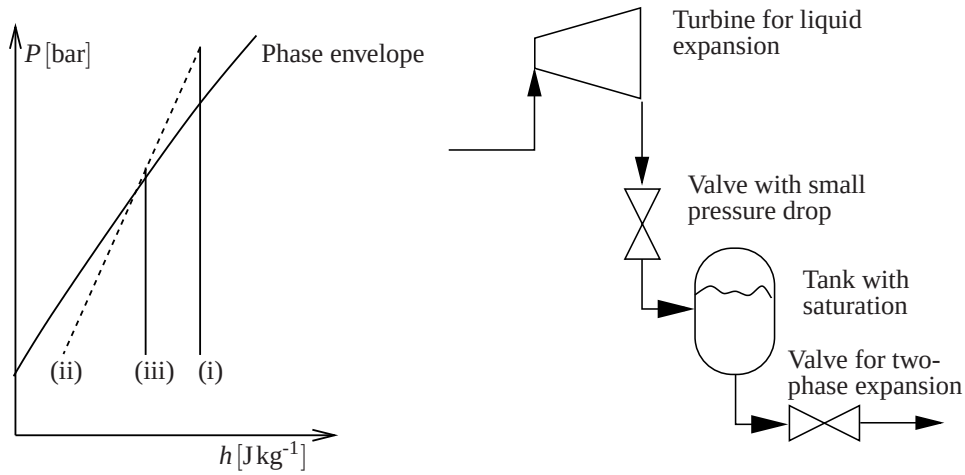

(a) Different expansion paths

(b) Liquid turbine and choke valve, path (iii)

Figure 2.3: Expansion in turbine increase the system performance. The left figure shows different expansion alternatives in a pressure enthalpy diagram; i) choke valve, ii) turbine and iii) combination of liquid turbine and choke valve, shown in right figure

The choke valve may be replaced by a turbine to improve the efficiency of the cycle. The pressure enthalpy diagram in Figure 2.3(a) illustrates the different paths for (i) isenthalpic expansion (choke valve) and (ii) isentropic expansion (ideal turbine). The vapour fraction (and specific enthalpy) into the evaporator is lower

with a turbine than for a choke valve so the COP_c is higher because $h_4 - h_3$ is larger without affecting $h_2 - h_1$. A practical problem of utilizing a turbine is that some of the liquid becomes vapour during expansion and this may cause wear in the turbine. A solution to this problem is to use a combination of a liquid turbine and a choke valve, illustrated in Figure 2.3(b) (Barclay and Yang, 2006). The turbine will then expand the liquid down to a pressure slightly higher than the saturation pressure and the choke valve will handle the remaining pressure drop into the two-phase region, see path (iii) in Figure 2.3(a). This is only useful if the liquid is sub-cooled before the expansion device, otherwise there will be no pressure drop for the liquid turbine.

The inclusion of a liquid turbine is considered in Chapter 6.

2.1.3 Condenser

The design of the condenser is important for the possible extra degree of freedom related to active charge. Two basic types of condensers are shown in Figure 2.4. Figure 2.4(a) shows a case where the liquid drains into a tank below the heat trans-

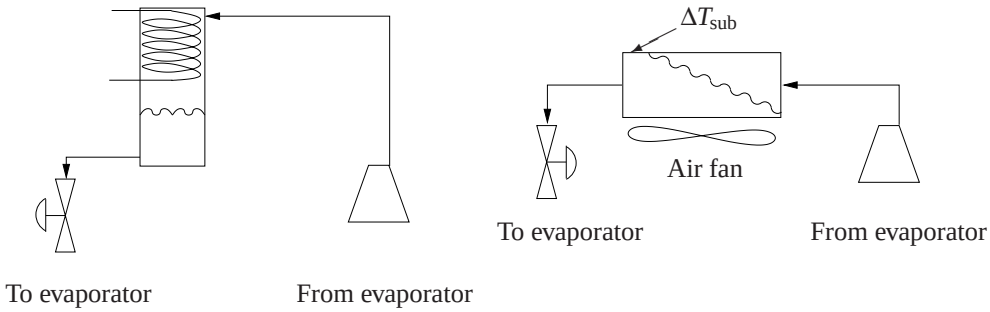

(a) Saturation at outlet (b) Plug-flow with possible sub-cooling

Figure 2.4: Two basic types of condensers

fer zone. With this design, there will be no sub-cooling in the condenser so there is no degree of freedom related to active charge since additional charge will only change the level in the tank below the condenser. An alternative design would be if the liquid covers part of the heat transfer zone, but this is not considered here.

Figure 2.4(b) shows a condenser with plug-flow. The refrigerant is first desuperheated, then condensed and finally sub-cooled. Here, the degree of freedom related

to active charge may be available (if we have means of changing it) because changing the charge will directly affect the pressure and sub-cooling in the condenser.

Remark. The plug-flow condenser may also give no sub-cooling by adding a liquid receiver after the condenser.

2.1.4 Evaporator

The design of the evaporator influences the degree of super-heating before the compressor. No super-heating is achieved with the flooded evaporator shown in Figure 2.5(a). Here, a float controller may adjust the choke valve to maintain a constant liquid level, but other strategies are also possible. Figure 2.5(b) shows a plug flow evaporator where we may have super-heating at the outlet. The super-heating may be controlled by a thermostatic expansion valve (TEV). The TEV will adjust its opening to give a certain degree of super-heating out of the evaporator. The TEV requires a certain degree of super-heating to be able to measure it and to assure that no liquid is fed to the compressor also dynamically. The super-heating is therefor typically controlled at 10 °C. Langley (2002, page 43).

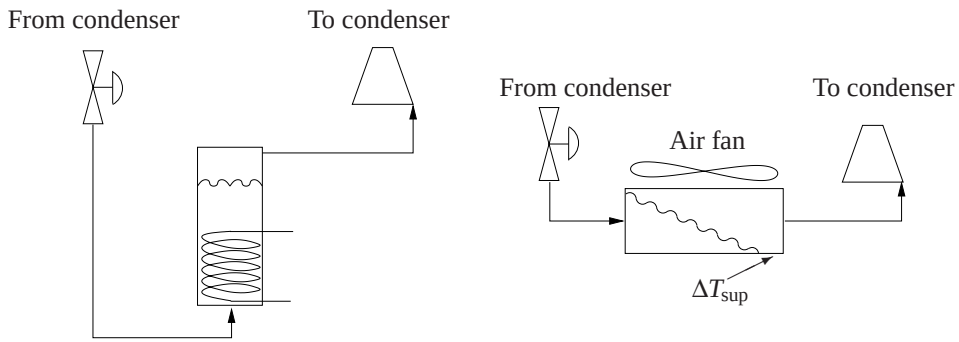

(a) Saturation at outlet (b) Plug-flow with possible super-heating

Figure 2.5: Two basic types of evaporators

Remark. The plug-flow evaporator may also give no super-heating by adding a liquid receiver after the evaporator.

2.1.5 Active charge

Consider first the simple case where both the condenser and evaporator are plug-flow heat exchangers, Figure 2.4(b) and 2.5(b) respectively. There is no additional liquid level in the cycle and we neglect the holdup in the piping, compressor and valve. We then have that the total charge in the system is $m_{\text{tot}} = m_{\text{evaporator}} + m_{\text{condenser}}$. An illustration is given in Figure 2.6. The compressor controls the load of the cycle and the choke valve controls the degree of super-heating. We assume that the flow of hot and cold source are kept constant so there are no degrees of freedom in the cycle. However, we have indicated an external filling/emptying system that may be used to adjust the charge in the system.

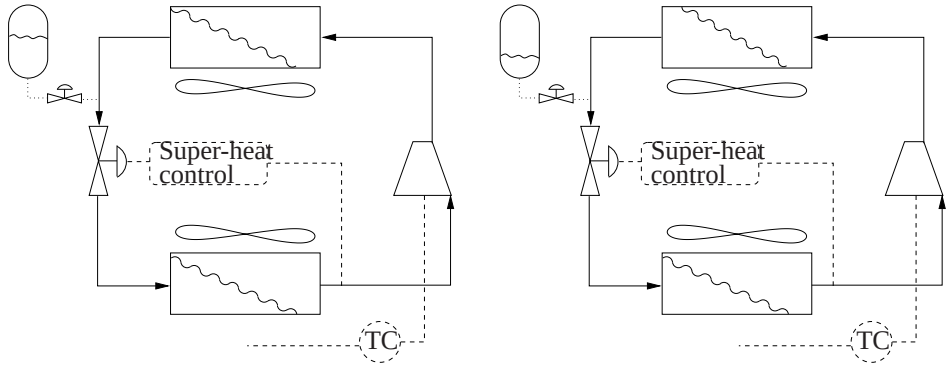

(a) Initial charge gives saturation at condenser outlet

(b) Increased charge gives sub-cooling at condenser outlet

Figure 2.6: A simple design with external filling/emptying system illustrating the degree of freedom related to active charge

In Figure 2.6(a) the charge is just enough to give saturation before the choke valve. If the charge is increased by filling from the external tank we will get the situation illustrated in Figure 2.6(b). The explanation is as follows:

Since the degree of super-heating out of the evaporator is controlled (by the choke valve) there will be no room for additional charge in the evaporator (except the increase due to higher density in vapour phase for higher pressure). The charge will therefor accumulate in the condenser where it will increase the pressure (and therefore the heat transfer) and give sub-cooling at the outlet. This illustrates that there is an extra degree of freedom related to the active charge. This degree of freedom is lost if the condenser design in Figure 2.4(a) is used.

The active charge may also be controlled without the external tank. This is discussed in Chapter 3.

Remark. If we remove refrigerant from the cycle in Figure 2.6(a) we may get to a point where the condenser pressure is to low to get full condensation. This illustrates why separate tank with a variable liquid level is desirable.

2.1.6 Operation of simple cycles

The simplest (and probably most well known) process using vapour compression cycle is the household refrigerator. The evaporator is mounted inside the refrigerator and the remaining equipment (compressor, condenser and choke valve) is mounted on the outside of the refrigerator.

Household refrigerators are usually controlled with a thermostat that switches the compressor on and off depending on the temperature inside the refrigerator. The expansion device is usually fixed, for example a capillary tube. Natural convection heat exchangers (no fans) are used. Thus, it is only one manipulated variable, namely the on/off switch for the compressor. Design and characteristics of refrigerators is discussed by Dossat (2002).

On/off control of the compressor is reasonable for a refrigerator since the compressor will operate at the design point with high efficiency most of the time (not during start-up). The use of a constant expansion device is also reasonable since the conditions are more or less constant (only small variations in the refrigerator and room temperature). However, for other applications it is necessary with continues capacity control. The compressor may then have variable speed and there are larger variations in the cycle such that a fixed valve position is inefficient. It is therefor normal to also have a variable valve. In addition it is common to have adjustable fans on the heat exchangers to improve heat transfer. This gives four manipulated variables, but as discussed above there may be a fifth manipulated variable. This fifth manipulated variable is related to the active charge in the cycle and depends on the design of the cycle.

The compressor is normally used to control the cooling load. The valve may be used to control the liquid level in the evaporator (or the degree of super-heating). As shown in Appendix B it is close to optimal to have the fans at constant speeds. We are then left with one degree of freedom that should optimize the operation. Good controlled variables are found in Chapter 4 and include the degree of sub-cooling (ΔT_{sub}) and the temperature difference at the condenser outlet. A possible control configuration is shown in Figure 2.7.

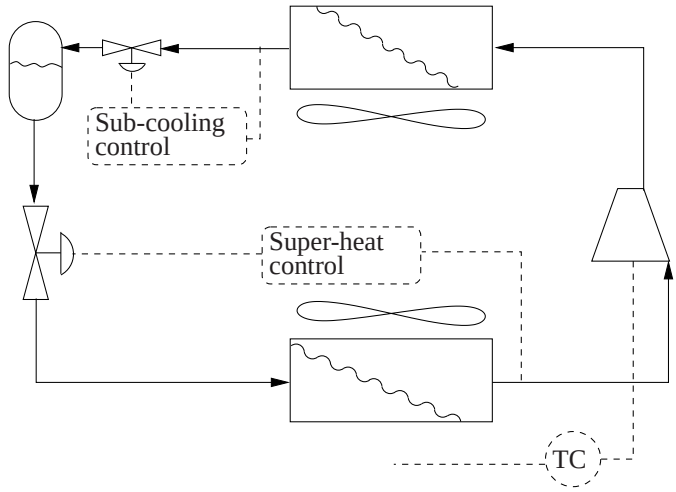

Figure 2.7: A possible control configuration for a simple refrigerant cycle. The fans are at constant speed

2.2 Some design features

The description in this section is based on refrigeration processes, but the same applies for heating cycles.

2.2.1 Constant versus varying temperature loads

The choice of refrigerant and configuration depends heavily on the cooling load. If the cooling load has a constant or close to constant temperature throughout the evaporator, a pure refrigerant will give a good temperature match. The refrigerant will evaporate at a slightly lower temperature than the cooling load (T_C). This is illustrated in Figure 2.8(a) where there is some super-heating (ΔT_{sup}). Note that this super-heating may be removed if the evaporator is designed as a flooded evaporator. We have assumed constant temperature loads in Chapter 3 and 4 by the use of cross-flow heat exchangers. Other cases of constant temperature loads are single component condensation or evaporation.

Often the cooling load change temperature as it is being cooled. If the temperature varies a lot, a single pure refrigerant will give large temperature differences in the warm end of the evaporator, illustrated in Figure 2.8(b). This large temperature difference gives a loss in terms of cycle efficiency, COP, so it may be economically attractive to consider alternatives to a single pure refrigerant cycle.

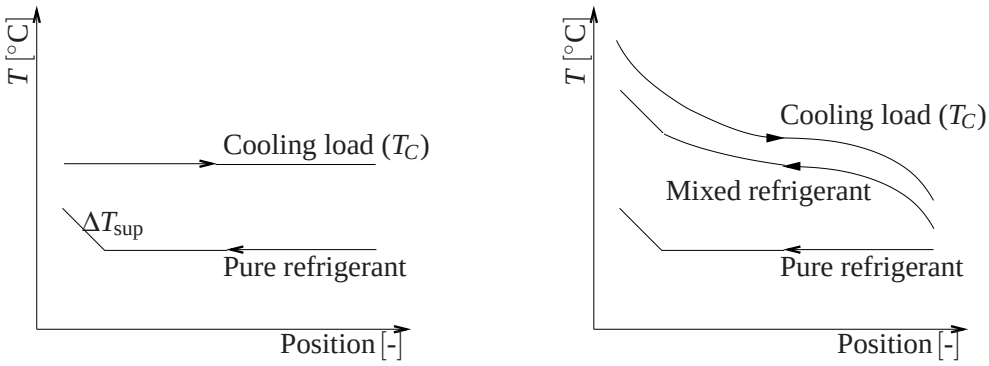

(a) Constant temperature load

(b) Variable temperature load

Figure 2.8: Evaporator temperature profile

Using a multicomponent refrigerant will give a gliding temperature also on the refrigerant side in the evaporator. This is illustrated in Figure 2.8(b). The refrigeration composition may be adjusted to optimize the performance of the system.

2.2.2 Two-stage expansion and two pressure levels

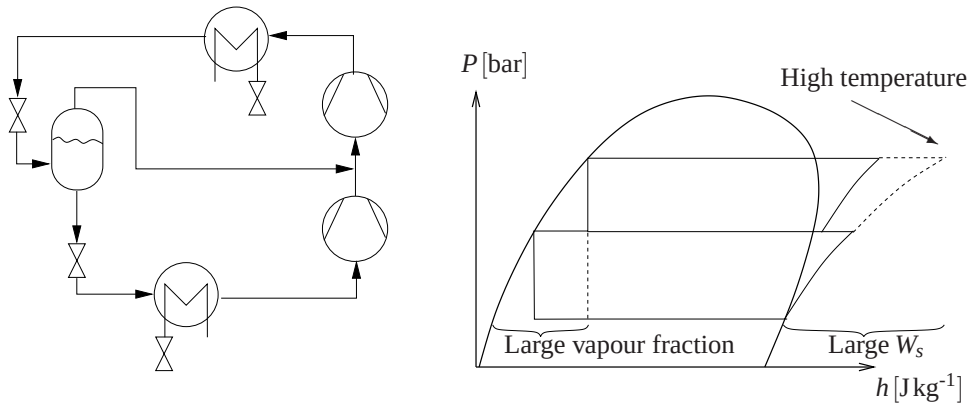

(a) Flowsheet

(b) Pressure enthalpy diagram, dotted cycle is conventional one-stage expansion

Figure 2.9: Two stage expansion improves cycle efficiency

If a high pressure ratio, $PR = \frac{P_h}{P_l}$ is required (because of large difference in T_H and T_C) there will be a large vapour fraction in the expansion process. All this vapour

has to be compressed back to the high pressure if the simple layout in Figure 2.1 is utilized. This is illustrated with the dotted cycle in Figure 2.9(b). The large vapour amount will not contribute to the cooling (except in the super-heating section) for a pure refrigerant and only give a minor contribution for mixed refrigerants. An improvement is to do the expansion in two (or more) stages, as illustrated in Figure 2.9(a). The vapour from the intermediate pressure level is fed either to the compressor as a side stream or between two compressors. This configuration has two effects making it more desirable:

- The vapour generated in the expansion down to the intermediate pressure is not expanded further so the necessary compressor power is reduced
- The vapour from the intermediate pressure level is colder than the vapour that has been compressed from the lowest pressure level so the mixing of the two streams will work as inter-cooling in the compressor and the necessary compressor power is reduced, as well as the outlet temperature

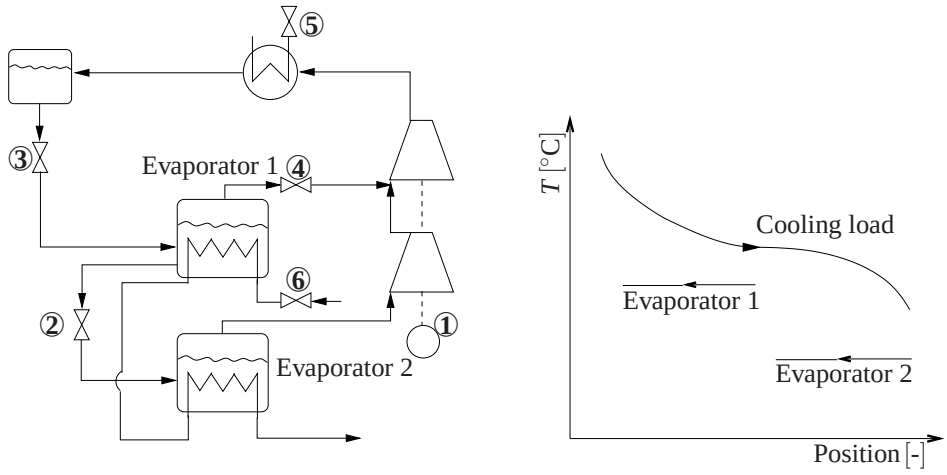

(a) Flowsheet (b) Temperature profile

Figure 2.10: Cooling at two pressure levels

An interesting use of two-stage expansion occur if cooling is needed at several temperature levels, e.g. a process stream that is cooled. One may then have an additional evaporator at the intermediate pressure level. This configuration is shown in Figure 2.10(a). The process stream is first cooled by the intermediate pressure level (Evaporator 1) and then by the low pressure level (Evaporator 2). The pressure enthalpy diagram is still as in Figure 2.9(b), but the amount of vapour at the intermediate pressure level is increased. The temperature profile in the evaporators may be illustrated by Figure 2.10(b). Control of such cycles are discussed by Wil-

son and Jones (1994) and we study degrees of freedom for this process in Chapter 8.

2.2.3 Internal heat exchange

Two ways of implementing internal heat exchange is illustrated in Figure 2.11. The configuration shown in Figure 2.11(a) is common for CO_2 cycles (Neksaa et al., 1998), but may also be used for other working fluid. The positive effect is that the expansion loss is reduced because of the extra sub-cooling before the expansion valve. However, the compressor inlet is heated which is negative for the efficiency. Depending on the working fluid and the operating point this kind of internal heat exchange may improve the efficiency (Radermacher, 1989). Also, if the suction line to the compressor will heat the vapour anyhow it is better to use this cooling internally.

The internal heat exchange configuration shown in Figure 2.11(b) is often used in LNG processes. Unless the internal heat exchanger may be bypassed it does not contribute to additional manipulated variables.

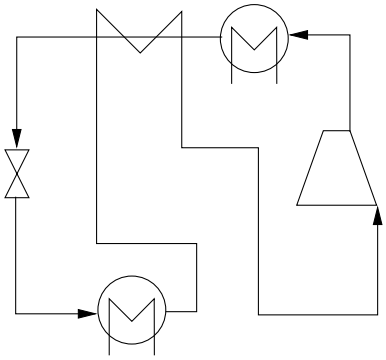

(a) May improve cycle efficiency also for pure fluids, often used for CO_2 cycles

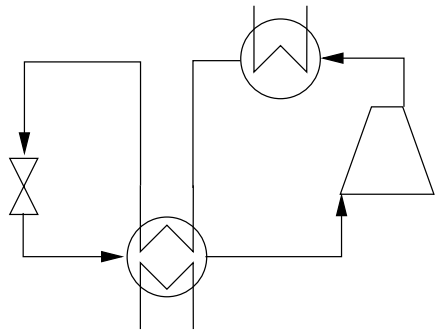

(b) No effect for pure refrigerants, often used in LNG processes

Figure 2.11: Internal heat exchange

2.2.4 Cascaded cycles

The configuration in Figure 2.12 shows two cycles in cascade, both with internal heat exchange. The refrigerant in the first cycle is condensed (partly of fully) by an

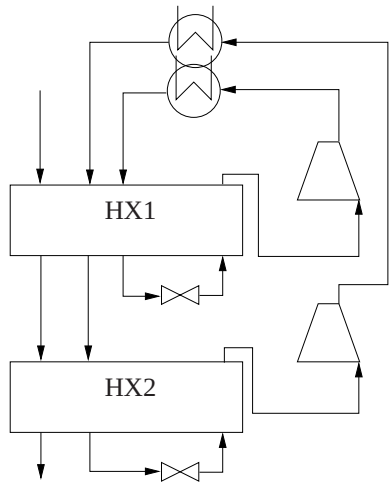

Figure 2.12: Cascaded cycles, shown with internal heat exchange

external fluid (e.g. air or water) and then further cooled in HX1. This refrigerant is used as cooling in HX1 after expansion. The refrigerant in the second cycle is cooled and possibly partly condensed with the same external fluid. Additional cooling is provided in both HX1 (by heat exchange with the first refrigerant cycle) and in HX2. The second refrigerant is expanded and vaporized through HX2 to provide the cooling at the lowest temperature. This layout shown in Figure 2.12 is often used for liquefaction of natural gas. The number of cycles typically varies from one to three and the refrigerant may be mixed or pure (then without internal heat exchange).

2.3 Conclusion

There are a number of design features that may be utilized in refrigeration processes based on the vapour compression cycle. It is not in the scope of this thesis to find which of these features are part of the truly optimal design, but rather to start from a given process design and study optimal operation. However, it seems that a study to quantify the energy improvements imposed by different design features is needed and may be an issue for further work.

Bibliography

Barclay, M. A. and Yang, C. C. (2006), Offshore LNG: The perfect starting point for the 2-phase expander?, *in* 'Offshore Technology Conference, Houston, Texas, USA'.

Dossat, R. J. (2002), *Principles of refrigeration*, Prentice Hall.

Langley, B. C. (2002), *Heat pump technology*, Prentice Hall.

Neksaa, P., Rekstad, H., Zakeri, G. R. and Schiefloe, P. A. (1998), 'CO_2-heat pump water heater: characteristics, system design and experimental results', *Int. J. Refrigeration* **21**, 172–179.

Radermacher, R. (1989), 'Thermodynamic and heat-transfer implications of working fluid mixtures in Rankine cycles', *Int. J. Heat Fluid Flow* **10**(2), 90–102.

Wilson, J. A. and Jones, W. E. (1994), 'The influence of plant design on refrigeration circuit control and operation', *European Symposium on Computer Aided Process Engineering (ESCAPE) 4, Dublin* pp. 215–221.

Chapter 3

Optimal operation of simple refrigeration cycles Part I: Degrees of freedom and optimality of sub-cooling

Published in Computers & Chemical Engineering (2007), 31, pages 712-721

The paper focuses on the operation of simple refrigeration cycles. With equipment given, there are, from a control and operational point of view, five steady state degrees of freedom; the compressor power, the heat transfer in the condenser, the heat transfer in the evaporator, the choke valve opening and the active charge in the cycle. Different designs for affecting the active charge, including the location of the liquid receiver, are discussed. With a given load (e.g. given cooling duty) the compressor power is set. Furthermore, it is usually optimal to maximize the heat transfer. The two remaining degrees of freedom (choke valve and active charge) may be used to set the degree of super-heating and sub-cooling. It is found that super-heating should be minimized, whereas some sub-cooling is optimal. For a simple ammonia cycle, sub-cooling gives savings in compressor power of about 2%. In this paper, refrigeration (cooling) cycles are considered, but the same principles apply to heat pumps.

3.1 Introduction

Cyclic processes for heating and cooling are widely used and their power ranges from less than 1 kW to above 100 MW. In both cases vapour compression cycle is used to "pump" energy from a low to a high temperature level.

The first application, in 1834, was to produce ice for storage of food, which led to the refrigerator found in most homes (Nagengast, 1976). Another well-known system is the air-conditioner (A/C). In colder regions a cycle operating in the opposite direction, the "heat pump", has recently become popular. These two applications have also merged together to give a system able to operate in both heating and cooling mode.

In Figure 3.1 a schematic drawing of a simple cycle is shown together with a typical pressure-enthalpy diagram for a sub-critical cycle. The cycle works as follows:

The low pressure vapour (4) is compressed by supplying work W_s to give a high pressure vapour with high temperature (1). The vapour is cooled to its saturation temperature in the first part of the condenser, condensed in the middle part and possibly sub-cooled in the last part to give the liquid (2). In the choke valve, the pressure is lowered to its original value, resulting in a two-phase mixture (3). This mixture is vaporized and possibly super-heated in the evaporator (4) closing the cycle.

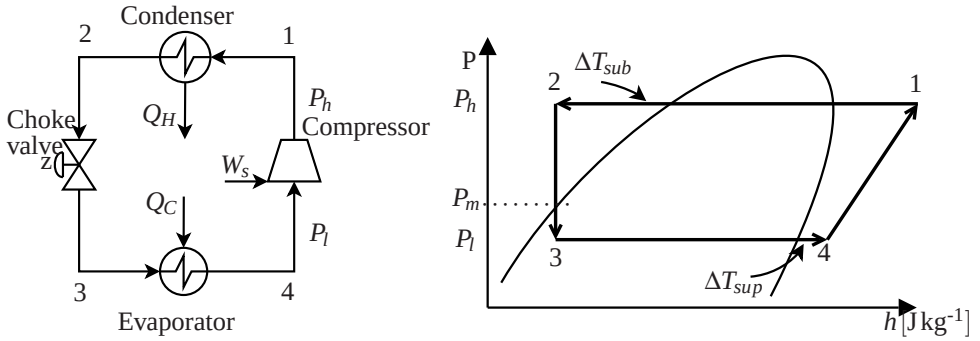

(a) (b)

Figure 3.1: (a) Simple refrigeration or heat pump cycle with (b) typical pressure-enthalpy diagram indicating both sub-cooling and super-heating

The choke valve may be replaced by an expander for improved efficiency, but this

Table 3.1: Structure of model equations

Heat exchangers (condenser and evaporator)
$Q = U \cdot \int \Delta T \, \mathrm{d}A = \dot{m} \cdot (h_{out} - h_{in})$
$P = P_{sat}(T_{sat})$
$m = \rho / V$
Valve
$\dot{m} = z \cdot C_V \sqrt{\Delta P \cdot \rho}$ $\qquad$ $h_{out} = h_{in}$
Compressor
$W_s = \dot{m}(h_{out} - h_{in}) = \dot{m} \cdot (h_s - h_{in}) / \eta$

is not considered here. The coefficient of performance for a refrigeration cycle (refrigerator, A/C) is defined as

$$COP = \frac{Q_c}{W_s} = \frac{\dot{m}(h_4 - h_3)}{\dot{m}(h_1 - h_4)} \tag{3.1}$$

The COP is typically around 3 which indicates that 33 % of the heat duty is added as work (e.g. electric power).

In this paper, the objective is to optimize the operation of a given cycle (Figure 3.1) in terms of maximize the COP, or specifically to minimize the compressor power W_s for a given cooling load Q_c. We consider only steady state operation. The model equations are summarized in Table 3.1. Note that pressure losses in piping and equipment are neglected. We also assume that the temperature of the hot (T_H) and cold (T_C) source are constant throughout the heat exchanger. This assumption holds for a cross flow heat exchanger. In practice, there may be some operational constraints, for example, maximum and minimum pressure constraints, which are not considered here.

In industrial processes, especially in cryogenic processes such as air separation and liquefaction of natural gas (LNG process), more complex refrigeration cycles are used in order to improve the thermodynamic efficiencies. These modifications lower the temperature differences in the heat exchangers and include cycles with mixed refrigerants, several pressure levels and cascaded cycles. Our long term objective is to study the operation of such processes. However, as a start we need to understand the simple cycle in Figure 3.1.

An important result from this study is the degree of freedom analysis given in Section 3.2. We find that the "active" charge plays an important role in operation of cyclic processes. This is also directly applicable to more complex designs. Unlike an open process, a closed cyclic process does not have boundary conditions on pressures imposed by the flows in and out of the system. Instead the pressure level

is indirectly given by the external temperatures, heat exchanger sizes, load and the active charge. *The active charge is defined as the total mass accumulated in the process equipment in the cycle, mainly in the condenser and evaporator, but excluding any adjustable mass in liquid receivers (tanks).*

The effect of a change in active charge on operation depends on the specific design. Intuitively, it seems that an increase in active charge must increase the pressure, and indeed this is true in most cases. For example, this is the case for the models used in this paper with plug-flow in the heat exchangers. Then more liquid in the condenser gives more sub-cooling which, effectively reduces cooling and pressure increases. Similarly more liquid in the evaporator gives less super-heating effectively increasing heat transfer and pressure increases. However, there may be designs where the effect of charge on pressure is opposite. For example, consider a well-mixed flooded condenser where the heat transfer coefficient U to liquid is larger than to vapour. An increase in charge (liquid) may then improve cooling and pressure decreases. In any case, the main point is that the "active" charge is a degree of freedom that affects the operation of the system, and this paper focuses on how to use it effectively.

Although there is a vast literature on the thermodynamic analysis of refrigeration cycles, there are very few authors who discuss their operation and control. Some discussions are found in text books such as Stoecker (1998), Langley (2002) and Dossat (2002), but these mainly deal with more practical aspects. Svensson (1994) and Larsen et al. (2003) discuss operational aspects. A more comprehensive recent study is that of Kim et al. (2004) who consider the operation of trans-critical CO_2 cycles. They discuss the effect of "active charge" and consider alternatives for placing the receiver.

The paper also discuss super-heating and sub-cooling. In the literature, it is generally taken for granted that there for a given cycle should be no sub-cooling and super-heating ($\Delta T_{sub} = 0\,^{\circ}\mathrm{C}$ and $\Delta T_{sup} = 0\,^{\circ}\mathrm{C}$) in optimal operation. For example, Stoecker (1998, page 57) states that

> *The refrigerant leaving industrial refrigeration condensers may be slightly sub-cooled, but sub-cooling is not normally desired since it indicates that some of the heat transfer surface that should be be used for condensation is used for sub-cooling. At the outlet of the evaporator it is crucial for protection of the compressor that there be no liquid, so to be safe it is preferable for the vapor to be slightly super-heated.*

In this study, we confirm that super-heating is not optimal. The issue of sub-cooling is less clear. Of course, sub-cooling in itself is always optimal, as less refrigerant needs to be circulated. The issue is whether sub-cooling is optimal

for a given cold source temperature and a given condenser area, because sub-cooling will reduce the temperature driving forces which must be compensated by increasing the pressure. We find, contrary to popular belief, that with given equipment, sub-cooling in the condenser may give savings in energy usage (compressor power) in the order of 2 %. An ammonia case study is presented to obtain numerical results.

3.2 Degrees of freedom in simple cycles

3.2.1 Design versus operation

Table 3.2 shows typical specifications for the simple refrigeration cycle in Figure 3.1 in design (find equipment) and in operation (given equipment). The five design specifications include the load, the two pressures, and the degree of sub-cooling and super-heating. Based on these five design specifications, external conditions and an assumed isentropic efficiency for the compression, we may obtain the following four equipment parameters which can be adjusted during operation: compression work (W_s) valve opening (z) and effective heat transfer (including UA-values) for the two heat exchangers. Initially, we were puzzled because we could not identify the missing fifth equipment parameter to be adjusted during operation. However, we finally realized that we can manipulate the "active charge" in the cycle, which affects the operation. The fact that the charge is an independent variable is unique for closed systems since there is no (external) boundary condition for pressure which would otherwise set the active charge.

Table 3.2: Typical specifications in design and operation

	Given	#
Design	Load (e.g. Q_h), P_l, P_h, ΔT_{sup} and ΔT_{sub}	5
Operation	W_s (load), choke valve opening (z), effective heat transfer (e.g. UA) in two heat exchangers and active charge	5

3.2.2 Active charge and holdup tanks

For the simple cycle in Figure 3.1 we have the following overall material balance:

$$m_{tot} = \underbrace{m_{\text{evap}} + m_{\text{con}} + m_{\text{valve}} + m_{\text{comp}}}_{m_{\text{active}}} + m_{\text{tanks}} \tag{3.2}$$

Normally the holdups in the valve and compressor are neglected and we get:

$$m_{tot} = \underbrace{m_{\text{evap}} + m_{\text{con}}}_{m_{\text{active}}} + m_{\text{tanks}} \tag{3.3}$$

With no filling, emptying or leaks, the total mass m_{tot} is fixed. We have not included a holdup tank in Figure 3.1, but in practice it is common to include a tank or receiver with variable liquid mass. It is assumed that a change in m_{tanks} (e.g. by filling or leaking) with a constant active charge (m_{active}) does not affect the operation of the cycle. This implies that the tank must contain both liquid and gas in equilibrium (saturated). Then we can move mass to or from the tank without affecting the pressure, and thus without affecting the rest of the cycle. Thus the liquid tank makes operation independent of the total charge in the system.

More importantly, the extra tank introduces an additional degree of freedom. This can be seen from Equation 3.3: With m_{tot} constant, we can by changing the mass (liquid) in the tank (m_{tank}), change the active charge (m_{active}). This shows that m_{tank} has an indirect steady state effect on the active charge, and can therefore be used for control purposes, of course provided that we have means of changing it.

Although it is possible to introduce several tanks in a cycle, we only have one material balance for each cycle, so from Equation 3.3 this will not add any steady-state degrees of freedom with respect to the active charge.

Rule 3.1 *In each closed cycle, we have one degree of freedom related to the active charge, which may be indirectly adjusted by introducing a variable liquid level (tank; receiver) in the cycle.*

Rule 3.2 *In each closed cycle, there will be one liquid holdup that does not need to be explicitly controlled, because the total mass is fixed. This is usually selected as the largest liquid volume in the closed system. The remaining liquid levels (holdups) must be controlled (to avoid overfilling or emptying of tanks).*

Remark 1 Note that in Rule 3.2 it says "does not need" rather than "must not". Thus, Rule 3.2 does not say that we cannot control all the liquid volumes in the system (including the largest one), but it just states that it is not strictly necessary. In fact, controlling all the liquid volumes, provides a way for explicitly controlling the active charge in the cycle (Rule 3.1).

Remark 2 Introducing additional liquid tanks may be useful for operation, but at least for pure fluids, these will not introduce any additional steady-state degrees of freedom because we can move mass from one tank to another without affecting operation. Also, to avoid that tanks fill up or empty, these additional levels must be controlled (Rule 3.2), either by self-regulation or feedback control.

Remark 3 In *mixed refrigerant* cycles two tanks may be used to indirectly change the composition of the circulating refrigerant. In this case the two tanks have different composition so moving mass from one tank to another does affect operation. For more complex cycles the maximum number of degrees of freedom related to tank holdups is the number of components in the refrigerant.

Adjusting the active charge

In order to freely adjust the active charge, we need to introduce a liquid tank (receiver) plus an extra valve. Kim et al. (2004) discuss alternative locations for the variable tank holdup (liquid receiver). In Figure 3.2, we show cycles for the two main cases where the tank is placed (a) on the high pressure side after the condenser and (b) on the low pressure side after the evaporator. Other placements and combinations are possible, but these are only variations of these two and will not add any steady-state degrees of freedom for pure refrigerants.

The most obvious way of introducing a means for adjusting the tank holdup is to add an extra valve before the tank as shown in Figure 3.2. In Figure 3.2(a), the

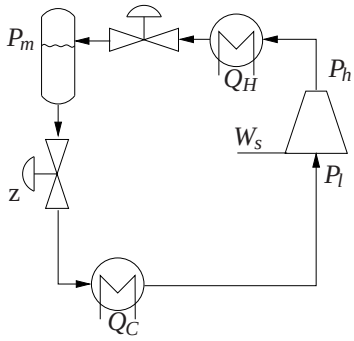

(a) Liquid tank and extra valve on high pressure side

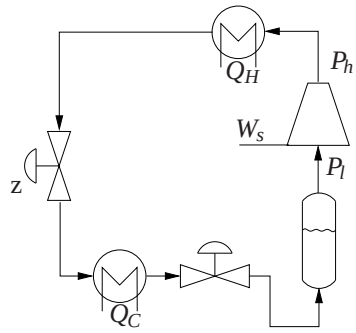

(b) Liquid tank and extra (non-optimal) valve on low pressure side

Figure 3.2: Simple cycle with variable active charge

liquid tank is located at an intermediate pressure P_m after the condenser. Since the extra valve is on the "same side" as the expansion valve (choke), the pressure drop over the extra valve will not effect the efficiency of the cycle. Since P_m is assumed to be the saturation pressure at the tank temperature, the exit stream from the condenser must be sub-cooled (or super-critical, but this is not considered in this paper). Thus, in Figure 3.2(a), the pressure drop across the valve may be used

to adjust the degree of sub-cooling in the condenser. To understand how the extra valve creates sub-cooling, consider the pressure-enthalpy diagram in Figure 3.1. The receiver (tank) with saturated liquid operates at saturation pressure P_m, and the pressure drop for the extra valve introduces a pressure drop $P_h - P_m$. As seen from Figure 3.1, the corresponding operating point 2 at the exit of the condenser must then be at a sub-cooled state.

Another possibility is to place the tank after the evaporator, as shown in Figure 3.2(b). With this design the stream exiting the evaporator is not fully evaporated and by lowering the pressure through the extra valve the vapour exiting the valve becomes saturated (see pressure-enthalpy diagram). However, in this case the valve introduces a pressure drop that must be compensated by increasing the compression power, so a valve here is generally not optimal.

A low pressure tank may not be desirable from a practical point of view, since the vapour velocity will be highest at this point in the cycle and the extra equipment will increase the pressure drop.

Extra valve removed

An extra valve is generally required to freely adjust the active charge. However, in many practical cases the extra valve in Figure 3.2(a) and 3.2(b) is removed. What effect does this have?

- High pressure tank without valve. Without the valve we have at steady state the same thermodynamic state at the exit of the condenser as at the exit from the tank. Thus, the exiting stream from the condenser will be saturated liquid. The most common design is shown in Figure 3.3, where the tank and condenser are merged together so that the saturated liquid from the condenser drains into the receiver. As we will show, this is not generally optimal. Thus, in this design we have used a degree of freedom ("fully open valve") to set the degree of sub-cooling to zero (not optimal).
- Low pressure tank without valve (Figure 3.4(a)). This gives saturated vapour to the compressor. Fortunately, this is generally optimal for the cycle as a whole, because the inlet temperature to the compressor should be as low as possible to minimize vapour volume and save compression power. Thus, in this design we have used a degree of freedom ("fully open valve") to set the degree of super-heating to zero (optimal). Two designs are shown in Figure 3.4(a), one with a separate receiver and one using a flooded evaporator. The designs are equivalent thermodynamically, but the heat transfer coefficient

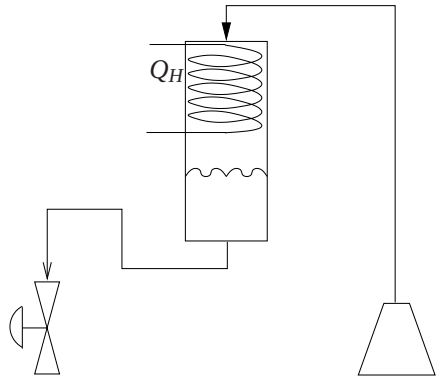

Figure 3.3: Condenser with saturation at outlet giving no sub-cooling (common design, but non-optimal)

and pressure drop will be different.

In summary, removing the valve gives saturation at the exit of the heat exchanger. In the case of high-pressure liquid tank we get a sub-optimal design if we remove the valve, whereas for the low-pressure tank we get an optimal design if the extra valve is removed.

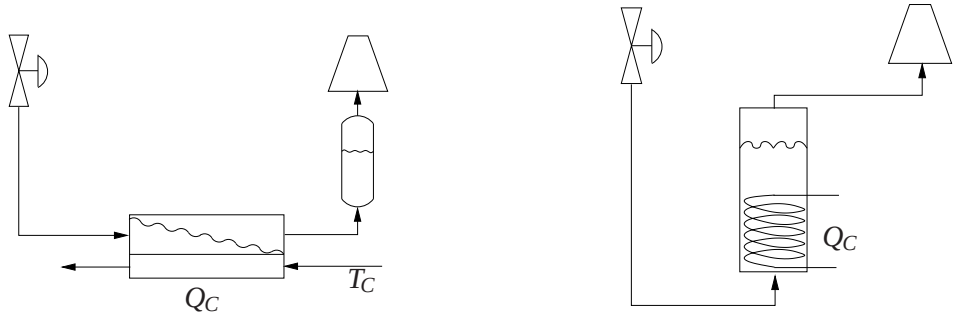

(a) With separate receiver (b) Flooded evaporator

Figure 3.4: Evaporator with saturation at outlet giving no super-heating (optimal)

3.2.3 Degrees of freedom for operation

In summary, we have the following five operational or control degrees of freedom for a simple refrigeration cycle (Figure 3.1):

1 Compressor power W_s. We assume here that it is used to set the "load" for the cycle.

2, 3 Effective heat transfer. There are two degrees of freedom related to adjusting the heat transferred in the condenser and evaporator. This may be done in many ways, for example, by introducing bypasses, changing the flowrates of coolant or using a flooded condenser or evaporator to change the effective UA-value. However, we generally find that it is optimal to maximize the effective heat transfer in the condenser and evaporator. There are exceptions where it may not be optimal to maximize the heat transfer in the condenser and evaporator, for example because, of costs related to pumps, fans or coolants, but these degrees of freedom are not considered in the following.

4 Choke valve opening (z)

5 Active charge (see Section 3.2.2)

In practice, we are then with a given load and maximum heat transfer left with two steady state degrees of freedom. These are the choke valve opening (z) and the active charge (m_{active}). These may be used to set the degree of super-heating and degree of sub-cooling. The pressure levels (P_h and P_l) are indirectly determined by the given (maximum) value of the heat transfer.

3.3 Discussion of some designs

As discussed in more detail in Section 3.4, we find that the thermodynamic efficiency is optimized by having no super-heating and some sub-cooling. With this in mind, we next discuss some alternative designs.

3.3.1 Optimal designs

Two potentially optimal designs are shown in Figure 3.5. The reason we say "potentially optimal" is because they will only be optimal if we use the optimal value for the sub-cooling and super-heating.

To avoid super-heating, we have in Figure 3.5(a) and 3.5(b) a low-pressure tank (receiver) after the evaporator. This tank will give saturated vapour out of the evaporator at steady state (optimal), and also by trapping the liquid it will avoid that we get liquid to the compressor during transient operation. To avoid super-heating we must have vapour-liquid equilibrium in the tank. This may be achieved

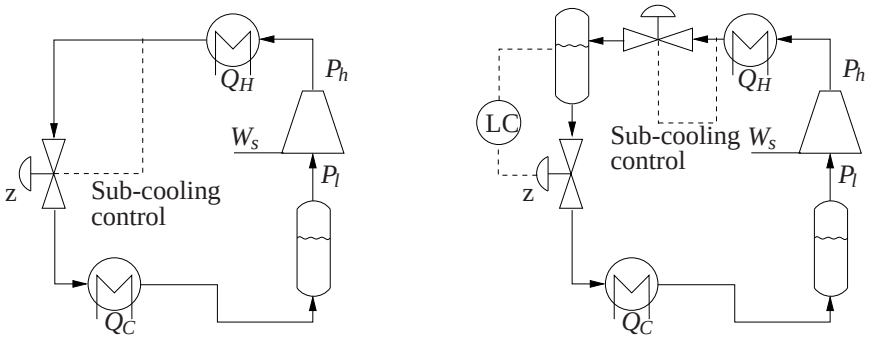

(a) Optimal with 1 tank

(b) Optimal with 2 tanks

Figure 3.5: Two potentially optimal designs with sub-cooling and no super-heating

by letting the vapour bubble through the tank. An alternative design is the flooded evaporator in Figure 3.4(b).

At the high-pressure side, we show optimal designs with both (a) no receiver and (b) a receiver and an extra valve. In (a) the choke is used to control the degree of sub-cooling (ΔT_{sub}). Also other control policies are possible, for example, keeping the choke valve position at its optimal value or controlling the pressure, but controlling ΔT_{sub} was found by Jensen and Skogestad (2005) to be a good self-optimizing controlled variable.

The design in Figure 3.5(b) is thermodynamically equivalent to Figure 3.5(a), but the addition of the tank may prevent that we get two-phase flow with vapour "blow out" through the choke. We here have two adjustable holdups, so from Rule 3.2 one of them must be controlled. In Figure 3.5(b) is shown the case where the choke valve is used to control the level in the high pressure tank, but alternatively it could control the level in the low pressure tank.

3.3.2 Non-optimal designs

Three non-optimal designs are shown in Figure 3.6. Figure 3.6(a) shows the design used in most applications except that the tank and condenser are often integrated as shown in Figure 3.3. This common design has two errors compared to the optimal solution: 1) There is no sub-cooling in the condenser and 2) there is super-heating in the evaporator. The super-heat control is in practice accomplished with a thermostatic expansion valve (TEV). In theory, one could get optimality by setting the

setpoint for super-heating to zero, but in practice this is not possible because this could give liquid out of the evaporator. The setpoint for super-heating is typically about 10 °C.

In Figure 3.6(b) we have two liquid tanks, one after the evaporator and one after the condenser. This design is better since there is no super-heating in the evaporator, but one error remains: There is no sub-cooling in the condenser. Note that we need to control one of the liquid levels in accordance with Rule 3.2.

Another non-optimal design is shown in Figure 3.6(c). Here we have introduced the possibility for sub-cooling, but we have super-heating which is generally not

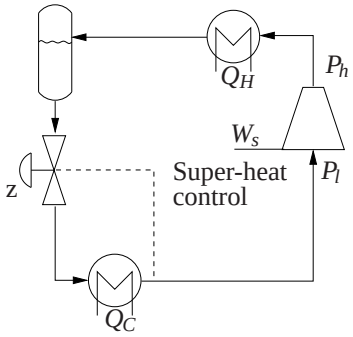

(a) Non-optimal 1. This design has two errors: 1) No sub-cooling and 2) Super-heating

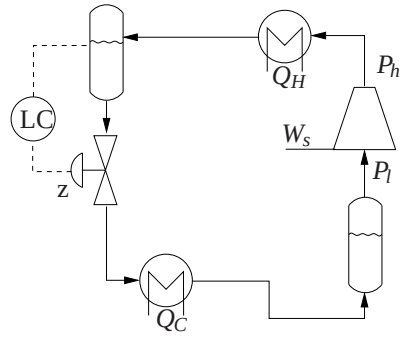

(b) Non-optimal 2. This design has one error: No sub-cooling

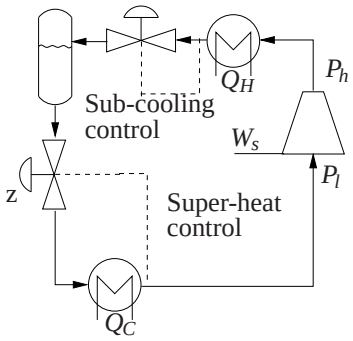

(c) Non-optimal 3, This design has one error: Super-heating

Figure 3.6: Three non-optimal designs

optimal.

3.4 Optimality of sub-cooling

We have several times made the claim that sub-cooling may be optimal. To justify this somewhat controversial claim, we start by considering a specific example.

3.4.1 Ammonia case study

The objective is to cool a storage building by removing heat (Q_C) as illustrated in Figure 3.7. The cycle operates between a cold medium of air inside the building ($T_C = T_{\text{room}}$) and hot medium of ambient air ($T_H = T_{\text{amb}}$). The steady state heat loss from the building is 20 kW and the cooling load Q_C is indirectly adjusted by the temperature controller which adjusts the compressor work (W_s) to maintain $T_C = T_C^s$.

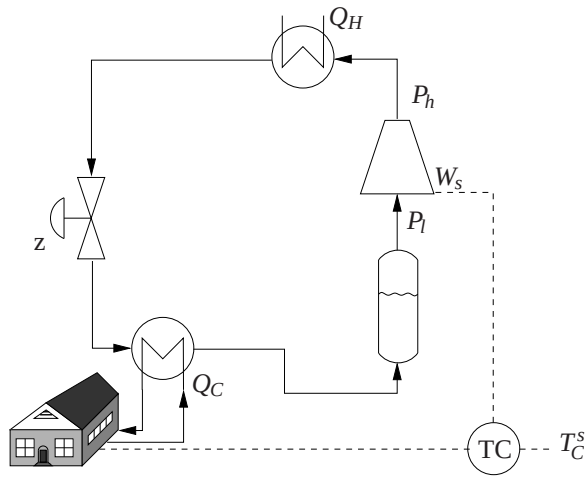

Figure 3.7: Cold warehouse with ammonia refrigeration unit

Some data for the cycle:

- Ambient temperature $T_H = 25\,^\circ\text{C}$
- Indoor temperature setpoint $T_C^s = -12\,^\circ\text{C}$
- Isentropic efficiency for compressor is 95 %

- Heat transfer coefficients (U) are 1000 and 500 $\mathrm{W\,m^{-2}\,K^{-1}}$ for the evaporator and condenser, respectively
- Heat exchangers with areas given in Table 3.3
- Thermodynamic calculations based on SRK equation of state

The equipment is given and we have 5 steady-state operational degrees of freedom (Section 3.2). With a given load and maximum heat transfer, we have two remaining steady state degrees of freedom, which may be viewed as the degree of sub-cooling (ΔT_{sub}) and the degree of super-heating (ΔT_{sup}). The performance of the cycle, measured by the compressor power W_s, was optimized with respect to the two degrees of freedom. We find as expected that super-heating is not optimal, but contrary to popular belief, the results in Table 3.3 show that sub-cooling by 4.66 °C reduces the compression work W_s by 1.74 % compared to the case with saturation out of the condenser. The high pressure P_h increases by 0.45 %, but this is more than compensated by a 2.12 % reduction in flowrate. The sub-cooling increases the condenser charge M_{con} by 5.01 %. Figure 3.8 shows the corresponding pressure enthalpy diagram for the two cases and Figure 3.9 shows the temperature profile in the condenser. Similar results are obtained if we use other thermodynamic data, if we change the compressor efficiency or if we let UA be smaller in the sub-cooling zone.

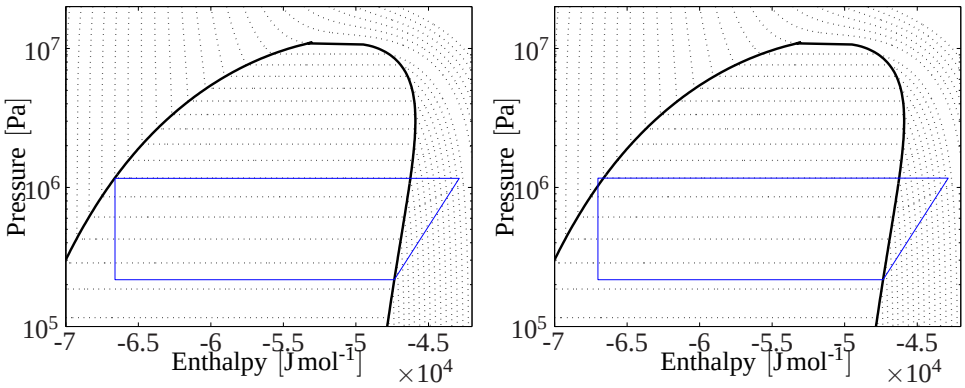

(a) Optimal operation without sub-cooling (Figure 3.6(b))

(b) Optimal operation with sub-cooling allowed (Figure 3.5)

Figure 3.8: Pressure-enthalpy diagrams with and without sub-cooling

The improvement of 2 % would be larger if the pressure drop in the piping and equipment was accounted for in the model, because the mass flowrate is reduced with an unchanged low pressure. Thus, the volumetric flowrate in the low pressure

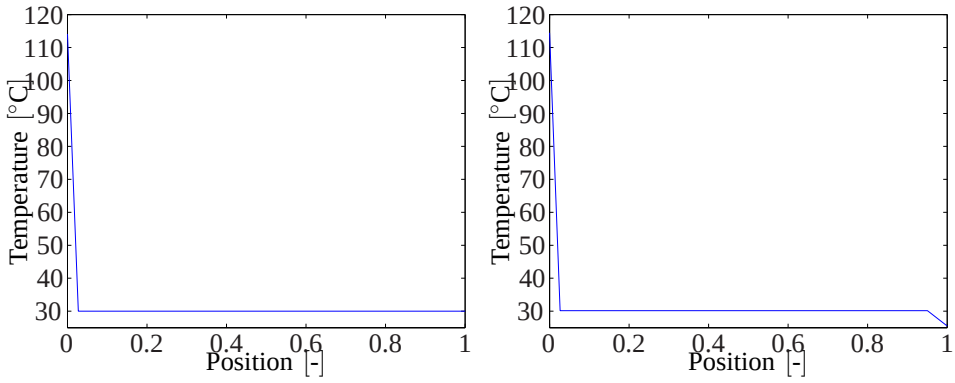

(a) Temperature profile without sub-cooling (b) Temperature profile with sub-cooling

Figure 3.9: Temperature profile in condenser

Table 3.3: Optimal operation with and without sub-cooling

	No sub-cooling	Optimal sub-cooling
W_s [W]	4648	4567
Q_C [kW]	20	20
$\dot{m}$ [kg s^{-1}]	0.0177	0.0173
M_{con} * [kg]	0.301	0.316
ΔT_{sub} [°C]	0.00	4.66
ΔT_{sup} [°C]	0.00	0.00
$\Delta T_{\text{min, con}}$ [°C]	5.00	0.491
P_h [bar]	11.63	11.68
P_l [bar]	2.17	2.17
A_{con} [m^2]	8.70	8.70
A_{vap} [m^2]	4.00	4.00

*Evaporator charge has no effect because of saturation (no super-heating) in the evaporator

side is reduced and this is important as pressure drop is most critical at low pressure. The pressure losses on the high pressure side will also be slightly reduced (because of smaller flowrate and higher pressure), but this is less important for the efficiency of the cycle.

3.4.2 Explanation

The irreversible isenthalpic expansion through the choke valve gives a thermodynamic loss. The reason for the improvement in efficiency by sub-cooling is that loss is reduced because less vapour is formed, see Figure 3.8. This more than compensates the increased irreversible loss due to larger temperature difference in the condenser. To understand this in more detail consider Figure 3.10 which shows a conceptual pressure enthalpy diagram of a typical vapour compression cycle. We have indicated a cycle without sub-cooling (solid line) and the same cycle with sub-cooling (dotted line). Note that since we in the latter case have a higher condenser pressure (and therefore also a higher temperature in the condensing section) we will with given equipment (UA-values) have more heat transfer, which gives a lower outlet temperature. The condenser outlet will follow the line "Con. out" with increasing pressure. The line will asymptotically approach the hot source temperature T_H and we want to find the optimal operating point on this line.

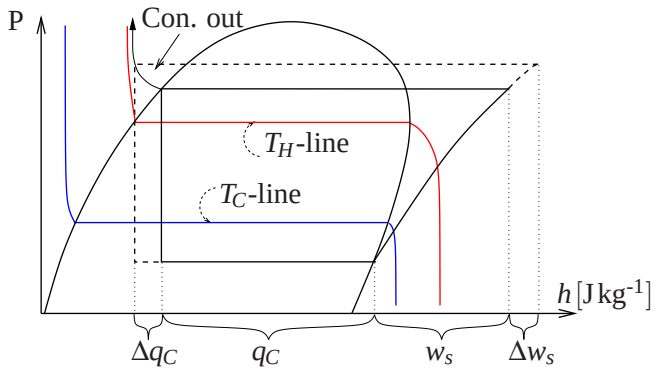

Figure 3.10: Pressure-enthalpy diagram for a cycle with and without sub-cooling

If we consider moving from one operating point to another we require an increase in the COP for the change to be optimal:

$$\Delta COP = \frac{q_C + \Delta q_C}{w_s + \Delta w_s} - \frac{q_C}{w_s} > 0 \tag{3.4}$$

$$COP \cdot \Delta w_s < \Delta q_C \tag{3.5}$$

where $q_C \cdot \dot{m} = Q_C$ and $w_s \cdot \dot{m} = W_s$. We assume that $Q_C\,[\mathrm{J\,s^{-1}}]$ is given, and that $\dot{m}\,[\mathrm{kg\,s^{-1}}]$ and $q_C\,[\mathrm{J\,kg^{-1}}]$ may vary. We use ΔT_{sub} as the independent variable and introduce differentials. The requirement for improving efficiency is then from Equation 3.5:

$$\left(\frac{\partial q_C}{\partial \Delta T_{sub}}\right)_{UA} > COP \cdot \left(\frac{\partial w_s}{\partial \Delta T_{sub}}\right)_{UA} \tag{3.6}$$

According to Equation 3.6, for an initial COP of 3, the increase in specific duty in the evaporator (Δq_C) should be 3 times larger than the increase in specific compressor power (Δw_s) to give improved performance. In Figure 3.10 we have that $\Delta q_C \approx \Delta w_s$, so the optimal degree of sub-cooling is clearly less than that indicated by this figure. Note however, that the "Con. out" line is much flatter for smaller Δq_C, so a small degree of sub-cooling may be optimal. The optimum is located at the degree of sub-cooling where the inequality in Equation 3.6 becomes an equality. In the case study we found that the optimum outlet temperature from the condenser (25.49 °C) is closer to T_H (25 °C) than the saturation temperature (30.15 °C).

Similar considerations on optimizing the pressure P_h have been made earlier for trans-critical CO_2-cycles (Kim et al., 2004). However, for sub-critical cycles like the ammonia cycle studied above, it has been assumed that the pressure is fixed by a saturation condition.

3.4.3 Discussion of sub-cooling: Why not found before?

The above results on optimality of sub-cooling is contrary to previous claims and popular belief. Why has this result not been found before?

Reason 1: Not allowed by design

The design of the condenser is often as shown in Figure 3.3, where the saturated liquid drains into a liquid receiver. In this design it is not possible to have sub-cooling.

Reason 2: Infinite area case

The optimal degree of sub-cooling becomes smaller as we increase the heat transfer (UA-values). In particular, with an infinite heat transfer area, sub-cooling is

not optimal. In this case the temperature at the condenser outlet is equal to the hot source temperature T_H. Neglecting the effect of pressure on liquid enthalpy, the enthalpy is also given. We then find that $\Delta q_C = 0$ and sub-cooling is not optimal as illustrated in Figure 3.11.

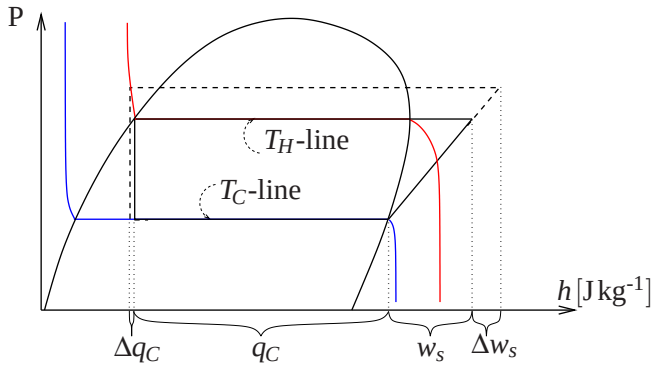

Figure 3.11: Pressure-enthalpy diagram for infinite area case where condenser outlet is at hot source temperature T_H

In practice, the enthalpy depends slightly on pressure (as indicated by the curved constant temperature lines in Figure 3.11) so Δq_C might be larger than zero, but this effect is too small to change the conclusion that sub-cooling is non-optimal with infinite area.

Reason 3: Specifying HRAT

The minimum approach temperature (ΔT_{min} or HRAT) is commonly used as a specification for design of processes with heat exchangers. The idea is to specify ΔT_{min} in order to get a reasonable balance between minimizing operating (energy) costs (favored by a small ΔT_{min}) and minimizing capital costs (favored by a large ΔT_{min}). Although specifying ΔT_{min} may be reasonable for obtaining initial estimates for stream data and areas, it should not be used for obtaining optimal design data - and especially not stream data (temperatures). This follows because specifying ΔT_{min} results in an optimum with no sub-cooling. This can be seen by letting the T_H-line in Figure 3.11 represent $T_H + \Delta T_{min}$. The condenser outlet temperature is then $T_H + \Delta T_{min}$ and similarly to the infinite area case we get $\Delta q_C = 0$ (neglecting the effect of pressure on liquid enthalpy), and sub-cooling is not optimal.

The results can also be understood because specifying ΔT_{min} favors designs with ΔT being as close as possible to ΔT_{min} throughout the heat exchanger, and this

clearly disfavour sub-cooling, see Figure 3.9(b).

A third way of understanding the difference is that we end up with two different optimization problems for design (Equation 3.7) and operation (Equation 3.8).

$$\begin{aligned} \min \quad & (W_s) \\ \text{subject to} \quad & T_C - T_C^S = 0 \\ & \Delta T_i - \Delta T_{\min,i} \geq 0 \end{aligned} \tag{3.7}$$

$$\begin{aligned} \min \quad & (W_s) \\ \text{subject to} \quad & T_C - T_C^S = 0 \\ & A_{\max,i} - A_i \geq 0 \end{aligned} \tag{3.8}$$

For the ammonia case study, solving 3.7 with $\Delta T_{min} = 5\,^{\circ}\text{C}$ gives the data for "No sub-cooling" in Table 3.3. Setting the resulting areas as A_{max}, and solving the optimization problem 3.8 results in A=A_{max} and the data for "Optimal sub-cooling" in Table 3.3. We see that specifying ΔT_{min} gives no sub-cooling, whereas fixing the heat exchanger areas to the same value gives $4.66\,^{\circ}\text{C}$ of sub-cooling.

3.5 Discussion

3.5.1 Super-heating by internal heat exchange

For the simple cycle in Figure 3.1, some sub-cooling in the condenser was found to be optimal, and we here discuss whether other means of obtaining further sub-cooling, in particular the use of internal heat exchange (Figure 3.12), may be beneficial.

Consider first the case when the vapour leaving the evaporator is saturated. In this case the internal heat exchange in Figure 3.12 has no effect on the overall process, at least for pure fluids. This can be understood because there is no effect on the pressure-enthalpy diagram.

Next, consider the case where the vapour is super-heated, which was previously, without internal heat exchange, found to be non-optimal. Depending on the properties of the fluid, this design may be desirable in some cases, even for pure refrigerants (Radermacher, 1989). In the ammonia case study presented above it is not optimal with internal heat exchange, but for a trans-critical CO_2 cycle, internal heat exchange with super-heating is optimal (Neksaa et al., 1998).

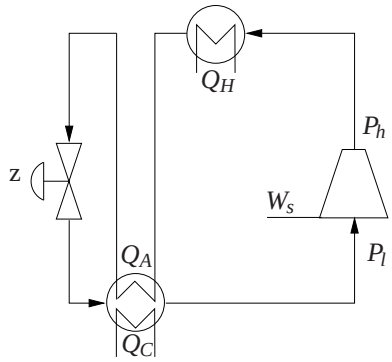

Figure 3.12: Internal heat exchange

3.5.2 Selection of controlled variable

Without internal heat exchange, we have found that it is generally optimal to have no super-heating ($\Delta T_{sup} = 0\,^{\circ}\mathrm{C}$) and some sub-cooling ($\Delta T_{sub} > 0\,^{\circ}\mathrm{C}$). In practice, no super-heating is easily obtained by use of a design with a low pressure tank as shown in Figure 3.4(a) and Figure 3.5. It is less clear how to get the right sub-cooling. In Figure 3.5 we show a strategy where a valve is used to control the degree of sub-cooling ΔT_{sub}. However, the optimal value of ΔT_{sub} will vary during operation, and also ΔT_{sub} may be difficult to measure and control, so it is not clear that this strategy is good. More generally, we could envisage an on-line optimization scheme where one continuously optimizes the operation (maximizes COP) by adjusting the valves. However, such schemes are quite complex and sensitive to uncertainty, so in practice one uses simpler schemes, like the one in Figure 3.5, where the valve controls some other variable. Such variables could be:

- Choke valve position setpoint z_s (that is, the valve is left in a constant position)
- High pressure (P_h)
- Low pressure (P_l)
- Temperature out of condenser (T_2)
- Degree of sub-cooling ($\Delta T_{sub} = T_2 - T_{sat}(P_h)$)
- Temperature out of evaporator (T_4)
- Degree of super-heating ($\Delta T_{sup} = T_4 - T_{sat}(P_l)$)
- Liquid level in storage tank (to adjust charge to rest of system)

- Pressure drop across the extra valve if the design in Figure 3.5(b) is used

The objective is to achieve "self-optimizing" control where a constant setpoint for the selected variable indirectly leads to near-optimal operation (Skogestad, 2000). The selection of "self-optimizing" controlled variables for simple refrigeration cycles is the main topic in Part II (Jensen and Skogestad, 2007).

3.6 Conclusion

The "active charge" in a closed cycle has a steady state effect. This is unlike open systems, where we have boundary conditions on pressure. To adjust the degree of freedom related to the "active charge" one needs a liquid tank (receiver) in the cycle. The key to make efficient use of this degree of freedom is to allow for sub-cooling in the condenser. Conventional wisdom says that one should avoid sub-cooling in the condenser to maximize the efficiency. However, we find that some sub-cooling is desirable. For the ammonia case study we get savings in the order of 2%, by using the design in Figure 3.5 that allows for sub-cooling. The savings would be even larger if we compared with the common design in Figure 3.6(a) which in addition to having no sub-cooling, also gives super-heating.

Nevertheless, the savings in themselves are not very large. More importantly, the results show that the active charge is a degree of freedom, and that the sub-cooling gives some decoupling between the high pressure P_h and the hot source temperature T_H. This is similar to that found for other cycles, including mixed (multi component) fluids and trans-critical CO_2.

Frictional pressure drops in the equipment have been neglected, but their inclusion would further favor sub-cooling which has a smaller mass flow.

Bibliography

Dossat, R. J. (2002), *Principles of refrigeration*, Prentice Hall.

Jensen, J. B. and Skogestad, S. (2005), Control and optimal operation of simple heat pump cycles, *in* 'European Symposium on Computer Aided Process Engineering (ESCAPE) 15, Barcelona'.

Jensen, J. B. and Skogestad, S. (2007), 'Optimal operation of a simple refrigeration cycles. Part II: Selection of controlled variables', *Comput. Chem Eng.* **31**, 1590–1601.

Kim, M., Pettersen, J. and Bullard, C. (2004), 'Fundamental process and system design issues in CO2 vapor compression systems', *Progress in energy and combustion science* **30**, 119–174.

Langley, B. C. (2002), *Heat pump technology*, Prentice Hall.

Larsen, L., Thybo, C., Stoustrup, J. and Rasmussen, H. (2003), Control methods utilizing energy optimizing schemes in refrigeration systems, *in* 'European Control Conference (ECC), Cambridge, U.K.'.

Nagengast, B. (1976), 'The revolution in small vapor compression refrigeration', *American Society of Heating, Refrigerating and Air-Conditioning Engineers (ASHRAE)* **18**(7), 36–40.

Neeraas, B. O., Brendeng, E., Wallentinsen, A. and Mangersnes, M. (2001), A new concept for small-scale LNG production, *in* 'AIChE Spring National Meeting'.

Neksaa, P., Rekstad, H., Zakeri, G. R. and Schiefloe, P. A. (1998), 'CO_2-heat pump water heater: characteristics, system design and experimental results', *Int. J. Refrigeration* **21**, 172–179.

Radermacher, R. (1989), 'Thermodynamic and heat-transfer implications of working fluid mixtures in Rankine cycles', *Int. J. Heat Fluid Flow* **10**(2), 90–102.

Skogestad, S. (2000), 'Plantwide control: the search for the self-optimizing control structure', *J. Process Contr.* **10**(5), 487–507.

Stoecker, W. F. (1998), *Industrial refrigeration handbook*, McGraw-Hill.

Svensson, M. C. (1994), Studies on on-line optimizing control, with application to a heat pump, PhD thesis, Norwegian University of Science and Technology, Trondheim.

Chapter 4

Optimal operation of simple refrigeration cycles Part II: Selection of controlled variables

Published in Computers & Chemical Engineering (2007), 31, pages 1590-1601

The paper focuses on operation of simple refrigeration cycles and considers the selection of controlled variables for two different cycles. One is a conventional sub-critical ammonia refrigeration cycle and the other is a trans-critical CO_2 refrigeration cycle. There is no fundamental difference between the two cycles in terms of degrees of freedom and operation. However, in practical operation there are differences. For the ammonia cycle, there are several simple control structures that give self-optimizing control, that is, which achieve in practice close-to-optimal operation with a constant setpoint policy. For the CO_2 cycle on the other hand, a combination of measurements is necessary to achieve self-optimizing control.

4.1 Introduction

Refrigeration and heat pump cycles are used both in homes, cars and in industry. The load and complexity varies, from small simple cycles, like a refrigerator or air-conditioner, to large complex industrial cycles, like the ones used in liquefaction of natural gas.

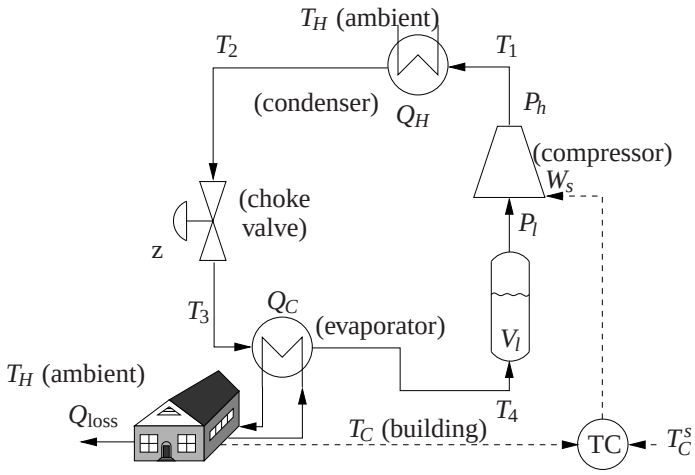

Figure 4.1: Simple refrigeration cycle studied in this paper (shown for the ammonia case)

The simple refrigeration process illustrated in Figure 4.1 is studied in this paper. In Part I (Jensen and Skogestad, 2007*b*) we showed that the cycle has five steady-state degrees of freedom; the compressor power, the heat transfer in the condenser, the heat transfer in the evaporator, the choke valve opening and the "active charge". Different designs for affecting the active charge, including the location of the liquid storage, were discussed in Part I.

It was found in Part I that there are normally three optimally active constraints; maximum heat transfer in condenser, maximum heat transfer in evaporator and minimum (zero) super-heating. The cycle in Figure 4.1 obtains the latter by having a liquid receiver before the compressor which gives saturated vapour entering the compressor. In addition, we assume that the load (e.g. cooling duty) is specified. There is then one remaining unconstrained steady-state degree of freedom, related to the outlet temperature of the condenser, which should be used to optimize the operation. The main theme of the paper is to select a "self-optimizing" controlled variable for this degree of freedom such that a constant setpoint policy (indirectly) achieves near-optimal operation.

We consider two systems:

- a conventional sub-critical ammonia cycle for cold storage ($T_C = -10\,^\circ$C)
- a trans-critical CO_2 cycle for cooling a home ($T_C = 20\,^\circ$C)

The CO_2 cycle is included since it always has an unconstrained degree of freedom that must be used for control. This is because there is no saturation condition on the

high pressure side, which is usually said to introduce one extra degree of freedom to the cycle (Kim et al., 2004). However, as shown in Part I (Jensen and Skogestad, 2007*b*), this "extra" degree of freedom is also available in a conventional sub-critical cycle if we allow for sub-cooling in the condenser. The sub-cooling will to some extent decouple the outlet temperature and the saturation pressure in the condenser. More importantly, some sub-cooling is actually positive in terms of thermodynamic efficiency (Jensen and Skogestad, 2007*b*). The ammonia cycle is included to show that there are no fundamental differences between a sub-critical and a trans-critical cycle. There is some confusion in the literature on this.

Although there is a vast literature on the thermodynamic analysis of closed refrigeration cycles, there are few authors who discuss the operation and control of such cycles. Some discussions are found in text books such as Stoecker (1998), Langley (2002) and Dossat (2002), but these mainly deal with more practical aspects. Svensson (1994) and Larsen et al. (2003) discuss operational aspects. A more comprehensive recent study is that of Kim et al. (2004) who consider the operation of trans-critical CO_2 cycles.

This paper considers steady-state operation and the objective is to find which controlled variables to fix. The compressor power is used as the objective function (cost $J = W_s$) for evaluating optimal operation.

4.2 Selection of controlled variable

We consider here the simple cycle in Figure 4.1 where the liquid receiver on the low pressure side ensures that the vapour entering the compressor is saturated. Note that there is no liquid receiver after the condenser, and thus no assumption of having saturated liquid at the condenser outlet. Furthermore, it is assumed that the heat transfer in both the condenser and evaporator are maximized. Finally, a temperature controller on the stream to be cooled (here the building temperature T_C) is used to adjust the compressor power.

There then remains one unconstrained degree of freedom (choke valve position z) which should be used to optimize the operation for all disturbances and operating points. We could envisage an real-time dynamic optimization scheme where one continuously optimizes the operation (minimize compressor power) by adjusting z. However, such schemes may be quite complex and sensitive to uncertainty. These problems can be reduced by selecting a good control variable, and ideally one get a simple constant setpoint scheme, with no need for real-time optimization. What should be controlled (and fixed, at least on the short time scale)? Some candidates

are:

- Valve position z (i.e., an open-loop policy where the valve is left in a constant position)
- High pressure (P_h)
- Low pressure (P_l)
- Temperature out of compressor (T_1)
- Temperature before valve (T_2)
- Degree of sub-cooling in the condenser* ($\Delta T_{\text{sub}} = T_2 - T_{sat}(P_h)$)
- Temperature approach in hot source heat exchanger ($T_2 - T_H$)
- Temperature out of evaporator (T_4)
- Degree of super-heating in the evaporator† ($\Delta T_{\text{sup}} = T_4 - T_{sat}(P_l)$)
- Liquid level in the receiver (V_l) to adjust the active charge in the rest of the system
- Liquid level in the condenser ($V_{l,con}$) or in the evaporator ($V_{l,vap}$)
- Pressure drop across the "extra" valve in Figure 4.11†

The objective is to achieve "self-optimizing" control where a constant setpoint for the selected variable indirectly leads to near-optimal operation (Skogestad, 2000). Note that the selection of a good controlled variable is equally important in an "advanced" control scheme like MPC which also is based on keeping the controlled variables close to given setpoints.

The selection of controlled variables is a challenging task, especially if one considers in detail all possible measurements, so we will first use a simple screening process based on a linear model.

4.2.1 Linear analysis

To find promising controlled variables, the "maximum gain" rule (Halvorsen et al., 2003) will be used. For the scalar case considered in this paper the rule is:
Prefer controlled variables with a large scaled gain $|G'|$ from the input (degree of

*Not relevant in the CO_2 cycle because of super-critical high pressure
†Not relevant for our design (Figure 4.1)

freedom) to the output (controlled variable)
Procedure scalar case:

1. Make a small perturbation in each disturbances d_i and re-optimize the operation to find the optimal disturbance sensitivity $\partial \Delta y_{\text{opt}}/\partial d_i$. Let Δd_i denote the expected magnitude of each disturbance and compute from this the overall optimal variation (here we choose the 2-norm):
   $\Delta y_{\text{opt}} = \sqrt{\sum_i \left(\frac{\partial \Delta y_{\text{opt}}}{\partial d_i} \cdot \Delta d_i\right)^2}$
2. Identify the expected implementation error n for each candidate controlled variable y (measurement).
3. Make a perturbation in the independent variables u (in our case u is the choke valve position z) to find the (unscaled) gain, $G = \Delta y/\Delta u$.
4. Scale the gain with the optimal span (span $y \equiv \Delta y_{\text{opt}} + n$), to obtain for each candidate output variable y, the scaled gain:
   $|G'| = \frac{|G|}{\text{span } y}$

The worst-case loss $L = J(u,d) - J_{\text{opt}}(u,d)$ (the difference between the cost with a constant setpoint and re-optimized operation) is then for the scalar case (Skogestad and Postlethwaite, 2005, page 394):

$$L = \frac{|J_{uu}|}{2} \frac{1}{|G'|^2} \tag{4.1}$$

where $J_{uu} = \partial^2 J/\partial u^2$ is the Hessian of the cost function J. In our case $J = W_s$ (compressor work). Note that J_{uu} is the same for all candidate controlled variables y.

The most promising controlled variables should then be tested on the non-linear model using realistic disturbances to check for non-linear effects, including feasibility problems.

4.2.2 Combination of measurements

If the losses with a fixed single measurement are large, as for the CO_2 case study, then one may consider combinations of measurements as controlled variables. The simple null space method (Alstad and Skogestad, 2007) gives a linear combination with zero local loss for the considered disturbances,

$$c = h_1 \cdot y_1 + h_2 \cdot y_2 + \ldots \tag{4.2}$$

The minimum number of measurements y to be included in the combination is $n_y = n_u + n_d$. In our case $n_u = 1$ and if we want to consider combinations of $n_y = 2$ measurements then only $n_d = 1$ disturbance can be accounted exactly for. With the "exact local method" (Halvorsen et al., 2003) or the "extended null space method" (Alstad and Skogestad, 2007) it is possible to consider additional disturbances. The local loss is then not zero, and we will minimize the 2-norm of the effect of disturbances on the loss.

4.3 Ammonia case study

The cycle operates between air inside a building ($T_C = T_{\text{room}} = -10\,^\circ\text{C}$) and ambient air ($T_H = T_{\text{amb}} = 20\,^\circ\text{C}$). This could be used in a cold storage building as illustrated in Figure 4.1. The heat loss from the building is

$$Q_{\text{loss}} = UA_{\text{loss}}(T_H - T_C) \tag{4.3}$$

The nominal heat loss is 15 kW. The temperature controller shown in Figure 4.1 maintains $T_C = -10\,^\circ\text{C}$ and will indirectly give $Q_C = Q_{\text{loss}}$ at steady-state.

4.3.1 Modelling

The structure of the model equations are given in Table 4.1 and the data are given in Table 4.2. The heat exchangers are modelled assuming "cross flow" with constant temperature on the air side ($T_H = 20\,^\circ\text{C}$ and $T_C = -10\,^\circ\text{C}$). The isentropic efficiency for the compressor is assumed constant. The SRK equation of state is used for the thermodynamic calculations. The gPROMS model is available on the internet (Jensen and Skogestad, 2007*a*).

Table 4.1: Structure of model equations

Heat exchangers (condenser and evaporator)
$Q = U \cdot \int \Delta T \, \mathrm{d}A = \dot{m} \cdot (h_{out} - h_{in})$
$P = P_{sat}(T_{sat})$
$m = \rho / V$
Valve
$\dot{m} = z \cdot C_V \sqrt{\Delta P \cdot \rho} \qquad h_{out} = h_{in}$
Compressor
$W_s = \dot{m}\,(h_{out} - h_{in}) = \dot{m} \cdot (h_s - h_{in}) / \eta$

Table 4.2: Data for the ammonia case study

$T_H = 20\,^{\circ}\mathrm{C}$
$T_C = T_C^s = -10\,^{\circ}\mathrm{C}$
Condenser: $(UA)_C = 2500\,\mathrm{W\,K^{-1}}$
Evaporator: $(UA)_E = 3000\,\mathrm{W\,K^{-1}}$
Compressor: isentropic efficiency $\eta = 0.95$
Choke valve: $C_V = 0.0017\,\mathrm{m}^2$
Building: $UA_{\mathrm{loss}} = 500\,\mathrm{W\,K^{-1}}$

4.3.2 Optimal steady-state operation

At nominal conditions the compressor power was minimized with respect to the degree of freedom (z). The optimal results are given in Table 4.3, and the corresponding pressure enthalpy diagram and temperature profile in the condenser are shown in Figure 4.2. Note that the optimal sub-cooling out of the condenser is 5.8 °C. This saves about 2.0 % in compressor power (W_s) compared to the conventional design with saturation.

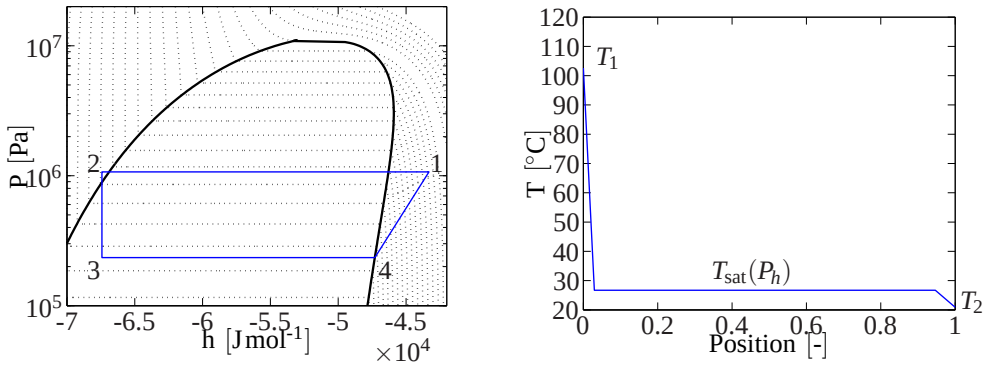

(a) Pressure enthalpy diagram

(b) Temperature profile in condenser

Figure 4.2: Optimal operation for the ammonia case study

4.3.3 Selection of controlled variables

There is one unconstrained degree of freedom (choke valve opening z) which should be adjusted to give optimal sub-cooling in the condenser. We want to find a good controlled variable (see Section 4.2 for candidates) to fix such that

Table 4.3: Optimal steady-state for ammonia case study

$W_s\,[\mathrm{kW}]$	2.975
$z\,[\text{-}]$	0.372
$P_h\,[\mathrm{bar}]$	10.70
$P_l\,[\mathrm{bar}]$	2.35
$Q_H\,[\mathrm{kW}]$	17.96
$\dot{m}\,[\mathrm{kg\,s^{-1}}]$	0.0127
$\Delta T_{\mathrm{sub}} = T_2 - T_{\mathrm{sat}}(P_h)\,[^\circ\mathrm{C}]$	5.80
$T_1\,[^\circ\mathrm{C}]$	102.6
$T_2\,[^\circ\mathrm{C}]$	20.9
$T_3\,[^\circ\mathrm{C}]$	-15.0
$T_4\,[^\circ\mathrm{C}]$	-15.0

we achieve close-to-optimal operation in spite of disturbances and implementation error ("self-optimizing control").

Linear analysis of alternative controlled variables

The following disturbance perturbations are used to calculate the optimal variation in the measurements y^*.

d_1: $\Delta T_H = \pm 10\,^\circ\mathrm{C}$

d_2: $\Delta T_C^s = \pm 5\,^\circ\mathrm{C}$

d_3: $\Delta UA_{\mathrm{loss}} = \pm 100\,\mathrm{W\,K^{-1}}$

The assumed implementation error (n) for each variable is given in Table 4.4 which also summarizes the linear analysis and gives the resulting scaled gains in order from low gain (poor) to high gain (promising).

Some notes about Table 4.4:

- P_l and T_4 have zero gains and cannot be controlled. The reason for the zero gains are that they both are indirectly determined by Q_{loss}.

$$Q_{\mathrm{loss}} = Q_C = (UA)_C\,(T_4 - T_C) \quad \text{and} \quad P_l = P_{sat}(T_4) \tag{4.4}$$

*In order to remain in the linear region, the optimal variations were computed for a disturbance of magnitude $1/100$ of this, and the resulting optimal variations were then multiplied by 100 to get $\Delta y_{\mathrm{opt}}(d_i)$

Table 4.4: Linear "maximum gain" analysis of candidate controlled variables y for ammonia case study

			$\lvert\Delta y_{\text{opt}}(d_i)\rvert$						
Variable (y)	Nom.	G	d_1 (T_H)	d_2 (T_C)	d_3 (UA_{loss})	$\lvert\Delta y_{\text{opt}}\rvert$	n	span y	$\lvert G'\rvert$
P_l [bar]	2.35	0.00	0.169	0.591	0.101	0.623	0.300	0.923	0.00
T_4 [°C]	-15.0	0.00	0.017	0.058	0.010	0.061	1.00	1.06	0.00
ΔT_{sup} [°C]	0.00	0.00	0.00	0.00	0.00	0.00	1.00	1.00	0.00
T_1 [°C]	102.6	-143.74	38	17.3	6.2	42.2	1.00	43.2	3.33
P_h [bar]	10.71	-17.39	4.12	0.41	0.460	4.17	1.00	5.17	3.37
z [-]	0.372	1	0.0517	0.0429	0.0632	0.092	0.05	0.142	7.03
T_2 [°C]	20.9	287.95	10.4	0.20	0.300	10.4	1.00	11.4	25.3
V_l [m^3]	1.00	5.1455	9e-03	0.011	1.2e-03	0.0143	0.05	0.064	80.1
ΔT_{sub} [°C]	5.80	-340.78	2.13	1.08	1.08	2.62	1.50	4.12	82.8
$V_{l,con}$ [m^3]	0.67	-5.7	5.8e-03	2.4e-03	1.4e-03	0.0064	0.05	0.056	101.0
$T_2 - T_H$ [°C]	0.89	-287.95	0.375	0.174	0.333	0.531	1.50	2.03	141.8

- The degree of super-heating ΔT_{sup} can obviously not be controlled in our case because it is fixed at $0\,^{\circ}$C (by design of the cycle).
- The loss is proportional to the inverse of squared scaled gain (see Equation 4.1). This implies, for example, that a constant condenser pressure (P_h), which has a scaled gain of 3.37, would result in a loss in compressor power $J = W_s$ that is $(82.8/3.37)^2 = 603$ times larger than a constant sub-cooling (ΔT_{sub}), which has a scaled gain of 82.8.
- The simple policies with a constant pressure (P_h) or constant valve position (z) are not promising with scaled gains of 3.37 and 7.03, respectively.
- A constant level in the liquid receiver (V_l) is a good choice with a scaled gain of 80.1. However, according to the linear analysis, the liquid level in the condenser ($V_{l,con}$) is even better with a scaled gain of 101.0.
- Controlling the degree of sub-cooling in the condenser ($\Delta T_{\text{sub}} = T_2 - T_{\text{sat}}(P_h)$) is also promising with a scaled gain of 82.8, but the most promising is the temperature approach at the condenser outlet ($T_2 - T_H$) with a scaled gain of 141.8.
- The ratio between the implementation error n and the optimal variation Δy_{opt} tells whether the implementation error or the effect of the disturbance is most important for a given control policy. For the most promising policies, we see from Table 4.4 that the contribution from the implementation error is most important.

Nonlinear analysis

The nonlinear model was subjected to the "full" disturbances to test more rigorously the effect of fixing alternative controlled variables. The main reason for

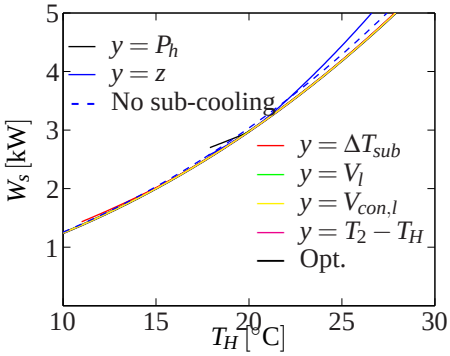

(a) Disturbance in T_H (d_1)

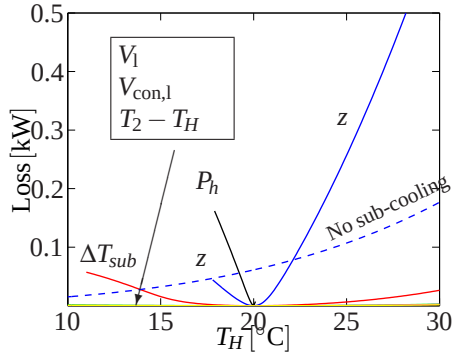

(b) Disturbance in T_H (d_1)

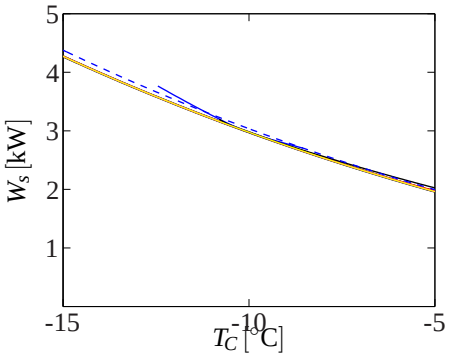

(c) Disturbance in T_C (d_2)

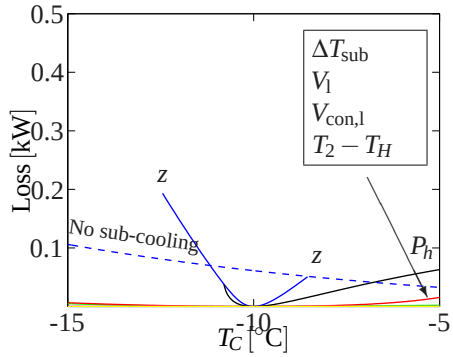

(d) Disturbance in T_C (d_2)

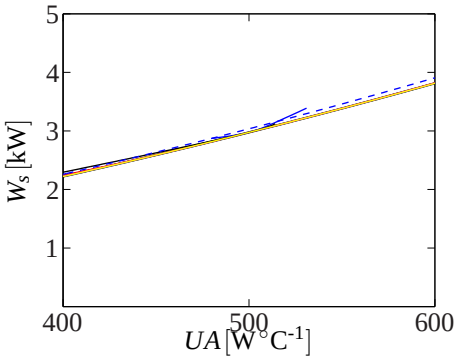

(e) Disturbance in UA_{loss} (d_3)

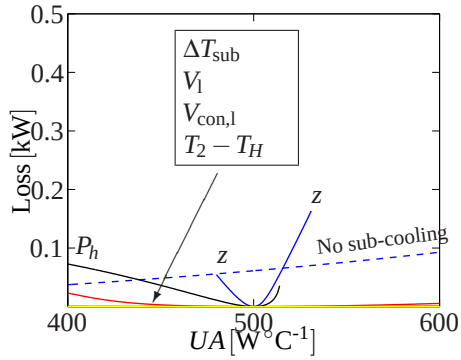

(f) Disturbance in UA_{loss} (d_3)

Figure 4.3: Ammonia case: Compressor power (left) and loss (right) for different disturbances and controlled variables. A line that ends corresponds to infeasible operation.

considering the full disturbances is to check for non-linear effects, in particular possible infeasible operation, which cannot be detected from the linear analysis. Figure 4.3 shows the compressor power W_s (left) and loss $L = W_s - W_{s,\text{opt}}$ (right) for disturbances in T_H (d_1), T_C (d_2) and UA_{loss} (d_3). $W_{s,\text{opt}}$ is obtained by re-optimizing the operation for the given disturbances. As predicted from the linear analysis, control of P_h or z should be avoided as it results in a large loss and even infeasibility (a line that ends corresponds to infeasible operation). Controlling the degree of sub-cooling ΔT_{sub} gives small losses for most disturbances, but gives infeasible operation when T_H is low. Controlling the liquid level, either in the receiver or in the condenser, gives small losses in all cases. Another good policy is to maintain a constant temperature approach out of the condenser ($T_2 - T_H$). This control policy was also the best in the linear analysis and has as far as we know not been suggested in the literature for ammonia cycles.

A common design for refrigeration cycles, also discussed in Part I, is to have no sub-cooling in the condenser. In practice, this might be realized with the design in Figure 4.1 by adding a liquid receiver after the condenser and using the choke valve to control this liquid level, or using the design in Figure 4.11 with the "extra" valve between the condenser and tank removed. The performance of this design ("no sub-cooling") is shown with the dashed line in Figure 4.3. The loss (right graphs) for this design is always nonzero, as it even at the nominal point has a loss of 0.06 kW, and the loss increases with the cooling duty of the cycle. Nevertheless, we note that the loss with this design is low (less than about 0.2 kW or 3.5 %) for all considered disturbances. This may be acceptable, although it is much higher than the best controlled variables (V_{l}, $V_{\text{con,l}}$ and $T_2 - T_H$) where the maximum losses are less than 0.005 kW.

Figure 4.4 shows the sensitivity to implementation error for the four best controlled variables. Controlling a temperature difference at the condenser exit (either $T_2 - T_H$ or ΔT_{sub}) has a small sensitivity to implementation error. On the other hand, controlling either of the two liquid levels (V_l or $V_{l,con}$) might lead to infeasible operation for relatively small implementation errors. In both cases the infeasibility is caused by vapour at the condenser exit. In practice, this vapour "blow out" may be "feasible", but certainly not desirable.

A third important issue is the sensitivity to the total charge of the system which is relevant for the case where we control the liquid level in the receiver ($y = V_l$). There is probably some uncertainty in the initial charge of the system, and maybe more importantly there might be a small leak that will reduce the total charge over time. Optimally the total charge has no steady-state effect (it will only affect the liquid level in the receiver). However, controlling the liquid level in the receiver ($y = V_{\text{l}}$) will make the operation depend on the total charge, and we have lost one

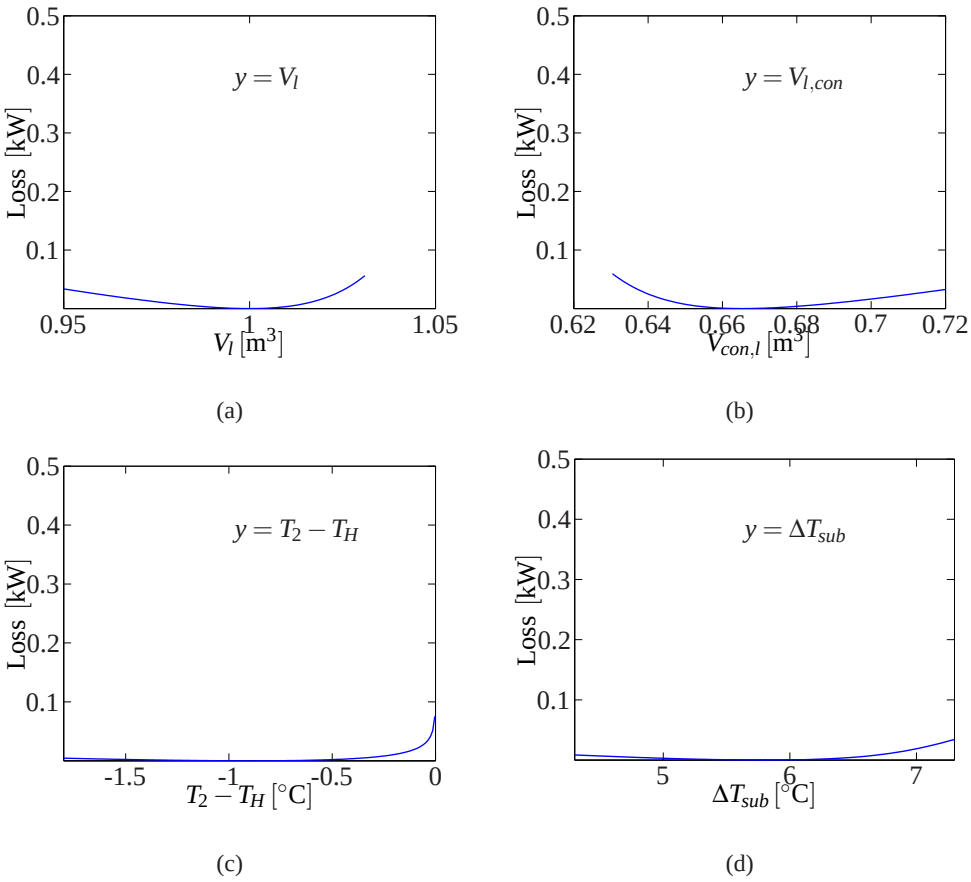

Figure 4.4: Ammonia case: Loss as function of implementation error

of the positive effects of having the liquid receiver. The other control structures will not be affected by varying total charge.

Conclusion ammonia case study

For the ammonia case, controlling the temperature approach at the condenser exit ($T_2 - T_H$) seems to be the best choice as the losses caused by implementation error (Figure 4.4) and disturbances (Figure 4.3) are very small. This control implementation is shown in Figure 4.5 where we also have introduced an inner "stabilizing" loop for pressure. However, the *setpoint* for the pressure is used as a degree of freedom so this loop does not affect the results of this study, which are based on steady-state. Although not optimal even nominally, another acceptable policy is

to use the conventional design with no sub-cooling (Figure 4.11 with the "extra valve" removed and minimum super-heating).

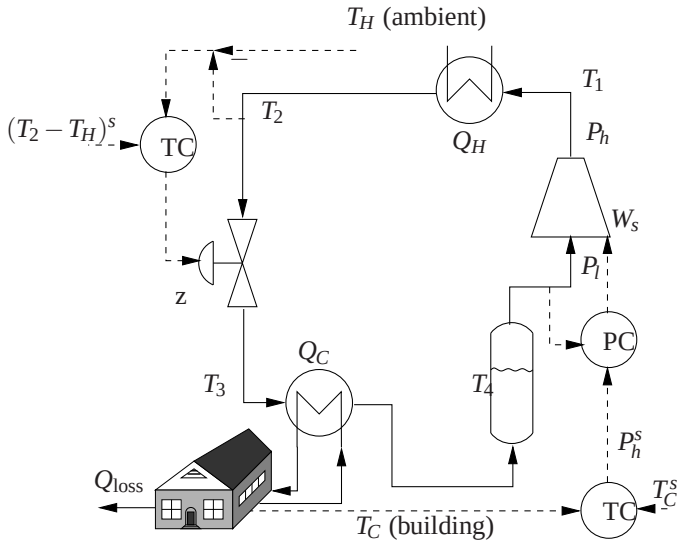

Figure 4.5: Proposed control structure for the ammonia cycle

4.4 CO_2 case study

Neksaa (2002) shows that CO_2 cycles are attractive for several applications, both from an efficiency point of view and from an environmental perspective. Skaugen (2002) gives a detailed analysis of the parameters that affect the performance of a CO_2 cycle and discusses pressure control in these systems.

The simple cycle studied in this paper, see Figure 4.6(a), operates between air inside a room ($T_C = 20\,^\circ$C) and ambient air ($T_H = 30\,^\circ$C). This could be an air-conditioner for a home as illustrated in Figure 4.6(a). The heat loss out of the building is given by Equation 4.3, and the temperature controller shown in Figure 4.6(a) indirectly gives $Q_C = Q_{\text{loss}}$. The nominal heat loss is 4.0 kW.

We consider a cycle with an internal heat exchanger, see Figure 4.6(a). This heat exchanger gives further cooling before the choke valve by super-heating the saturated vapour from the evaporator outlet. This has the advantage of reducing the expansion loss through the valve, although super-heating increases the compressor power. For the CO_2 cycle it has been found that the internal heat exchanger improves efficiency for some operating points (Domanski et al., 1994). For the

CO_2 cycle, we find that the internal heat exchanger gives a nominal reduction of 9.9% in W_s. For the ammonia cycle, the effect of internal heat exchange to give super-heating is always negative in terms of efficiency.

4.4.1 Modelling

Table 4.1 shows the structure of the model equations and the data are given in Table 4.5. Constant air temperature is assumed in the evaporator (T_C). The gas cooler and internal heat exchanger are modelled as counter-current heat exchangers with 6 control volumes each. The Span-Wagner equation of state (1996) is used for the thermodynamic calculations. The MATLAB model is available on the internet (Jensen and Skogestad, 2007*a*).

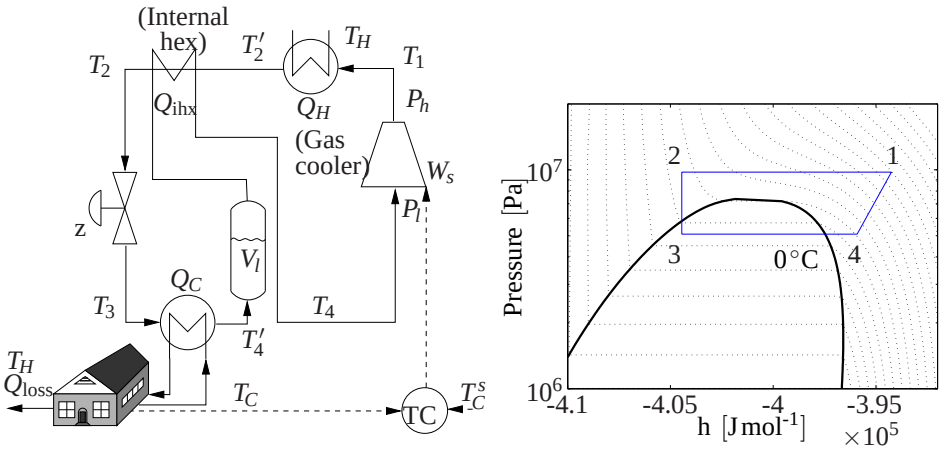

(a) The CO_2 cycle (b) Pressure enthalpy diagram

Figure 4.6: The CO_2 cycle operates trans-critical and is designed with an internal heat exchanger

4.4.2 Optimal operation

Some key parameters for optimal operation of the CO_2 cycle are summarized in Table 4.6 and the pressure enthalpy diagram is given in Figure 4.6(b). Figure 4.7 shows the optimal temperature profiles in the gas cooler and in the internal heat exchanger.

Table 4.5: Conditions for the CO_2 case study

Evaporator: $(UA)_{\text{vap}} = 798\,\text{W}^\circ\text{C}^{-1}$
Gas cooler: $(UA)_{\text{gco}} = 795\,\text{W}^\circ\text{C}^{-1}$
Internal heat exchanger: $(UA)_{\text{ihx}} = 153\,\text{W}^\circ\text{C}^{-1}$
Compressor: isentropic efficiency $\eta = 0.75$
Ambient: $T_H = 30\,^\circ\text{C}$
Air flow gas cooler: $\dot{m}c_p = 250\,\text{J}^\circ\text{C}^{-1}\,\text{s}^{-1}$
Room: $T_C = T_C^s = 20\,^\circ\text{C}$
Room: $UA_{\text{loss}} = 400\,\text{W}^\circ\text{C}^{-1}$
Choke valve: $C_V = 1.21 \cdot 10^{-6}\,\text{m}^2$

Table 4.6: Optimal operation for CO_2 case

$W_s\,[\text{W}]$	958
$z\,[\text{-}]$	0.34
$P_h\,[\text{bar}]$	97.61
$P_l\,[\text{bar}]$	50.83
$Q_H\,[\text{W}]$	-4958
$Q_{\text{ihx}}\,[\text{W}]$	889
$\dot{m}\,[\text{kg}\,\text{s}^{-1}]$	0.025
$T_1\,[^\circ\text{C}]$	89.6
$T_2\,[^\circ\text{C}]$	25.5
$T_3\,[^\circ\text{C}]$	15.0
$T_4\,[^\circ\text{C}]$	31.2

Note that when the ambient air goes below approximately $T_H = 25\,^\circ\text{C}$ the optimal pressure in the gas cooler is sub-critical. We will only consider trans-critical operation, so we assume that the air-conditioner is not used below $25\,^\circ\text{C}$.

4.4.3 Selection of controlled variable

We want to find what the valve should control. In addition to the variables listed in Section 4.2, we also consider internal temperature measurements in the gas cooler and internal heat exchanger. Note that the "no sub-cooling" policy is not possible for the CO_2 cycle because it operates trans-critical.

As discussed in more detail below, there are no obvious single measurements to control for this application. One exception is the holdup m on the high pressure side of the cycle. However, measuring the holdup of a super-critical fluid is not

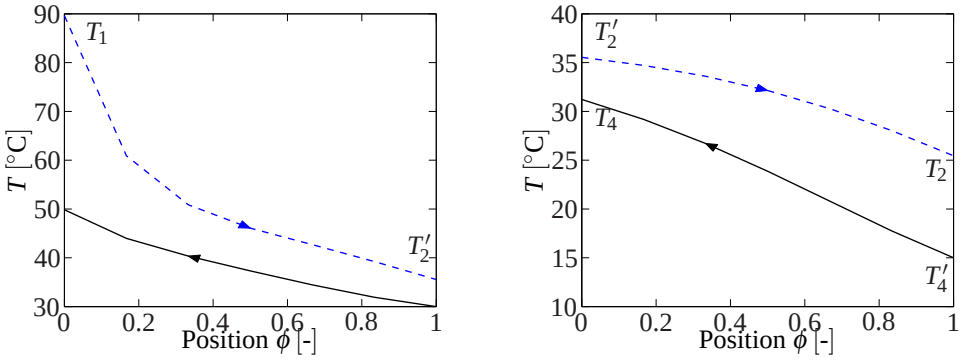

(a) Gas cooler

(b) Internal heat exchanger

Figure 4.7: CO_2 case: Temperature profile in gas cooler and internal heat exchanger

easy (one might use some kind of scale, but this will be to expensive in most applications). Thus, we will consider measurement combinations. First, we will try to combine two measurements, and if this is not acceptable for all disturbances, we may try more measurements. Any two measurements can be combined, and we choose here to combine P_h and T_2. The reason is that P_h is normally controlled anyway for dynamic reasons, and T_2 is simple to measure and is promising from the linear analysis. Also, temperature corrected setpoint for pressure has been proposed before (Kim et al., 2004). We use the "exact local method" (Alstad and Skogestad, 2007) and minimize the 2-norm of $M_d = HFW_d$, where $F = \partial y_{\text{opt}}/\partial d_i$ is the optimal sensitivity of $y' = [P_h \quad T_2]$ with respect to disturbances $d' = [T_H \quad T_C \quad (UA)_{\text{loss}}]$. The magnitude of the disturbances are given in W_d. We find that the linear combination $c = h_1 \cdot P_h + h_2 \cdot T_2$ with $k = h_2/h_1 = -8.53\,\text{bar}^\circ\text{C}^{-1}$ minimizes the 2-norm of the three disturbances on the loss. This can be implemented in practice by controlling the combined pressure and temperature

$$P_{h,combine} = P_h + k \cdot \left(T_2 - T_{2,\text{opt}}\right) \tag{4.5}$$

where $T_{2,\text{opt}} = 25.5\,^\circ\text{C}$ and $k = -8.53\,\text{bar}^\circ\text{C}^{-1}$. An alternative is to use a more physically-based combination. For an ideal gas we have $m = \frac{PV \cdot MW}{RT}$, and since the gas cooler holdup m_{gco} seems to be a good variable to control, we will include P/T in the gas cooler as a candidate controlled variable.

Table 4.7: Linear "maximum gain" analysis of controlled variables for CO_2 case

			$\lvert\Delta y_{\text{opt}}(d_i)\rvert$						
Variable (y)	Nom.	G	d_1 (T_H)	d_2 (T_C)	d_3 (UA_{loss})	$\lvert\Delta y_{\text{opt}}\rvert$	n	span y	$\lvert G'\rvert$
P_h/T_2' [bar °C^{-1}]	0.32	-0.291	0.140	-0.047	0.093	0.174	0.0033	0.177	0.25
P_h [bar]	97.61	-78.85	48.3	-15.5	31.0	59.4	1.0	60.4	1.31
T_2' [°C]	35.5	36.7	16.27	-2.93	7.64	18.21	1	19.2	1.91
$T_2' - T_H$ [°C]	3.62	24	4.10	-1.92	5.00	6.75	1.5	8.25	2.91
z [-]	0.34	1	0.15	-0.04	0.18	0.24	0.05	0.29	3.45
V_l [m^3]	0.07	0.03	-0.02	0.005	-0.03	0.006	0.001	0.007	4.77
T_2 [°C]	25.5	60.14	8.37	0.90	3.18	9.00	1	10.0	6.02
$P_{h,\text{combine}}$ [bar]	97.61	-592.0	-23.1	-23.1	3.91	33.0	9.53	42.5	13.9
m_{gco} [kg]	4.83	-11.18	0.151	-0.136	0.119	0.235	0.44	0.675	16.55

Linear method

We first use the linear "maximum gain" method to find promising controlled variables. The following disturbances* are considered:

d_1: $\Delta T_H = \pm 10\,^\circ\text{C}$

d_2: $\Delta T_C = \pm 5\,^\circ\text{C}$

d_3: ΔUA_{loss} from -100 to $+40\,\text{W}\,^\circ\text{C}^{-1}$

The linear results are summarized in Table 4.7. Some controlled variables (P_l, T_4', ΔT_{sub} and ΔT_{sup}) are not considered because they, as discussed earlier, can not be fixed or are not relevant for this cycle. The ratio P_h/T_2' in the gas cooler is not favourable with a small scaled gain. This is probably, because the fluid in the gas cooler is far from ideal gas so P_h/T_2' is not a good estimate of the holdup m_{gco}. From Table 4.7 the most promising controlled variables are the holdup in the gas cooler (m_{gco}) and the linear combination ($P_{h,\text{combine}}$). Fixing the valve opening z_s (no control) or the liquid level in the receiver (V_l) are also quite good.

Non-linear analysis

Figure 4.8 shows the compressor power (left) and loss (right) for some selected controlled variables. We see that the two most important disturbances are the temperatures T_H and T_C which gives larger losses than disturbance in the heat loss out of the building. Controlling the pressure P_h gives infeasible operation for small

*In order to remain in the linear region, the optimal variations were computed for a disturbance of magnitude $1/100$ of this, and the resulting optimal variations were then multiplied by 100 to get $\Delta y_{\text{opt}}(d_i)$

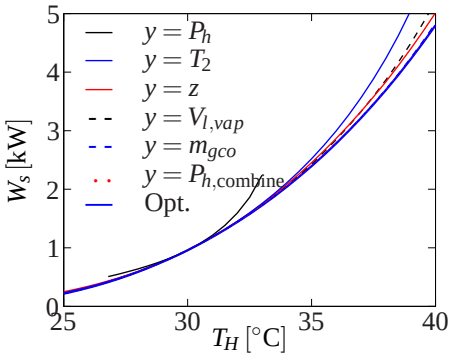

(a) Disturbances in T_H (d_1)

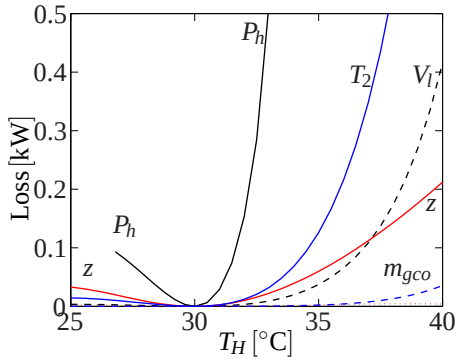

(b) Disturbance in T_H (d_1)

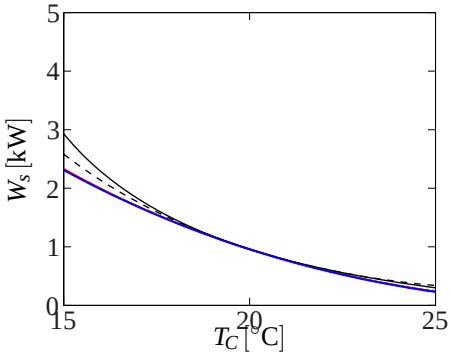

(c) Disturbance in T_C (d_2)

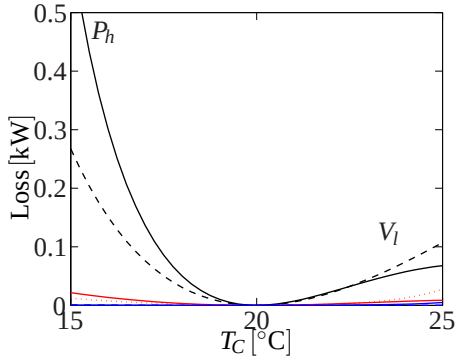

(d) Disturbance in T_C (d_2)

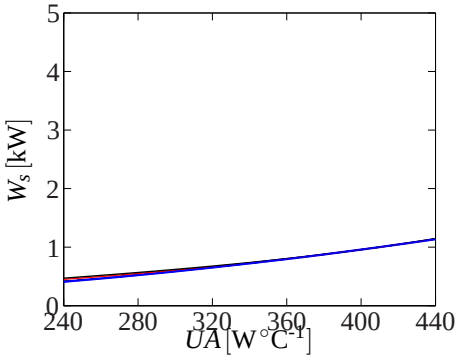

(e) Disturbance in UA_{loss} (d_3)

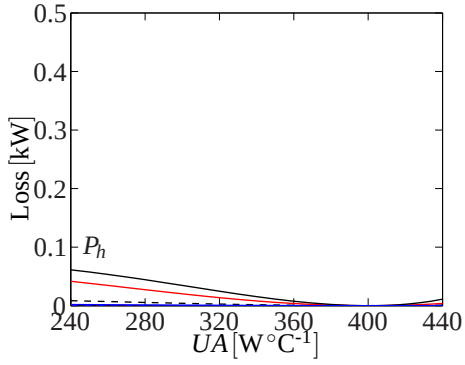

(f) Disturbance in UA_{loss} (d_4)

Figure 4.8: CO_2 case: Compressor power (left) and loss (right) for different disturbances and controlled variables. A line that ends corresponds to infeasible operation.

disturbances in the ambient air temperature (T_H). The nonlinear results confirm the linear gain analysis with small losses for $P_{h,\text{combine}}$ and m_{gco}.

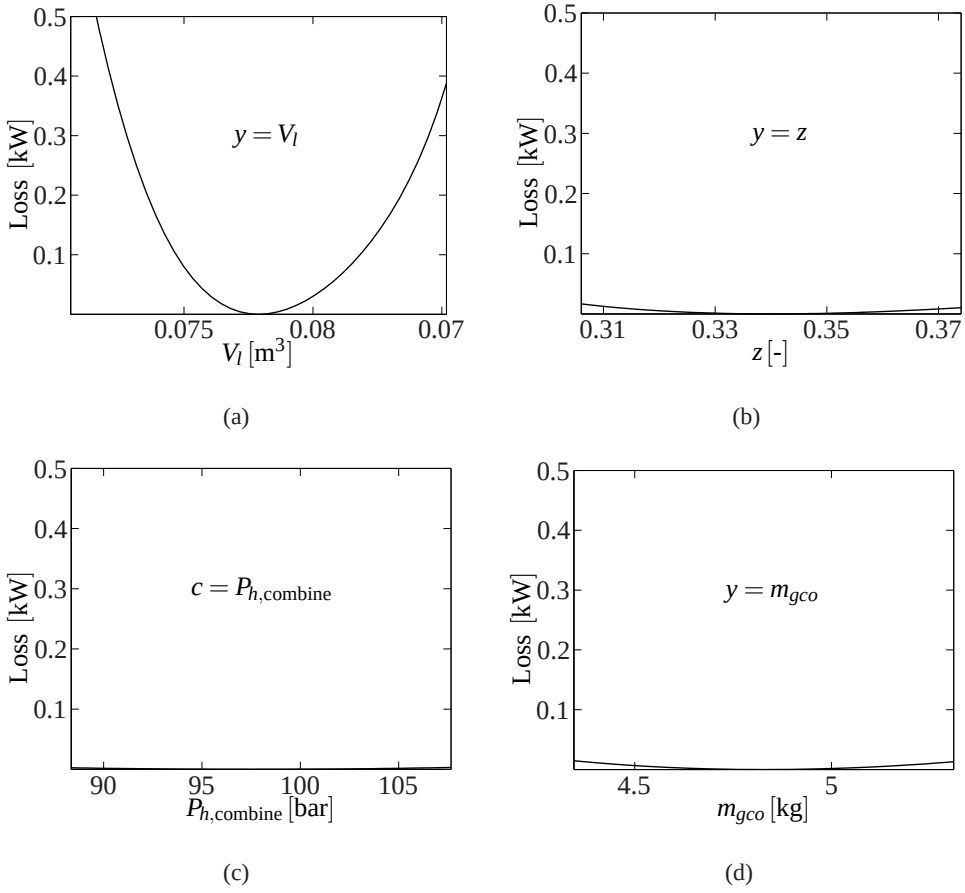

Figure 4.9: CO_2 case: Loss as function of implementation error

Another important issue is the sensitivity to implementation error. From Figure 4.9 we see that the sensitivity to implementation error is very large for $y = V_l$. The three best controlled variables are constant valve opening (z), constant holdup in the gas cooler (m_{gco}) and the linear combination ($P_{h,\text{combine}}$).

Conclusion CO_2 case study

For this CO_2 refrigeration cycle we find that fixing the holdup in the gas cooler m_{gco} gives close to optimal operation. However, since the fluid is super-critical,

holdup is not easily measured. Thus, in practice, the best *single* measurement is a constant valve opening z ("no control"). A better alternative is to use *combinations* of measurements. We obtained the combination $P_{h,\text{combine}} = P_h + k \cdot (T_2 - T_{2,\text{opt}})$ using the "exact local method". This implementation is shown in Figure 4.10. The disturbance loss compared with single measurements is significantly reduced and the sensitivity to implementation error is very small.

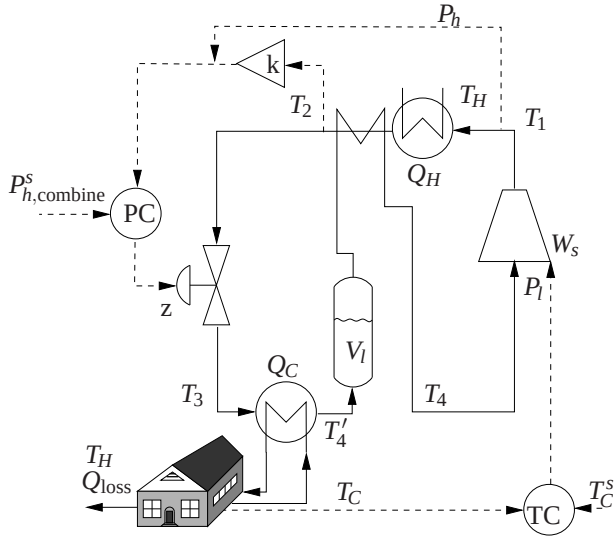

Figure 4.10: Proposed control structure for the CO_2 cycle

4.5 Discussion

4.5.1 Super-heating

An important practical requirement is that the material entering the compressor must be vapour (either saturated or super-heated). Saturation can be achieved by having a liquid receiver before the compressor as shown in Figure 4.1. However, in many designs the receiver is located at the high pressure side and super-heating may be controlled with the choke valve (e.g. thermostatic expansion valve TEV) as shown in Figure 4.11. A minimum degree of super-heating is required to handle disturbances and measurement errors. Since super-heating is not thermodynamically efficient (except for some cases with internal heat exchange), this minimal degree of super-heating becomes an active constraint. With the configuration in Figure 4.11, the "extra" valve is the unconstrained degree of freedom (u) that

should be adjusted to achieve optimal operation. Otherwise the results from the study hold, both for the ammonia and CO_2 cycle.

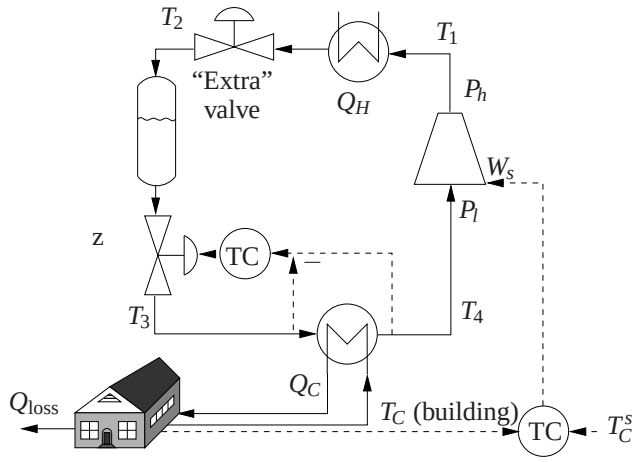

Figure 4.11: Alternative refrigeration cycle with liquid receiver on high pressure side and control of super-heating

4.5.2 Heat transfer coefficients

We have assumed constant heat transfer coefficients in the heat exchangers. Normally, the heat transfer coefficient will depend on several variables such as phase fraction, velocity of the fluid and heat transfer rate. However, a sensitivity analysis (not included) shows that changing the heat transfer coefficients does not affect the conclusions in this paper. For the CO_2 cycle, we did some simulations using a constant air temperature in the gas cooler, which may represent a cross flow heat exchanger and is an indirect way of changing the effective UA value. We found that the losses for a constant liquid level control policy ($y = V_l$) was slightly smaller, but the analysis presented here is still valid and the conclusion that a combination of measurements is necessary to give acceptable performance, remains the same.

4.5.3 Pressure control

This paper has only considered steady-state operation. For dynamic reasons, in order to "stabilize" the operation, a degree of freedom is often used to control one pressure (P_l or P_h). However, the *setpoint* for the pressure may be used as a degree of freedom at steady-state, so this will not change the results of this study. An

example of a practical implementation using cascade control is shown in Figure 4.5 where the temperature difference at the condenser outlet is controlled which was found to be the best policy for the ammonia case study. The load in the cycle is controlled by adjusting the setpoint to the pressure controller that stabilize the low pressure (P_l).

4.6 Conclusion

For a simple cycle, there is one unconstrained degree of freedom that should be used to optimize the operation. For the sub-critical ammonia refrigeration cycle a good policy is to have no sub-cooling. Further savings at about 2% are obtained with some sub-cooling where a good control strategy is to fix the temperature approach at the condenser exit ($T_2 - T_H$), see Figure 4.5. One may argue that 2% savings is very little for all the effort, but larger savings are expected for cases with smaller heat exchanger areas (Jensen and Skogestad, 2007*b*), and allowing for sub-cooling shows that there is no fundamental difference with the CO_2 case.

For the trans-critical CO_2 cycle, the only single "self-optimizing" measurement seems to be the holdup in the super-critical gas cooler (m_{gco}). However, since this holdup is difficult to measure a combination of measurements is needed. We propose to fix a linear combination of pressure and temperature, $P_{h,combine} = P_h + k \cdot (T_2 - T_{2,\text{opt}})$, see Figure 4.10. This is a "self-optimizing" control structure with small losses for expected disturbances and implementation errors.

Acknowledgment

The contributions of Tore Haug-Warberg and Ingrid Kristine Wold on implementing the thermodynamic models are gratefully acknowledged.

Bibliography

Alstad, V. and Skogestad, S. (2007), 'The null space method for selecting optimal measurement combinations as controlled variables', *Ind. Eng. Chem. Res.* .

Domanski, P. A., Didion, D. A. and Doyle, J. P. (1994), 'Evaluation of suction-line/liquid-line heat exchange in the refrigeration cycle,', *Int. J. Refrig.* **17**, 487–493.

Dossat, R. J. (2002), *Principles of refrigeration*, Prentice Hall.

Halvorsen, I. J., Skogestad, S., Morud, J. C. and Alstad, V. (2003), 'Optimal selection of controlled variables', *Ind. Eng. Chem. Res.* **42**, 3273–3284.

Jensen, J. B. and Skogestad, S. (2007*a*). gPROMS and MATLAB model code for ammonia and CO_2 cycles. See additional material for paper at homepage of S. Skogestad.

Jensen, J. B. and Skogestad, S. (2007*b*), 'Optimal operation of simple refrigeration cycles. Part I: Degrees of freedom and optimality of sub-cooling', *Comput. Chem. Eng.* **31**, 712–721.

Kim, M., Pettersen, J. and Bullard, C. (2004), 'Fundamental process and system design issues in CO2 vapor compression systems', *Progress in energy and combustion science* **30**, 119–174.

Langley, B. C. (2002), *Heat pump technology*, Prentice Hall.

Larsen, L., Thybo, C., Stoustrup, J. and Rasmussen, H. (2003), Control methods utilizing energy optimizing schemes in refrigeration systems, *in* 'European Control Conference (ECC), Cambridge, U.K.'.

Neksaa, P. (2002), 'CO_2 heat pump systems', *Int. J. Refrigeration* **25**, 421–427.

Skaugen, G. (2002), Investigation of Transcritical CO_2 Vapour Compression Systems by Simulation and Laboratory Experiments, PhD thesis, Norwegian University of Science and Technology.

Skogestad, S. (2000), 'Plantwide control: the search for the self-optimizing control structure', *J. Process Contr.* **10**(5), 487–507.

Skogestad, S. and Postlethwaite, I. (2005), *Multivariable feedback control*, Second edn, John Wiley & Sons.

Span, R. and Wagner, W. (1996), 'A new equation of state for carbon dioxide covering the fluid region from the triple-point temperature to 1100 K at pressures up to 800 MPa', *J. Phys. Chem. Ref. Data* **25**(6), 1509–1596.

Stoecker, W. F. (1998), *Industrial refrigeration handbook*, McGraw-Hill.

Svensson, M. C. (1994), Studies on on-line optimizing control, with application to a heat pump, PhD thesis, Norwegian University of Science and Technology, Trondheim.

Chapter 5

Problems with specifying $\Delta T_{\mathbf{min}}$ in design of processes with heat exchangers

Accepted for publication in Industrial & Engineering Chemistry Research

We show in this paper that the common method of specifying ΔT_{min} for individual heat exchangers may lead to wrong decisions and should be used with care when designing heat exchanger systems. In particular, design with constraints on ΔT_{min} may result in operation conditions which are not optimal when the resulting areas are installed. In addition, different U-values for the heat exchangers are not easily handled. We propose an alternative method (simplified TAC) to avoid these problems and compare it with the ΔT_{min}-method on three vapour compression (refrigeration) cycle case studies.

5.1 Introduction

In process design one seeks to optimize the future income of the plant. This might be realized by minimizing the total annualized cost (TAC), $J_{\mathrm{TAC}} = J_{\mathrm{operation}} + J_{\mathrm{capital}}$ [\$year^{-1}]; see Problem 5.1 below. However, finding J_{TAC} requires detailed equipment and cost data, which is not available at an early design stage.

An alternative simple and common approach for design of processes with heat exchangers, especially at an early design stage, is to specify the exchanger minimum approach temperature (EMAT $= \Delta T_{\mathrm{min}}$) in each heat exchanger; see Problem 5.2

below. The idea is that this specification should give a reasonable balance between minimizing operating costs $J_{\text{operation}}$ (favored by a small $\Delta T_{\min}$) and minimizing capital costs J_{capital} (favored by a large $\Delta T_{\min}$).

As an example, Figure 5.1 shows a hot stream (T_2) transferring heat to a cold stream with constant temperature (T_1). Stream 2 may be hot exhaust gas which is cooled to recover its energy and this is done by vaporizing water in stream 1. A small value of $\Delta T_{\min}$ means that a lot of the energy is recovered, but it requires a large heat exchanger. On the other hand, a larger value of $\Delta T_{\min}$ requires less area, but the outlet temperature T_2 will be higher and less energy is recovered. There exists many rules of thumb for the value of $\Delta T_{\min}$. For example Turton et al. (1998, page 250) recommends 10 °C for fluids and 5 °C for refrigerants.

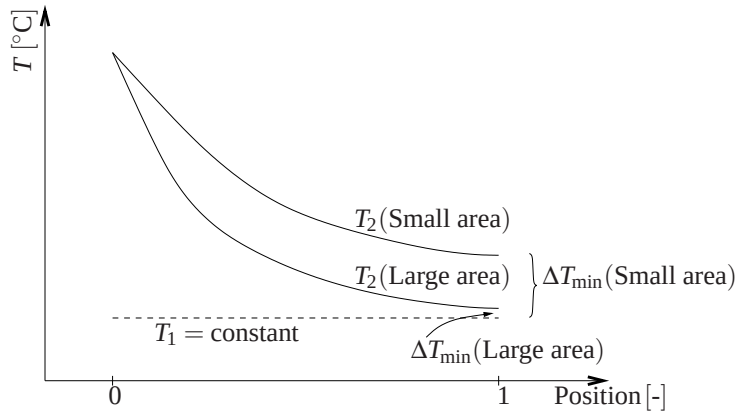

Figure 5.1: The effect of different values for $\Delta T_{\min}$

Note that what we call $\Delta T_{\min}$ in this paper is the individual exchanger minimum approach temperature (EMAT). This should not be confused with the "pinch temperature" (heat recovery approach temperature, HRAT) used in design of heat exchanger networks.

The use of $\Delta T_{\min}$ as a constraint is only used for *design*, as it is reasonably well known that we should never specify $\Delta T_{\min}$ during operation (here the areas should be used as constraints rather than $\Delta T_{\min}$). However, even when it comes to design, specifying $\Delta T_{\min}$ (and maybe varying it in an outer loop), does not always result in a good design, except for simple cases. To understand why specifying $\Delta T_{\min}$ in design may not be correct, consider the following three problems:

Problem 5.1 Detailed optimal design *based on minimizing TAC* [\$year^{-1}] *(e.g. Biegler et al., 1997):*

$$\min_{u_1} \left(J_{operation} + J_{capital} \right) \tag{5.1}$$

subject to model equations and operational constraints (this applies to all problems in this paper). The degrees of freedom, u_1, include all the equipment data (sizes) and operating variables. The annualized capital cost is often obtained as:

$$J_{\text{capital}} = \sum_{i \in \text{Units}} \left(C_{\text{fixed,i}} + C_{\text{variable,i}} \cdot S_i^{n_i} \right) / T \tag{5.2}$$

Here S_i is the characteristic size for the unit (area in m^2 for heat exchangers), and the cost factors ($C_{\text{fixed,i}}$ and $C_{\text{variable,i}}$) and cost scaling factor n_i are constants for each unit (e.g. heat exchangers). T is the capital depreciation time, e.g. $T = 10\,\text{years}$. The operating cost $J_{\text{operation}}$ are given by the prices of feeds, products and utilities (energy) plus other fixed and variable operating costs; e.g. see Equation 5.8 below.

Problem 5.2 Simplified optimal design *with specified* ΔT_{min}*:*

$$\begin{aligned} & \min_{u_2} (J_{operation}) \\ \textit{subject to} \quad & \Delta T_i - \Delta T_{\min} \geq 0 \end{aligned} \tag{5.3}$$

Here, the degrees of freedom, u_2, include the heat transfer in the heat exchanger (Q_i) and the operating variables (flows, works, splits etc.). After solving this problem one can calculate the heat exchanger areas A_i from the resulting temperatures (using $Q_i = \int U_i \Delta T_i \, \mathrm{d}A_i$). Note that Problem 5.2 will favor designs where the temperature difference ΔT is close to $\Delta T_{\min}$ throughout the heat exchangers because this improves energy efficiency but does not cost anything. Specifying $\Delta T_{\min}$ will therefore tend to give designs with large heat exchanger areas. In addition, different U-values can not be handled easily as they are not part of the optimization problem in Equation 5.3. An indirect approach is too use different $\Delta T_{\text{min, i}}$ for each heat exchanger in Equation 5.3.

Let us now consider steady-state operation, where the equipment data, including heat exchanger areas, are given and the degrees of freedom u_3 include only the operating variables. For each heat exchanger, there is at steady-state one operating variable which may be chosen as the *effective* area A_i (in practice, A_i may be changed using a bypass). However, we must require $A_i \leq A_i^{\max}$ where $A_i^{\max}$ is the "installed area" e.g. found from Problem 5.1 or 5.2. We then have:

Problem 5.3 Optimal operation *with given heat exchanger areas.*

$$\begin{aligned} & \min_{u_3} (J_{operation}) \\ \textit{subject to} \quad & A_i - A_{\max,i} \leq 0 \end{aligned} \tag{5.4}$$

Note that in many cases, including the examples in this paper, it is optimal to have $A_i = A_{\max,i}$.

The solution to Problem 5.3 in terms of optimal stream data (temperatures) will be the same as to Problem 5.1, but *not* generally the same as to Problem 5.2; see the motivating example below. To understand this, note that in Problem 5.3, with the areas given, there is no particular incentive to make the temperature difference ΔT "even" (due to $\Delta T_{\min}$) throughout the heat exchangers. Provided there are degrees of freedom, we will therefore find that ΔT from Problem 5.3 varies more through the heat exchangers than ΔT from Problem 5.2. In particular, the $\Delta T_{\min}$ obtained from Problem 5.3 is often smaller than that specified in design (Problem 5.2), see the introductory example below. Thus, the optimal nominal operating point (solution to Problem 5.3) is not the same as the nominal simplified design point (solution to Problem 5.2). From this it is clear that specifying $\Delta T_{\min}$ in design is not a good approach.

The objective of this paper is to study the $\Delta T_{\min}$-method (Problem 5.2) in more detail and suggest an alternative simple design method (called the simplified TAC-method) for heat exchanger systems. The optimization problems are solved using the gPROMS software.

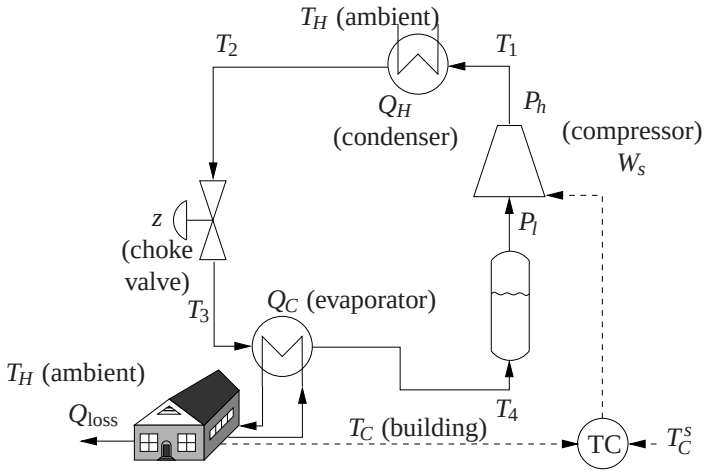

Figure 5.2: An ammonia refrigeration system

5.2 Motivating example: Ammonia refrigeration cycle

The ammonia refrigeration cycle for cold storage presented in Jensen and Skogestad (2007*a*) is shown in Figure 5.2. We use the following conditions:

Table 5.1: Structure of model equations for the ammonia case study

Heat exchangers (condenser and evaporator)
$Q = \int U \Delta T \, \mathrm{d}A = \dot{m} \cdot (h_{out} - h_{in})$
$P = P_{sat}(T_{sat})$
$m = \rho / V$
Valve
$\dot{m} = z \cdot C_V \sqrt{\Delta P \cdot \rho} \qquad h_{out} = h_{in}$
Compressor
$W_s = \dot{m}(h_{out} - h_{in}) = \dot{m} \cdot (h_s - h_{in}) / \eta$

- $Q_{\text{loss}} = 20\,\text{kW}$
- Ambient temperature $T_H = 25\,^{\circ}\text{C}$
- Cold storage (indoor) temperature set point $T_C^s = -12\,^{\circ}\text{C}$
- Heat transfer coefficient for the evaporator and condenser, $U = 500\,\text{W}\,\text{m}^{-2}\,^{\circ}\text{C}^{-1}$
- The ammonia leaving the evaporator is saturated vapour (which is always optimal for this cycle, Jensen and Skogestad (2007*b*))

The temperature controller is assumed to adjust the compressor power to maintain $T_C = T_C^s$ which indirectly sets the load $Q_C = Q_{\text{loss}}$. The main model equations are given in Table 5.1.

5.2.1 ΔT_{min} design-method

The operational cost is given by the compressor power ($J_{\text{operation}} = W_s$), so with the ΔT_{min}-method, the optimal design problem, see Problem 5.2, becomes:

$$\begin{aligned} & \min_{u_2}(W_s) \\ \text{subject to} \quad & \Delta T_{\text{vap}} - \Delta T_{\text{min, vap}} \geq 0 \\ & \Delta T_{\text{con}} - \Delta T_{\text{min,con}} \geq 0 \end{aligned} \tag{5.5}$$

where the degrees of freedom u_2 include the heat transfered in the two heat exchangers (Q_i) (but note that $Q_C = 20\,\text{kW}$) plus three other operating variables* (e.g. two pressures and refrigerant flow). We choose $\Delta T_{\text{min}} = 10\,^{\circ}\text{C}$ in both the

*The simple cycle in Figure 5.2 has five operating variables (Jensen and Skogestad, 2007*b*), but two of these have been specified (given load and saturated vapour)

evaporator and the condenser (Shelton and Grossmann, 1986). The resulting heat exchanger areas A are then obtained from $Q = \int (U \cdot \Delta T)\, \mathrm{d}A$.

As noted in the introduction, the solution to Equation 5.5 does not generally give optimal operation with the resulting areas. The re-optimized operation problem with given areas, see Problem 5.3, becomes:

$$\begin{aligned} & \min_{u_3}(W_s) \\ \text{subject to} \quad & A_{\text{vap}} - A_{\text{vap}}^{\max} \leq 0 \\ & A_{\text{con}} - A_{\text{con}}^{\max} \leq 0 \end{aligned} \tag{5.6}$$

where $A_{\text{vap}}^{\max}$ and $A_{\text{con}}^{\max}$ are the result of the $\Delta T_{\min}$-method design problem (Equation 5.5). The degrees of freedom u_3 include A_{vap} and A_{con} (which in this case are optimally equal to their maximum design values) plus the three other operating variables (e.g. two pressures and refrigerant flow).

The results for the two problems are summarized in the two left columns of Table 5.2 and we note that re-optimization reduces the operating cost (W_s) by 3.2 %. Figure 5.3 shows the corresponding temperature profiles in the condenser.

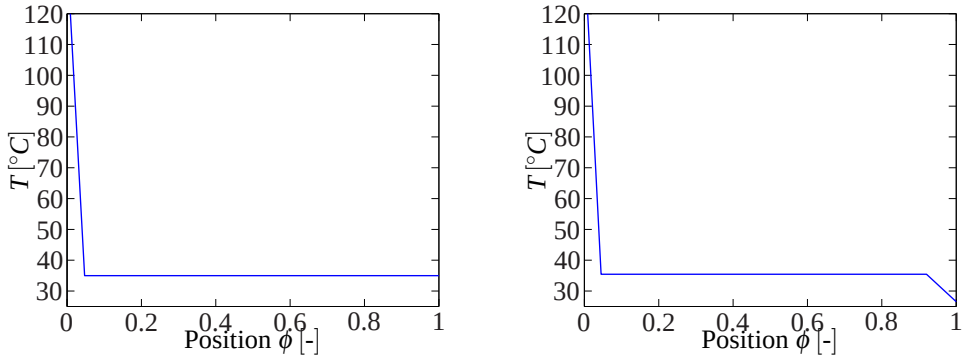

(a) Optimal design with specified $\Delta T_{\min}$

(b) Re-optimized operation with specified A

Figure 5.3: Temperature profile in the condenser for the $\Delta T_{\min}$-method

- In the design case (5.5) (with fixed $\Delta T_{\min}$) there is no sub-cooling of ammonia in the condenser. In the re-optimized operation (5.6) however, there is a sub-cooling of 8.9 °C. The optimality of sub-cooling in simple refrigeration cycles is discussed in detail in Jensen and Skogestad (2007*b*).
- The high pressure P_h is increased by 0.7 % in the re-optimized case, but this is more than compensated for by a 3.7 % reduction in flowrate.

Table 5.2: Ammonia case study

	$\Delta T_{\min}$-method		Simplified TAC (Eq. 5.9)	
	Design (5.5) $\Delta T_{\min} = 10\,^{\circ}\mathrm{C}$	Operation (5.6) Re-optimized	$C_0 = 818^*$	$C_0 = 8250^{\dagger}$
$\Delta T_{\min}^{\mathrm{vap}}$ [°C]	**10.0**	10.0	9.13	26.7
$\Delta T_{\min}^{\mathrm{con}}$ [°C]	**10.0**	1.53	1.84	**10.0**
A_{con} [m^2]	4.50	**4.50**	4.12	1.47
A_{vap} [m^2]	4.00	**4.00**	4.38	1.50
A_{tot} [m^2]	8.50	8.50	**8.50**	2.97
HX cost [-]	1.00	1.00	1.00	0.51
P_l [bar]	1.74	1.74	1.81	0.77
P_h [bar]	13.5	13.6	14.0	28.4
ΔT_{sub} [°C]	0.0	8.9	9.6	28.5
$\dot{m}$ [mol s^{-1}]	1.07	1.03	1.03	1.10
$\mathbf{W_s}$ [W]	6019	5824	5803	12479
COP [-]	3.32	3.43	3.45	1.60

Given data is shown in boldface

$^*C_0$ adjusted to get same total heat exchanger area as the $\Delta T_{\min}$-method

$^{\dagger}C_0$ adjusted to get same $\Delta T_{\min}$ as used in the $\Delta T_{\min}$-method

In summary, we find that the $\Delta T_{\min}$ design-method does not result in optimal operating variables for the given example. A better design method is therefore needed!

5.3 Proposed simplified TAC method

The original cost function for Problem 5.1 requires quite detailed cost data plus a lot of other information which is not available at an early design stage. The simplified Problem 5.2 on the other hand, is easy to formulate and solve, but here we cannot easily handle different U-values for heat exchangers and the optimal design point is not generally the same as the optimal operating point (even nominally). Therefore, the objective is to find a better simplified formulation. The starting point is to replace the equipment cost (Equation 5.2) in Problem 5.1 with a simplified expression. First, we assume that the structure of the design is given such that we need not consider the fixed cost terms (i.e. we set $C_{\mathrm{fixed,i}} = 0$). Second, we only consider heat exchanger costs. For a vapour compression cycle this is justified if the capital cost for the compressor is proportional to the compressor power W_s, which corresponds to assuming $n_i = 1$ for the cost exponent for the compressor. We can then include the capital cost for the compressor in the operating cost of the compressor. Third, we assume that all heat exchangers have the same

cost factors ($C_{\text{variable,i}} = C_0$ and $n_i = n$).

The resulting "simplified TAC" optimal design problem becomes:

Problem 5.4 Simplified optimal design *with simplified TAC*

$$\min_{u_4} \left(J_{operation} + C_0 \cdot \sum_i A_i^n \right) \tag{5.7}$$

subject to model equations and operating constraints, and where u_4 includes the heat exchanger areas A_i plus the operating variables. In the general case:

$$J_{\text{operation}} = \sum p_{F_i} F_i - \sum p_{P_j} P_j + \sum p_{Q_k} Q_k + \sum p_{W_{s,l}} W_{s,l} \quad [\$\,\text{year}^{-1}] \tag{5.8}$$

where F_i are feeds, P_j are products, Q_k are utilities (energy), $W_{s,l}$ are the mechanical work the p's are respective prices. For a heat exchanger network problem this can be reduced to $J_{\text{operation}} = \sum p_{Q_i} Q_i\,[\$\,\text{year}^{-1}]$ which in many cases simplifies to $J_{\text{operation}} = Q_H\,[\$\,\text{year}^{-1}]$, where Q_H is the supplied heat (Gundersen and Naess, 1988). For the refrigeration cycles considered in this paper, $J_{\text{operation}} = W_s\,[\$\,\text{year}^{-1}]$.

In the examples, we choose $n = 0.65$ for the heat exchangers and use C_0 as the single adjustable parameter (to replace $\Delta T_{\min}$). There are several benefits compared with the $\Delta T_{\min}$-method:

- The heat exchanger temperatures depend on $U_i A_i$ for each heat exchanger. Thus, different U-values for each exchanger are easily included.
- The optimal design (Equation 5.7) and the optimal operation (Problem 5.3) have the same solution in terms of optimal stream data. This follows since the term $C_0 \sum_i A_i^n$ is constant in operation.
- The assumption of using the same C_0 for all heat exchangers is generally a much better than assuming the same $\Delta T_{\min}$.

On the other hand, compared to the $\Delta T_{\min}$ design method, the simplified TAC design method requires calculation of ΔT inside all exchangers during the optimization, and the optimization problem is also a bit more difficult to solve. However, the proposed method does not require any additional data compared with the $\Delta T_{\min}$ method.

5.3.1 Revisit of ammonia case study

The optimization problem (Equation 5.7) for the proposed simplified TAC-method becomes*:

$$\min(W_s + C_0 \cdot (A_{\text{con}}^n + A_{\text{vap}}^n)) \tag{5.9}$$

The right two columns of Table 5.2 shows the optimal design with $n = 0.65$ and two different values of C_0. First, $C_0 = 818$ gives the same total heat exchanger area and almost the same capital cost as the $\Delta T_{\min}$-method, but the area is better distributed between the evaporator and condenser. This results in a 3.60% reduction in operating cost (W_s) compared with the $\Delta T_{\min}$-method (0.36% after re-optimizing the operating point for the $\Delta T_{\min}$-method). Second, $C_0 = 8250$ gives $\Delta T_{\min} = 10.0\,^{\circ}\text{C}$ as specified in the $\Delta T_{\min}$ method. The compressor work is increased with 107% (114%), but the heat exchanger area is reduced by 60%, and this is the only design that truly satisfies the $\Delta T_{\min}$ we selected initially.

The simplified TAC method confirms that sub-cooling is optimal, and we see that the degree of sub-cooling increases with decreasing heat transfer area (increased C_0).

Note that the heat transfer coefficients U_i were assumed to be equal, but the simplified TAC method will automatically distribute the heat transfer area optimally, also if the heat exchangers have different heat transfer coefficients. For example, with $U_{\text{vap}} = 2U_{\text{con}}$ the energy savings (for the same heat exchangers cost) are even larger (6%) using the simplified TAC method compared with the $\Delta T_{\min}$-method.

5.4 Other case studies

We here briefly present results from two other case studies.

5.4.1 CO_2 air-conditioner

CO_2 as a working fluid in air-conditioners and heat-pumps is gaining increased popularity because of its low environmental impact (Lorentzen, 1995; Neksaa, 2002). We consider a trans-critical CO_2 air-condition unit with the following data:

*In a more realistic design, one may also consider additional constraints such as maximum compressor suction volumes and pressure ratio, but this is not discussed here.

Table 5.3: CO_2 air-conditioner

	$\Delta T_{\min}$-method		Simplified TAC		
	Design $\Delta T_{\min} = 5\,^{\circ}\mathrm{C}$	Operation Re-optimized	$C_0 = 253^{*}$	$C_0 = 185^{\dagger}$	$C_0 = 877^{\ddagger}$
$\Delta T_{\min}^{\mathrm{gco}}\,[^{\circ}\mathrm{C}]$	**5.00**	3.56	2.41	2.07	**5.00**
$\Delta T_{\min}^{\mathrm{vap}}\,[^{\circ}\mathrm{C}]$	**5.00**	5.00	5.78	5.01	11.5
$\Delta T_{\min}^{\mathrm{ihx}}\,[^{\circ}\mathrm{C}]$	**5.00**	4.75	-	-	-
$A_{\mathrm{gco}}\,[\mathrm{m}^2]$	1.31	**1.31**	1.76	2.02	0.92
$A_{\mathrm{vap}}\,[\mathrm{m}^2]$	1.60	**1.60**	1.38	1.60	0.70
$A_{\mathrm{ihx}}\,[\mathrm{m}^2]$	0.23	**0.23**	0	0	0
$A_{tot}\,[\mathrm{m}^2]$	3.14	3.14	**3.14**	3.62	1.61
HX cost [-]	1.00	1.00	0.91	**1.00**	0.59
$P_h\,[\mathrm{bar}]$	87.8	91.6	92.8	91.0	107.0
$P_l\,[\mathrm{bar}]$	50.8	50.8	49.9	50.8	43.3
$\dot{m}\,[\mathrm{mol\,s^{-1}}]$	0.65	0.59	0.69	0.70	0.67
$\mathbf{W_s}\,[\mathrm{W}]$	892	859	871	814	1328
COP [-]	4.49	4.65	4.59	4.92	3.01

Given data is shown in boldface
$^{*}C_0$ adjusted to get same total area as $\Delta T_{\min}$-method
$^{\dagger}C_0$ adjusted to get same heat exchanger cost as the $\Delta T_{\min}$-method
$^{\ddagger}C_0$ adjusted to get same $\Delta T_{\min}$ as used in the $\Delta T_{\min}$-method

- Heat transfer coefficient: $U = 500\,\mathrm{W\,m^{-2}\,K^{-1}}$ for the evaporator, condenser and internal heat exchanger
- Ambient temperature: $T_H = 30\,^{\circ}\mathrm{C}$
- Set point for room temperature: $T_C = 20\,^{\circ}\mathrm{C}$
- Heat loss into the room: $Q_{\mathrm{loss}} = 4.0\,\mathrm{kW}$

The details about the model are found in Jensen and Skogestad (2007*a*). In the optimization we have included an internal heat exchanger (with area A_{ihx}) that transfers heat from before the compressor to before the valve. Otherwise the flowsheet is as for the ammonia cycle shown in Figure 5.2.

For solving Problem 5.2, we use a design $\Delta T_{\min} = 5.0\,^{\circ}\mathrm{C}$ in all heat exchangers. Again we find that re-optimizing for operation (Problem 5.3) gives a better operating point with 3.70% less compressor power. The results given in Table 5.3 are similar to the ammonia cooling cycle, although there is no sub-cooling since P_h is above the critical pressure.

Interestingly with the simplified TAC method we obtain $A_{\mathrm{ihx}} = 0.0\,\mathrm{m}^2$, which means that it is not optimal from an economical point of view to pay for the area for

the internal heat exchanger (although the internal heat exchanger would of course be used if it were available free of charge). This is a bit surprising since we have not included the fixed cost of installing a heat exchanger, which would make it even less desirable to invest in an internal heat exchanger. On the other hand, if we require a lot of super-heating before the compressor then it might be better to achieve this super-heating in an internal heat exchanger, but this is not discussed here.

With $C_0 = 253$ we get the same total heat transfer area as for the $\Delta T_{\min}$-method, but the shaft work is reduced by 4.26% (0.58% compared to re-optimized). $C_0 = 185$ gives the same cost of heat exchanger area (without even considering the savings of completely removing a heat exchanger) and W_s is reduced by 12.22% (8.85%). With $C_0 = 877$ we get the only design with $\Delta T_{\min} = 5.0\,^{\circ}\mathrm{C}$. The heat exchanger cost is reduced by 41% and the compressor power is increased by 49% (55%) compared with the $\Delta T_{\min}$-method.

5.4.2 PRICO LNG process

The PRICO LNG process (Price and Mortko, 1996) is a simple configuration utilizing mixed refrigerants. Details about the model is presented elsewhere (Jensen, 2008). Note that we are not considering constraints on compressor suction volume and pressure ratio for the compressor. This will be important in an actual design, but we have tried to keep the case study simple to illustrate the effect of specifying $\Delta T_{\min}$.

A design $\Delta T_{\min}$ of $2.0\,^{\circ}\mathrm{C}$ is used for the $\Delta T_{\min}$ method. From Table 5.4 we see that re-optimizing reduces the energy usage (W_s) by 4.8%. This is achieved by increasing the pressure ratio (by 25.5%) and reducing the refrigerant flowrate (by 16.7%). The composition of the refrigerant is also slightly changed, but this is not shown in Table 5.4. We were quite surprised by the rather large improvement obtained by re-optimizing with fixed heat transfer areas considering the relatively low value for the initial $\Delta T_{\min}$.

With the simplified TAC method we get a 4.1% reduction (0.2% increase compared to re-optimized) in W_s for the same total heat transfer area ($C_0 = 2135$). The small increase in W_s compared with the re-optimized $\Delta T_{\min}$ design is because the simplified TAC method minimizes the heat exchanger cost and not the total area. With the same cost ($C_0 = 2090$), the TAC-method gives a reduction in compressor power of 4.3% (0.1%). The saving compared with the re-optimized case is small because of the small $\Delta T_{\min}$ resulting in very large heat exchangers. A more reasonable design is achieved with $C_0 = 7350$, which gives a design with a true $\Delta T_{\min}$

Table 5.4: PRICO LNG process

	$\Delta T_{\min}$-method		Simplified TAC		
	Design $\Delta T_{\min} = 2\,^{\circ}\mathrm{C}$	Operation Re-optimized	$C_0 =$ 2135*	$C_0 =$ 2090†	$C_0 =$ 7350‡
$\Delta T_{min,HOT}\,[^{\circ}\mathrm{C}]$	**2.00**	0.89	0.90	0.86	**2.00**
$\Delta T_{min,NG}\,[^{\circ}\mathrm{C}]$	**2.00**	0.98	1.09	1.08	2.22
$A_{HOT} \cdot 10^{-3}\,[\mathrm{m}^2]$	98.2	**98.2**	101.2	102.7	43.1
$A_{NG} \cdot 10^{-3}\,[\mathrm{m}^2]$	29.9	**29.9**	26.9	27.2	14.5
$A_{Tot} \cdot 10^{-3}\,[\mathrm{m}^2]$	128.1	128.1	**128.1**	129.9	57.7
HX cost [-]	1.00	1.00	0.99	**1.00**	0.60
P_h [bar]	20.1	27.1	27.0	26.8	37.8
P_l [bar]	2.7	2.9	2.9	2.9	1.91
$\dot{m}\,[\mathrm{kmol\,s^{-1}}]$	3.0	2.5	2.5	2.5	2.3
$\mathbf{W_s}$ [MW]	18.94	18.14	18.17	18.12	22.16

Given data is shown in boldface
*C_0 adjusted to get same total area as $\Delta T_{\min}$-method
†C_0 adjusted to get same heat exchanger cost as the $\Delta T_{\min}$-method
‡C_0adjusted to get same $\Delta T_{\min}$ as used in the $\Delta T_{\min}$-method

of 2.0 °C. The heat exchanger capital cost is reduced by 40 % but the compressor power is increased by 17.0 % (22.2 %).

5.5 Discussion

5.5.1 $\Delta T_{\min}$-method

There are some main points that are important to note from this analysis of the $\Delta T_{\min}$-method

1. $\Delta T_{\min}$ is treated as an important parameter in heat exchanger design, but the theoretical basis seems weak as "violating" $\Delta T_{\min}$ in operation may give lower operating cost.
2. The $\Delta T_{\min}$-method will not always give the optimal operating point, so sub-optimal setpoints might be implemented.
3. The size distribution between the heat exchanger will not be optimal, although this may be partly corrected for by individually adjusting the value of $\Delta T_{\min}$ for each heat exchanger.
4. More seriously, the results might lead to wrong structural decisions and this

can not be changed by iterating on the $\Delta T_{\min}$-values. In the ammonia case study, one would incorrectly conclude that sub-cooling is not optimal and thus implement a liquid receiver after the condenser. This would during operation achieve no sub-cooling. From the true optimum however, we see that some sub-cooling is optimal.

5. One potential advantage with the $\Delta T_{\min}$-method is that it only requires an overall energy balance for the heat exchangers. However, for more complex cases a more detailed model of the heat exchangers is needed so in the general cases this advantage is lost.

In summary, the $\Delta T_{\min}$-method is not satisfactory for realistic design problems.

5.5.2 Other approaches

The question is whether there are other ways of specifying temperature differences. In terms of area, rather than specifying $\Delta T_{\min}$, it would be better to specify the mean temperature difference $\overline{\Delta T} = \frac{1}{A}\int \Delta T\, dA$, since $\overline{\Delta T}$ is directly linked to the heat transfer area by (assuming constant heat transfer coefficient):

$$Q = UA\overline{\Delta T} \tag{5.10}$$

However, this method has several drawbacks that makes it unattractive to use. First, it might be cumbersome to calculate the integral of the temperature and second, and more importantly there are no general rules in selecting values for $\overline{\Delta T}$. We therefore propose to use the simplified TAC-method.

5.5.3 Heat exchanger network design

The results in this paper show that one should not use a constraint on $\Delta T_{\min}$ (EMAT) for the design of individual heat exchangers. What about the standard heat exchanger network (HEN) design problem (e.g. Gundersen and Naess, 1988), where a constraint on the heat recovery approach temperature $\Delta T_{\min}$ (HRAT) for the network is used? Our results do not invalidate this approach. First, the stream data (inlet and outlet temperatures and flows) are fixed for the standard HEN problem. It then follows, that specifying $\Delta T_{\min}$ (HRAT) is equivalent to specifying the heat recovery, or equivalently the required hot utility (Q_H). The solution to this particular design problem will therefore result in optimal operating data if we install the resulting areas (and remove the $\Delta T_{\min}$ specification). However, note that the simplified TAC-formulation in Equation 5.7 with $J_{\text{operation}} = \sum_i p_{Q_i} Q_i$ is much

more general than the standard heat exchanger network design problem, where the stream data are specified.

5.6 Conclusion

We have shown that the method of specifying $\Delta T_{\min}$ for design of heat exchangers, ($\min\ J$ subject to $\Delta T \geq \Delta T_{\min}$), may fail to give an optimal operating point. In the ammonia refrigeration case study, the $\Delta T_{\min}$-method fails to find that sub-cooling in the condenser is optimal. As a simple alternative we propose the simplified total annualized cost (TAC) method ($\min\,(J + C_0 \sum_i A_i^n)$), where C_0 replaces $\Delta T_{\min}$ as the adjustable parameter. A high value of C_0 corresponds to increasing the investment (capital) costs relative to the operating (energy) costs and favors small areas and a larger $\Delta T_{\min}$. Thus, C_0 can be adjusted to get a desired value for $\Delta T_{\min}$ or the total area or it can be obtained from cost data. With the alternative method, different heat transfer coefficients U_i can also be accounted for.

Another important conclusion is related to the temperature difference profile in the heat exchanger. According to exergy or entropy minimization rules of thumb (e.g. Sauer et al., 1996) it is optimal to have even driving forces, which suggests that ΔT should be constant in heat exchangers. The results presented here however, suggest that this is not true. The $\Delta T_{\min}$ approach (Problem 5.2) favors a more constant ΔT profile (see Figure 5.3(a)), but in optimal operation (Problem 5.3) we find that the temperature difference is small in one end (see Figure 5.3(b)).

Bibliography

Biegler, L. T., Grossmann, I. E. and Westerberg, A. W. (1997), *Systematic Methods of Chemical Process Design*, Prentice Hall.

Gundersen, T. and Naess, L. (1988), 'The synthesis of cost optimal heat exchangers networks', *Comput. Chem Eng.* **12**(6), 503–530.

Jensen, J. B. (2008), Optimal operation of cyclic processes. With application to LNG processes, PhD thesis, Norwegian University of Science and Technology.

Jensen, J. B. and Skogestad, S. (2007*a*), 'Optimal operation of a simple refrigeration cycles. Part II: Selection of controlled variables', *Comput. Chem Eng.* **31**, 1590–1601.

Jensen, J. B. and Skogestad, S. (2007*b*), 'Optimal operation of simple refrigeration cycles. Part I: Degrees of freedom and optimality of sub-cooling', *Comput. Chem. Eng.* **31**, 712–721.

Lorentzen, G. (1995), 'The use of natural refrigerants: a complete solution to the CFC/HCFC predicament', *Int. Journal of Refrigeration* **18**, 190–197.

Neksaa, P. (2002), 'CO_2 heat pump systems', *Int. J. Refrigeration* **25**, 421–427.

Price, B. C. and Mortko, R. A. (1996), PRICO - a simple, flexible proven approach to natural gas liquefaction, *in* 'GASTECH, LNG, Natural Gas, LPG international conference , Vienna'.

Sauer, E., Ratkje, S. K. and Lien, K. M. (1996), 'Equipartition of forces: A new principle for process design and optimization', *Ind. Eng. Chem. Res.* **35**, 4147–4153.

Shelton, M. R. and Grossmann, I. E. (1986), 'Optimal synthesis of integrated refrigeration systems—i : Mixed-integer programming model', *Comput. Chem. Eng.* **10**(5), 445–459.

Turton, R., Bailie, R. C., Whiting, W. B. and Shaeiwitz, J. A. (1998), *Analysis, synthesis, and design of chemical processes*, Pearson Education Ltd.

Chapter 6

Optimal design of a simple LNG process

In this chapter we discuss the design optimization of a single cycle mixed fluid LNG process, the PRICO process. A simple objective function is stated and used on nine different cases with varying constraints. Important constraints are discussed and the results are compared with the commercial PRICO process and with other publications.

6.1 Introduction

Large amounts of natural gas are found at locations that makes it infeasible or not economical to transport it in gaseous state to the customers. The most economic way of transporting natural gas over long distances is to first produce liquefied natural gas (LNG) and then transport the LNG by ships. LNG has approximately 600 times the density of gaseous natural gas.

At atmospheric pressure, LNG has at saturated conditions a temperature of approximately $-162\,^{\circ}\mathrm{C}$, so the process requires large amounts of energy to generate the necessary cooling. Several different process designs are used and they can be grouped roughly as follows:

1. Pure fluid cascade process: The refrigerants are pure fluids, but several cycles are used to improve the efficiency.
2. Mixed fluid refrigerant: The refrigerant composition is adjusted to match the cooling curve of the natural gas.

3. Mixed fluid cascade process: Combination of the two where energy efficiency is further improved by using several mixed refrigerant cycles.

The PRICO LNG process considered in this paper, see Figure 6.1, belongs to the second group and has a single cycle with a mixed refrigerant. The mixed refrigerant gives a good temperature match throughout the heat exchanger compared with using pure component cycles (group 1). However, compared with multiple mixed refrigerant processes the thermodynamic efficiency is lower, so the process is mainly used for smaller plants (e.g. peak shaving plants) up to 2 MTPA (million tons per annum).

Stebbing and O'Brien (1975) reports on the performance of the first commercial PRICO plants in operation. Price and Mortko (1996) from the Black & Veatch company discuss the process and give some key values for several of their plants. With respect to academic work, Lee et al. (2002) used the PRICO process as one of their case studies for testing their approach to design optimization. The same group later published some updated results (Del Nogal et al., 2005).

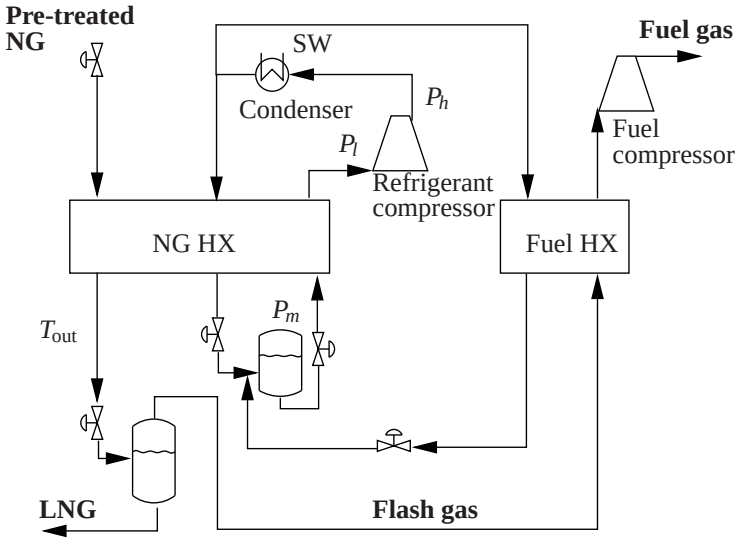

Figure 6.1: Simplified flowsheet of the PRICO process also showing flash gas heating and recompression (not considered here).

6.1.1 Optimal design

Mathematically, optimal design may be expressed as the solution to the following optimization problem:

$$\begin{aligned} \min \quad & J_{\text{TAC}} = J_{\text{operation}} + J_{\text{capital}} \\ \text{subject to} \quad & c \leq 0 \end{aligned} \tag{6.1}$$

where J_{capital} [\$ year^{-1}] is the annualized cost of the equipment and $J_{\text{operation}}$ [\$ year^{-1}] is the annual operating cost ($J_{\text{operation}} = J_{\text{utility}} + J_{\text{feeds}} + J_{\text{products}}$). The total annualized cost (TAC) is minimized with respect to the design variables, which includes both the structure (integer variables) and the design parameters. c is a set of design constraints (i.e. maximum design pressure, non-negative flows and feed composition).

The truly optimal design is a complex task involving mixed integer non-linear programming. In our case, however, we start from a given process structure so we may use a simpler approach with no integer variables.

For heat exchanger design, a common approach is to minimize only the operating cost, but subject to a minimum approach temperature in all heat exchangers (Lee et al., 2002; Del Nogal et al., 2005), that is, $\Delta T_i \geq \Delta T_{\text{min}}$ is introduced as a design constraint. The idea is that the heat exchanger minimum approach temperature*, ΔT_{min}, gives a balance between low operating cost (favored by low ΔT_{min}) and low capital cost (favored by high ΔT_{min}). This approach will however, not generally result in a true optimal design, even when iterating on ΔT_{min}. Specifically, re-optimizing to find the optimal operation given the resulting equipment, will usually result in a lower optimal value of ΔT_{min} (Chapter 5). This also implies that a design approach based on specifying ΔT_{min} and altering it in an outer loop, will not work.

Therefore, we choose to use the simplified total annual cost (sTAC) method presented in Chapter 5. The capital cost is often expressed as a fixed and a variable contribution, $J_{\text{capital}} = \sum_i \left(C_{\text{fixed,i}} + C_{\text{variable,i}} \cdot S_i^{n_i}\right)/T$, where S_i is the characteristic size for the unit (area in m^2 for heat exchangers). The cost factors ($C_{\text{fixed,i}}$ and $C_{\text{variable,i}}$) and the scaling factor n_i are assumed constants for each unit. T is the capital depreciation time, e.g. $T = 10$ years. First, if the structure of the network is fixed, the size independent parameter does not matter (so we may use $C_{\text{fixed,i}} = 0$). Second, we here consider only the compressor and heat exchanger costs (main equipment). Third, we assume that the exponent $n = 1$ for the compressors. We can then add the operation and capital cost for the compressor into a single term,

*ΔT_{min} in this paper refers to the individual exchanger approach temperature (ERAT) and not the heat recovery approach temperature (HRAT) or "pinch" temperature of the entire network

see Equation 6.2 below. Fourth, we assume that the size dependent parameter and the exponent are equal for all heat exchanger ($C_{\text{variable,i}} = C_0$ and $n_i = n$). We choose to fix $n = 0.65$ for the heat exchanger areas and use C_0 as a single adjustable parameter.

The resulting "simplified TAC" design problem with the cost factors C_0 and k as parameters becomes:

$$\min \left(k \cdot W_s + \underbrace{p_{\text{feed}} \cdot \dot{m}_{\text{feed}} - p_{\text{LNG}} \cdot \dot{m}_{\text{LNG}} - p_{\text{fuel}} \cdot \dot{m}_{\text{fuel}}}_{J_{\text{flows}}} + C_0 \cdot \sum_i A_i^n \right) \text{ [\$/year]} \tag{6.2}$$

This minimization is subject to some design constraints, see Section 6.1.2. A_i is the heat transfer area for the two hot streams in the main heat exchanger (natural gas and warm refrigerant) and for the sea water heat exchanger. Note that k is not only the price of the compressor energy as it also includes the annualized capital cost for the compressor. One may view k [\$/MW/year] as the price of "renting" a compressor.

With no capacity limits, this problem (Equation 6.2) is actually ill-posed as it is optimal to have infinite feed (capacity). In practice, one either designs for a given feed or imposes constraints that limit the capacity. In this paper, we assume that we wish to find the optimal design with a given maximum compressor shaft power $W_s^{\max}$. The factor k then does not matter as the term kW_s is fixed. We also do not include the condenser in the design, and instead specify the outlet temperature of the condenser. A mass balance gives $\dot{m}_{\text{fuel}} = \dot{m}_{\text{feed}} - \dot{m}_{\text{LNG}}$ and we may write $J_{\text{flows}} = \dot{m}_{\text{feed}} (p_{\text{feed}} - p_{\text{fuel}}) - \dot{m}_{\text{LNG}} (p_{\text{LNG}} - p_{\text{fuel}}) = -\dot{m}_{\text{LNG}} (p_{\text{LNG}} - p_{\text{fuel}})$, where we have assumed $p_{\text{feed}} = p_{\text{fuel}}$. This is reasonable since feed may be used as a fuel. Since W_s is constrained, the optimal design problem (Equation 6.2) simplifies to:

$$\begin{aligned} & \min \left(-\dot{m}_{\text{LNG}} + \hat{C}_0 \left(A_{\text{HOT}}^{0.65} + A_{\text{NG}}^{0.65} \right) \right) \\ \text{subject to} \quad & W_s \leq W_s^{\max} \\ & m_{\text{fuel}} \leq m_{\text{fuel}}^{\max} \\ & c \leq 0 \end{aligned} \tag{6.3}$$

The minimization is with respect to design parameters (A_{HOT} and A_{NG}) operating parameters (flows, pressures, splits etc.). We may adjust the parameter $\hat{C}_0$ in Equation 6.3 to obtain a reasonable $\Delta T_{\min}$. This will unlike the "$\Delta T_{\min}$-method" (where we maximize $\dot{m}_{\text{LNG}}$ with $\Delta T_i \geq \Delta T_{\min}$ as constraints) give the same operating point if one re-optimizes the operation with the areas fixed at the optimal design values. The set c is constraints that may vary for the different cases.

6.1.2 Design constraints

In design it is necessary to impose some constraints for the optimization to assure that a feasible solution is found.

Pressure: There are typically constraints on pressures in the process. These constraints may be related to equipment manufacturing limits. For example, a large conventional centrifugal compressor has a maximum pressure in the order of 30 to 40 bar, while a vertical split centrifugal compressor may have outlet pressure up to about 80 bar (General Electric Oil and Gas, January 2007). Constraints may also arise from the fact that higher pressures are not desirable from a safety point of view (e.g. explosion danger). One may also constrain certain pressures to simplify the objective function by removing the pressure dependence (higher pressure requires more expensive piping, heat exchangers etc.).

Temperatures: There may be constraints on temperature gradients (e.g. in heat exchangers) or on absolute temperatures. Both of these may be related to mechanical issues such as stress. *This has not been considered here.*

Compressor suction volume ($\dot{V}_{\mathbf{suc}}$): In operation the compressor suction volume and compressor head are linked to the speed of rotation through the characteristic curve. In design one may have to limit the compressor size to keep it within physical limits (e.g. by limiting the compressor suction volume). The current maximum limit for a single flow centrifugal compressor seems to be $380000\,\mathrm{m^3\,h^{-1}}$ (General Electric Oil and Gas, January 2007).

Compressor head: A simple correlation for the maximum head (or specific enthalpy rise) per compressor wheel is for a centrifugal compressor (see Equation 1.73 on page 37 in Lüdtke, 2004):

$$\text{Head} = \Delta h = s \cdot u^2 \qquad [\mathrm{kJ\,kg^{-1}}] \tag{6.4}$$

where $s \approx 0.57 - 0.66$ is the work input factor and $u\,[\mathrm{m\,s^{-1}}]$ is the velocity at the wheel tip. Adding the numbers for each wheel gives the total head for the compressor. For example, one compressor wheel with 1.7 m diameter and a rotational speed $\omega = 3600\,\mathrm{RPM}$ gives the following head:

$$u = \frac{3600\,\mathrm{min^{-1}}}{60\,\mathrm{s\,min^{-1}}} \cdot \pi \cdot 1.7\,\mathrm{m} = 320\,\mathrm{m\,s^{-1}} \tag{6.5}$$

$$\Delta h = (320\,\mathrm{m\,s^{-1}})^2 \cdot s \approx 58 - 68\,\mathrm{kJ\,kg^{-1}} \tag{6.6}$$

Table 6.1 gives the head for different rotational speeds and wheel diameters ($s = 0.57$). For large compressors, the number of wheels is typically six or less (up to eight for the barrel type).

Table 6.1: Maximum head, $\Delta h\,[\mathrm{kJ\,kg^{-1}}]$, per compressor wheel for different wheel diameters and rotational speeds (Equation 6.4 with $s = 0.57$). The last column shows the total head for a compressor with one of each of the wheels in the table.

	Wheel diameter						
Rotational speed	1.7 m	1.6 m	1.5 m	1.4 m	1.3 m	1.2 m	**Sum 6 wheels**
3600 RPM	59.6	52.8	46.4	40.4	34.8	29.7	**263.6**
3000 RPM	41.4	36.6	32.2	28.0	24.2	20.6	**183.0**

Compressor pressure ratio (Pr): The maximum compressor pressure ratio is an alternative simple way of limiting the compressor head (e.g. Price and Mortko (1996) report the value of 5.5 for their compressor), but this approach is less exact since the head also depends on the mass flowrate. The use of Equation 6.4 is therefore preferred.

Compressor shaft work (W_s^{max}): A maximum value for the compressor shaft work may be imposed for example due to physical limitations in the driver to the compressor or the compressor itself or in the available power supply.

Mach number: The gas velocity must be below the sonic velocity (Mach number less than one). High Mach numbers are typically a problem at low pressures, so this is an issue at the compressor inlet. However, the velocity is only known at the compressor outlet (the tip speed) so it is common to report the machine Mach number as the tip speed over the sonic velocity at the inlet. The machine Mach number may be higher than one (as high as 1.25 according to Lüdtke (2004)) without having an actual Mach number higher than one. *We have not considered this constraint.*

LNG outlet conditions: There may be constraints on the LNG heating value and composition. *This is not considered here*. We have however, assumed storage as saturated liquid at $P = 1.1\,\mathrm{bar}$.

Fuel specifications: There may be constraints on the fuel heating value and composition. *This is not considered here*. We have limited the maximum amount of fuel to a value somewhat larger than the energy needed by the refrigerant compressor (by combustion in a gas turbine).

6.2 Process description

Figure 6.1 shows a simplified flowsheet of the PRICO process. *Natural gas* is fed to the main heat exchanger (NG HX) after some pretreatment (removal of water,

CO_2 etc.) which is not included in this paper. The natural gas is cooled, liquefied and sub-cooled by heat exchange in NG HX with the cold refrigerant. To further lower the temperature, the sub-cooled liquid is then expanded and the liquid is separated from the vapour (flash gas) and sent to storage as LNG. The vapour (flash gas) is heated, re-compressed and used as fuel, but this part of the plant has not been included in this work. Instead the flash gas is considered as a product with a given fuel prize. The further simplified process considered in this work is shown in Figure 6.2.

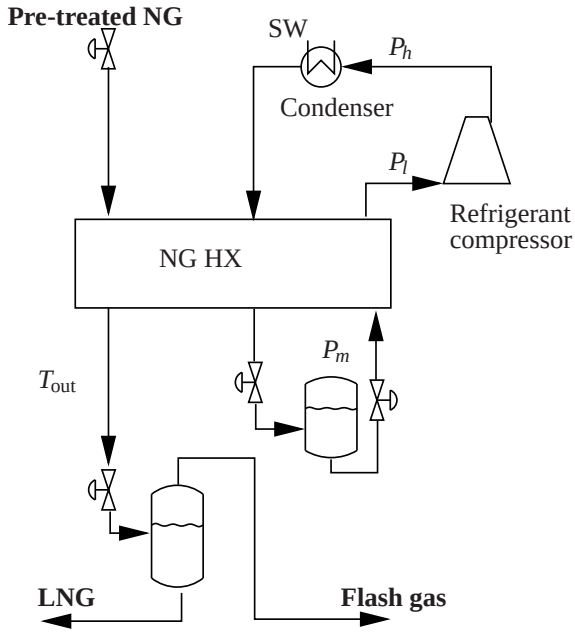

Figure 6.2: Further simplified flowsheet of the PRICO process used in this work

The *refrigerant* is partially condensed in the sea water (SW) cooler (condenser). The main part (all in our case, see Figure 6.2) of the refrigerant is fed to the NG HX and is cooled together with the natural gas stream. The refrigerant is a sub-cooled liquid at the outlet of NG HX and is expanded to the low pressure (P_l). The resulting two-phase mixture provides the cooling in NG HX by vaporization. The outlet from the heat exchanger (NG HX) is slightly super-heated, partly to avoid damage to the compressor. We have assumed $\Delta T_{\text{sup}} = 10\,^{\circ}\text{C}$ in most cases.

We have made some simplifications compared to the process described in Price and Mortko (1996). *First*, we do not consider removal of heavy components from the natural gas feed. This removal may be done upstream or integrated in the refrigeration process (as shown by Price and Mortko (1996)). A more detailed discussion

on this is given below. *Second*, we have not included the refrigerant separator and refrigerant pump indicated by Price and Mortko (1996). This, however, will not change the thermodynamics if the pump work is neglected. *Third*, as already mentioned we have not considered the flash gas heating (Fuel HX) and compression. The resulting flowsheet is shown in Figure 6.2.

Some of the data reported by Price and Mortko (1996), which we have used as design constraints, is shown in Table 6.2. In *addition*, we use the following:

- Composition of natural gas (mole-%): 89.7% methane, 5.5% ethane, 1.8% propane, 0.1% n-butane and 2.8% nitrogen. Note that this composition is more methane rich than that reported in Price and Mortko (1996) (89.7% versus 83.2%). The mole weight is $MW = 0.0176\,\mathrm{kg}\,mol^{-1}$.
- The temperature after the refrigerant condenser and the temperature in the natural gas feed are both 30 °C. Price and Mortko (1996) report 29 °C and 32 °C, respectively.
- Pressure drops:
  - 5 bar on natural gas side in main heat exchanger
  - 0.1 bar in SW cooler
  - 4 bar for hot refrigerant in main heat exchanger
  - 1 bar for cold refrigerant in main heat exchanger
  - 0.3 bar from main heat exchanger to compressor
- Constant heat transfer coefficients
- The refrigerant is a mix of nitrogen (N_2), methane (C_1), ethane (C_2), propane (C_3) and n-butane (nC_4) and the composition is found by optimization. Price and Mortko (1996) use hydrocarbons ranging from C_1 to iC_5.
- The SRK equation of state is used for the thermodynamic calculations.

6.3 Results for optimal design

The numerical results from the optimization for nine cases are reported in Table 6.3. Boldface numbers indicate specifications or active contraints. We have adjusted $\hat{C}_0$ in Equation 6.3 to obtain $\Delta T_{\min} \approx 2.0\,^{\circ}\mathrm{C}$ in the main heat exchanger (NG HX) for all cases. We have assumed 10 °C super-heating at the compressor inlet

Table 6.2: Design constraints based on data from Price and Mortko (1996)

P_{feed} [bar]	40
W_s [MW] (max)	77.5
$\dot{V}_{\text{suc}}$ [$\text{m}^3\,\text{s}^{-1}$] (max)	88*
P_h [bar] (max)	22
Pr [-] (max)	5.5

*This was reported as $317\,\text{m}^3\,\text{s}^{-1}$, but this is probably a misprint and should be $317000\,\text{m}^3\,\text{h}^{-1}$

($\Delta T_{\text{sup}} = 10\,^\circ\text{C}$) except in Cases 6.3 and 6.4. Note from the results that it is optimal in all cases to have no C_3H_8 in the refrigerant.

Table 6.3: Optimal design results for nine different cases

Case	6.1	6.2	6.3	6.4	6.5	6.6	6.7	6.8	6.9
$\dot{m}_{\text{feed}}$ [$\text{kg}\,\text{s}^{-1}$]	52.2	45.0	45.3	44.8	49.6	49.6	51.4	76.1	80.8
$\dot{m}_{\text{LNG}}$ [$\text{kg}\,\text{s}^{-1}$]	44.6	41.7	42.0	41.5	46.3	46.3	48.1	71.1	75.8
$\dot{m}_{\text{fuel}}$ [$\text{kg}\,\text{s}^{-1}$]	7.7	**3.33**	**3.33**	**3.33**	**3.33**	**3.33**	**3.33**	**5.0**	**5.0**
$\dot{m}_{REF}$ [$\text{kg}\,\text{s}^{-1}$]	478	475	472	443	251	298	320	611	617
T_{out} [°C]	**-144**	-156	-156	-156	-157	-157	-157	-157	-156
ΔT_{sup} [°C]	**10.0**	**10.0**	11.6	**25.7**	**10.0**	**10.0**	**10.0**	**10.0**	**10.0**
ΔT_{min} [°C]	1.96	1.97	1.95	2.03	1.97	1.94	1.94	2.00	2.04
η [%]	82.8	82.8	82.8	82.8	82.8	82.8	82.8	82.8	82.8
W_s [MW]	**77.5**	**77.5**	**77.5**	**77.5**	**77.5**	**77.5**	**77.5**	**120**	**120**
P_h [bar]	**22.0**	**22.0**	**22.0**	**22.0**	50.4	**30.0**	**37.0**	**30.0**	**30.0**
Pressure ratio [-]	**5.5**	**5.5**	**5.5**	**5.5**	22.5	16.6	11.7	7.3	7.2
P_l [bar]	4.0	4.0	4.0	4.0	2.24	1.81	3.17	4.11	4.16
Head [$\text{kJ}\,\text{kg}^{-1}$]	134	135	136	145	256	216	200	162	161
V_{suc} [$\text{m}^3\,\text{s}^{-1}$]	84.3	83.3	84.0	83.9	75.1	**106**	**70**	**106**	**106**
UA_{HOT} [$\text{MW}\,^\circ\text{C}^{-1}$]	38.4	40.9	41.3	39.8	18.7	22.9	26.8	51.8	52.2
UA_{NG} [$\text{MW}\,^\circ\text{C}^{-1}$]	4.8	4.4	4.4	4.6	5.7	5.5	5.8	8.0	8.2
UA_{tot} [$\text{MW}\,^\circ\text{C}^{-1}$]	43.1	45.3	45.7	44.4	24.4	28.4	32.6	59.8	60.4
$\hat{C}_0 \cdot 10^{-3}$ [$\text{kg}\,\text{s}^{-1}\,\text{m}^{-1.3}$]*	**110**	**120**	**130**	**107**	**37**	**51**	**54**	**3000**	**3000**
Refrigerant composition:									
x_{CH_4} [mole-%]	33.3	32.3	32.3	32.5	31.1	29.2	31.9	32.5	33.2
$x_{C_2H_6}$ [mole-%]	35.3	33.2	33.4	34.7	32.3	32.9	32.7	32.9	33.5
$x_{C_3H_8}$ [mole-%]	0.0	0.0	0.0	0.0	0.0	0.0	0.0	0.0	0.0
$x_{n-C_4H_{10}}$ [mole-%]	25.0	24.6	24.3	22.8	26.7	30.3	25.2	23.4	23.5
x_{N_2} [mole-%]	6.4	9.9	10.0	10.0	9.9	7.6	10.2	11.2	9.8

*$\hat{C}_0$ adjusted to obtain $\Delta T_{\text{min}} \approx 2.0\,^\circ\text{C}$

Case 6.1 *Nominal design using data from Price and Mortko (1996) in Table 6.2.*

We specify the LNG temperature at the exit of NG HX (T_{out}) to $-144\,^{\circ}\text{C}$ (Price and Mortko, 1996). The LNG production ($\dot{m} = 2.52\,\text{kmole}\,\text{s}^{-1} = 44.6\,\text{kg}\,\text{s}^{-1}$) is slightly larger (3.7%) than that reported by Price and Mortko (1996) ($\dot{m}_{\text{LNG}} = 2.43\,\text{kmol}\,\text{s}^{-1}$*), but note that the feed composition is different and that we have neglected the removal of heavy components. On the other hand, we have not included the heating of flash gas (in Fuel HX) before re-compression to turbine fuel which would have further increased the LNG production by providing some cooling for free.

The resulting flash gas is $7.7\,\text{kg}\,\text{s}^{-1}$ and will produce about 230 MW of energy by combustion in a gas turbine (assuming 60% efficiency and $50\,\text{MJ}\,\text{kg}^{-1}$). This is too high considering that the refrigerant compressor consumes less than 80 MW. In the remaining cases we have therefore limited the amount of flash gas to $3.33\,\text{kg}\,\text{s}^{-1}$ to achieve about 100 MW equivalents of fuel, which replaces the specification on T_{out}.

Case 6.2 *Constraint on the amount of flash gas after expansion (*$3.33\,\text{kg}\,\text{s}^{-1}$*) such that it gives about* 100 MW *worth of energy in a gas turbine.*

Note that the temperature out of the heat exchanger (T_{out}) is reduced from -144 to $-156\,^{\circ}\text{C}$ to reduce the amount of flash gas. This results in a 6.0% reduction in production compared with Case 6.1 ($\dot{m}_{\text{LNG}}$ drops from $44.6\,\text{kg}\,\text{s}^{-1}$ to $41.7\,\text{kg}\,\text{s}^{-1}$). This is because we are unable to cool as much natural gas and this is not compensated for by the increased liquid fraction after expansion. The effect of the outlet temperature (T_{out}) is further discussed below.

Case 6.3 *Optimized super-heating.*

We find by removing the constraint on super-heating, that ΔT_{sup} increases from $10.0\,^{\circ}\text{C}$ to the optimal value of $11.6\,^{\circ}\text{C}$. This gives an 0.8% increase in LNG production compared with Case 6.2. This illustrates, as discussed by Jensen and Skogestad (2007), that the optimal super-heating is not zero for a system with internal heat exchange.

Case 6.4 *Higher degree of super-heating.*

In this case we specify a higher degree of super-heating ($25.7\,^{\circ}\text{C}$ compared to the optimal of $11.6\,^{\circ}\text{C}$). This gives only a 1.3% reduction in LNG production compared to Case 6.3, which shows that the optimum is "flat" in terms of super-heating. With $0.22\,^{\circ}\text{C}$ super-heating we get a reduction of 2.3% in LNG production compared with Case 6.3.

*Calculated from $4.71\,\text{MNm}^3\,\text{day}^{-1}$

In reality, we expect that the heat transfer coefficient is lower in the super-heating section than in the vaporization section. This suggests that the optimal degree of super-heating will be lower than what we find with constant heat transfer coefficients.

Until now we have fixed the two refrigerant pressures. Specifically, the discharge pressure P_h is fixed at 22 bar and the pressure ratio, $Pr = P_h/P_l$ at 5.5 (Table 6.3). However, some authors have published optimization results with discharge pressure much higher than 22.0 bar (Lee et al., 2002; Del Nogal et al., 2005). They also claim that the refrigerant flowrate should be about 3-4 times the flowrate of natural gas on mole basis. For the cases up till now we have obtained a ratio of about 6, which is about 50 % higher. These two observations are closely related as the amount of refrigerant depends on the pressure ratio (Pr).

Case 6.5 *No pressure constraints*

Here we optimize the process without the constraint on discharge pressure and pressure ratio. We see that the production is increased from 41.7 kg s^{-1} to 46.3 kg s^{-1} (11 %) while the refrigerant amount is reduced from 14.7 kmole s^{-1} to 7.64 kmole s^{-1} (which gives a ratio 2.9 between refrigerant and LNG flowrate). To achieve this, the high pressure is increased to $P_h = 50.4$ bar and the pressure ratio is $Pr = 22$.

Some other interesting results to note are:

- the compressor suction volume decreases
- the necessary heat transfer area for the warm refrigerant stream is less than half, UA is 18.8 MW/°C compared to 40.9 MW/°C for Case 6.2

Both these effects are related to the fact that much less refrigerant is needed, but how can this be explained? The cooling duty per kg of refrigerant is closely related to the compressor head, [kJ kg^{-1}], which again is closely related to the pressure ratio. So increasing the compressor head (and pressure ratio) will increase the cooling duty per kg of refrigerant and thus decrease the required amount of refrigerant.

There is a potential problem with this design. A high pressure ratio usually requires more compressor stages (casings) and this may not be desirable, although some of the extra capital cost related to the extra compressor casing and higher pressure will be offset by the reduction in heat transfer area.

We wish to limit the PRICO process to one compressor casing, which may not be feasible with the high pressure ratio of 22 in Case 6.5. To get a realistic design we use performance specifications for the MCL1800 series compressor from General Electric Oil and Gas (January 2007).

Case 6.6 *MCL1800 series compressor.*

MCL1800 is a centrifugal compressor with casing diameter of 1800 mm. The reported maximum suction volume is 380000 $m^3 h^{-1}$ or about 106 $m^3 s^{-1}$, the maximum discharge pressure is 30 bar and the maximum shaft work is 120 MW (General Electric Oil and Gas, January 2007). In this case we keep 77.5 MW as the maximum compressor shaft work to compare with the other cases, and specify a maximum compressor suction volume of 106 $m^3 s^{-1}$ and maximum pressure of 30 bar.

Interestingly, the results show that we are able to almost match the production and pressure ratios obtained in Case 6.5 with realistic specifications and one compressor casing. The total head in the compressor may be achieved with one compressor casing with 5 wheels and a rotational speed of 3600 RPM, see Table 6.1.

Note that the suction volume V_{suc} is an active constraint for the three last cases in Table 6.3 where actual compressor data are utilized.

The MCL1800 compressor seems a bit large for the specified duty, so let us try a smaller compressor.

Case 6.7 *MCL1400 series compressor.*

MCL1400 is a centrifugal compressor with a casing diameter of 1400 mm. The reported maximum suction volume is 250000 $m^3 h^{-1}$ or about 70 $m^3 s^{-1}$, the maximum discharge pressure is 37 bar and the maximum shaft work is 75 MW (General Electric Oil and Gas, January 2007). We have assumed that it is possible to use 77.5 MW power.

We get a slightly higher production (3.6 %) compared with Case 6.6. This illustrates that the increase in outlet pressure (from 30 bar to 37 bar) more than compensates for the reduction in compressor suction volume (from 106 $m^3 s^{-1}$ to 70 $m^3 s^{-1}$). The reqired head is slightly reduced because of a higher suction pressure. However, the maximum head is reduced compared with the MCL1800 compressor because of a reduced tip speed. The total achievable head in the compressor is strongly affected by the reduction in wheel diameter throughout the compressor casing. Using a 7.0 cm reduction from one wheel to the next and an intial wheel diameter of 1.35 m gives an estimated maximum total head of 172 $kJ kg^{-1}$ with 6 compressor wheels. This is significantly less than the required amount and we believe that the design in Case 6.7 is infeasible with one compressor casing, but a detailed compressor design is necessary to verify this conclusion.

Finally, we would like to find the maximum train capacity limit for the PRICO process with a single compressor casing.

Case 6.8 *Again we utilize the larger MCL1800, but we allow for more shaft power, namely* 120 MW

We find that we may produce 71.1 kg s^{-1} LNG in a single PRICO train with one compressor casing using realistic design data. Note that the required compressor head is reduced from 216 kJ kg^{-1} to 162 kJ kg^{-1} compared to Case 6.6 so for this case we may use a slower driver (see Table 6.1), for example a Frame 9 gas turbine with rotational speed of 3000 RPM (General Electric Oil and Gas, January 2007).

Note that the cost factor $\hat{C}_0 = 3000$ is increased tenfolds compared to the other cases. This was necessary to achieve $\Delta T_{\min} = 2.0\,^{\circ}\mathrm{C}$. There seems to be no practical reasons for this large increase in the cost factor and an alternative design optimization is given below.

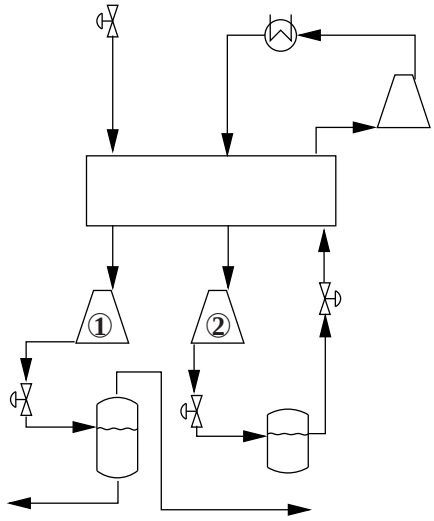

Figure 6.3: A flowsheet of the PRICO process illustrating the use of liquid turbine and valve as expansion device

The LNG expansion valve and the refrigerant expansion valve shown in Figure 6.1 may be exchanged with a combination of liquid turbine and valve, see Figure 6.3. Ideally, one would do the entire expansion in a turbine, but two-phase turbines are to our knowledge not in use so it is necessary to use the combination of a liquid turbine and a valve (Barclay and Yang, 2006). The liquid turbine will then take the pressure down to slightly above the saturation pressure and the expansion valve will take care of the two-phase expansion. The main advantage with this solution is not that power is generated by the liquid turbine (this is actually quite small), but rather the extra cooling provided by the isentropic expansion in the turbine compared to isenthalpic expansion in the valve. This reduces; i) the amount of

flash gas that does not contribute to the product for LNG expansion and ii) the amount of flash gas that does not contribute significantly to the cooling, but still needs to be compressed by the compressor for the refrigerant expansion.

Case 6.9 *A liquid turbine is included in the expansion of the natural gas* ① *and in the expansion of the refrigerant* ②.

The production is further increased by 6.6% compared with Case 6.8. The total heat transfer area is increased by 1.0%. Note that also for this case we had to specify a high $\hat{C}_0$ to obtain $\Delta T_{\min} \approx 2.0\,^{\circ}\mathrm{C}$.

We have assumed an isentropic efficiency of 80% in the liquid turbines. We have used a back-off from saturation at the turbine outlet of 2.0 bar. A turbine will be even more advantageous for cases with higher pressures, both in the refrigerant cycle and in the natural gas stream.

In summary, we see that some design constraints strongly affect the optimal solution. These constraints are related to the compressor performance; maximum suction volume, maximum discharge pressure, maximum head and maximum shaft work. The changes given by these constraints are illustrated in cases 6.5 to 6.8. Other constraints have less influence on the optimal solution; these are the degree of super-heating and the amount of flash gas (determined by the temperature after cooling or the amount of flash gas). The changes given by these constraints are illustrated by the first four cases.

6.3.1 An alternative design optimization

Above we adjusted the cost factor $\hat{C}_0$ to achieve $\Delta T_{\min} \approx 2.0\,^{\circ}\mathrm{C}$. For Case 6.8 this resulted in a cost factor unrealistically much larger than for the other cases. We suspect that this is due to the non-linear behaviour of $\Delta T_{\min}$. A better approach may be to fix $\hat{C}_0$. Here $\hat{C}_0 = 110 \cdot 10^3\,\mathrm{kg\,s^{-1}}\left(\mathrm{m^{-2}}\right)^{0.65}$ is used for all cases.

Table 6.4 shows key results for all nine cases with the same specifications for super-heating, maximum work and pressures as before. Note that for Case 6.8 we get an increase by 8.6% in the LNG production compared to the corresponding case in Table 6.3 where $\hat{C}_0 = 3000 \cdot 10^3\,\mathrm{kg\,s^{-1}}\left(\mathrm{m^{-2}}\right)^{0.65}$. This is achieved by increasing the total heat transfer area by 24.7% and $\Delta T_{\min}$ is reduced from 2.0 °C to 1.5 °C. A similar increased production and heat transfer areas is achieved for Case 6.9. For cases 6.5 to 6.7 the production is reduced compared to the results in Table 6.3.

The results in Table 6.4 are obtained more easily than the results in Table 6.3,

Table 6.4: Optimal design with $C_0 = 110 \cdot 10^3 \,\mathrm{kg\,s^{-1}} \left(\mathrm{m^{-2}}\right)^{0.65}$

Alternative Case	6.1	6.2	6.3	6.4	6.5	6.6	6.7	6.8	6.9
$\dot{m}_{\mathrm{LNG}}\,[\mathrm{kg\,s^{-1}}]$	44.6	45.4	45.8	44.3	36.5	42.6	45.1	77.2	81.4
$\Delta T_{\mathrm{min}}\,[^\circ\mathrm{C}]$	1.96	1.96	1.86	2.04	2.89	2.51	2.37	1.48	1.65
$UA_{\mathrm{HOT}}\,[\mathrm{MW\,^\circ C^{-1}}]$	38.4	41.7	42.3	39.7	8.0	18.4	22.5	64.2	62.8
$UA_{\mathrm{NG}}\,[\mathrm{MW\,^\circ C^{-1}}]$	4.8	4.6	4.7	4.5	2.9	4.1	4.6	10.3	10.4
$UA_{\mathrm{tot}}\,[\mathrm{MW\,^\circ C^{-1}}]$	43.1	46.4	46.9	44.2	10.9	22.5	27.1	74.6	73.2
Change compared with Table 6.3									
$\Delta\dot{m}_{\mathrm{LNG}}\,[\%]$	0.0	8.9	9.0	-1.1	-21.2	-8.0	-6.2	8.6	7.4
$\Delta UA_{\mathrm{tot}}\,[\%]$	0.0	2.4	2.6	-0.45	-55.5	-21.0	-16.9	24.7	21.2

where it was necessary to adjust $\hat{C}_0$ until we got $\Delta T_{\mathrm{min}} \approx 2.0\,^\circ\mathrm{C}$.

In terms of optimality it seems better to fix the cost factor $\hat{C}_0$ rather than the ΔT_{min}.

In Cases 6.2 and 6.3 the relative (percent) increase in production ($\dot{m}_{\mathrm{LNG}}$) is more than three times the relative increase in heat transfer area (UA_{tot}), even though the work W_s is constant. This indicates strongly that the cost factor $\hat{C}_0$ is too high. An alternative approach would therefore be to adjust $\hat{C}_0$ such that the relative increase in $\dot{m}_{\mathrm{LNG}}$ and UA_{tot} are similar.

6.4 Discussion

6.4.1 Compressor

The number of impellers, or wheels, in the compressor will affect the achievable head. Lüdtke (2004) reports that centrifugal compressor may be manufactured with up to ten impellers in one casing, but that more than five impellers usually gives a cost in terms of reduced efficiency. General Electric Oil and Gas (January 2007) indicates that their compressors may be delivered with up to eight impellers. Based on the numbers for maximum head per impeller in Table 6.1 we have no difficulty achieving the necessary head for the cases presented with the MCL1800 compressor, see Table 6.3. However, there is some uncertainty:

- The wheel diameter is decreasing through the compressor, and finding the optimal design requires a detailed analysis of the compressor.
- The number of wheels may affect the efficiency, which we have assumed constant at 82.8 %.

Price and Mortko (1996) report that the PRICO process uses an axial compressor. The efficiency may be slightly higher for an axial compressor than for a centrifugal compressor.

6.4.2 Heavy extraction

We have neglected the process for removing heavy components from the natural gas stream. The paper by Price and Mortko (1996) shows that this process is integrated in the refrigeration process as shown in Figure 6.4(a). The natural gas is taken out of the heat exchanger after being cooled somewhat. The heavy components are then in the liquid phase and is extracted (methane and ethane in the liquid is recovered and mixed with the LNG product). The vapour stream is sent back to the heat exchanger for further cooling.

Alternatively, one may have the removal of heavy components before the refrigeration process. This is shown in Figure 6.4(b).

The choice between upstream and integrated NGL recovery depends on several factors and will not be treated here.

The fraction of NGL in the natural gas feed is quite small for the case we have considered, so we believe inclusion of an integrated NGL extraction will not have a large impact on our results.

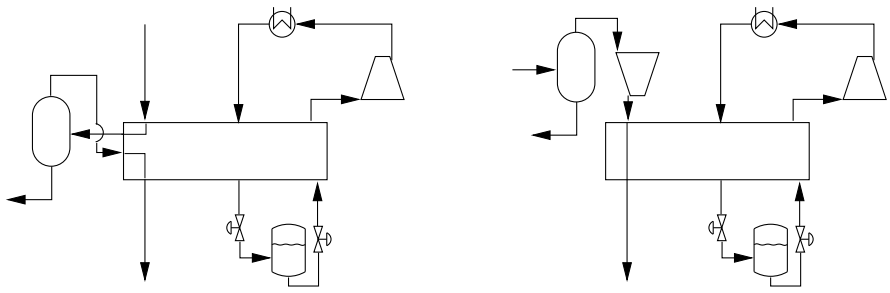

(a) Integrated NGL recovery (b) Upstream NGL recovery

Figure 6.4: Alternative locations of the NGL recovery

6.4.3 Feed pressure

Higher feed pressure gives higher maximum production because the main part of the cooling will be at a higher temperature (since the condensation temperature range is higher with increased pressure). Figure 6.5 shows the maximum production as function of feed pressure. However, this effect is not for free since a feed compressor is needed. For example, compressing the feed from 40 bar to 60 bar requires a compressor with about 5.3 MW power for the natural gas flowrate in Case 6.8. To find the optimal feed pressure it is necessary to also consider the feed compressor and the extra capital cost related to higher pressure in the heat exchanger and piping.

The feed pressure increase is limited if the NGL extraction is integrated (because the separation in NGL extraction is harder at higher pressure, e.g. propane has a critical pressure of about 42 bar) so very high feed pressures are only feasible for plants with NGL extraction prior to refrigeration.

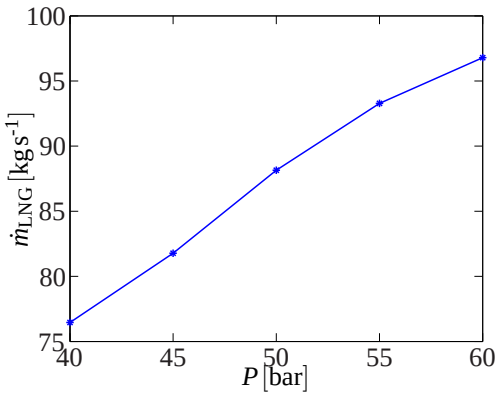

Figure 6.5: Maximum LNG production as function of feed pressure for Case 6.9

6.4.4 Large PRICO plants?

Larger production rates requires more than one compressor, so one then has the choice of using more PRICO trains in parallel or to use more cycles in cascade with one compressor for each cycle. An obvious advantage with choosing more parallel PRICO trains is that one may operate on part load if one compressor shuts down. But important issues are thermodynamic efficiency and capital cost compared with cascaded cycles.

Based on Case 6.9 in Table 6.3 we get a maximum LNG production of about

$76\,\mathrm{kg\,s^{-1}}$, see Figure 6.5 with $P = 40\,\mathrm{bar}$. This is about 2.2 MTPA based on 335 operating days per year so two trains in parallel gives about 4.4 MTPA while three trains in parallel gives about 6.6 MTPA. However, if a large plant is constructed one may wish to have the NGL extraction up front and install a feed compressor prior to the refrigeration process. From Figure 6.5 we see that a feed pressure of 60 bar gives a maximum production of about $97\,\mathrm{kg\,s^{-1}}$ or 2.8 MTPA per train. This results in a maximum production of 5.6 MTPA and 8.4 MTPA for two and three parallel trains respectively. Even higher feed pressures may be feasible.

The specific work is $439\,\mathrm{kWh\,t^{-1}}$ for 40 bar feed pressure and $344\,\mathrm{kwh\,t^{-1}}$ for 60 bar feed pressure for the process with liquid turbine for expansion of LNG and refrigerant. This is without considering the shaft work generated by the turbines and required by the feed and fuel compressor.

Roberts et al. (2004) presents different driver configurations for the AP-X process from the Air Products company. The configuration with the highest production (10 MTPA) is with three Frame 9 gas turbines and and additional 10 MW from the helper/starter motor, giving a total of 400 MW. We have assumed 130 MW for each Frame 9 gas turbine; this the ISO rating (General Electric Oil and Gas, January 2007). With the same available shaft work we would achieve

$$\frac{2.8\,\mathrm{MTPA}}{120\,\mathrm{MW}} \cdot 400\,\mathrm{MW} = 9.3\,\mathrm{MTPA}$$

for the PRICO process with 60 bar feed pressure and liquid turbine for expansion of both LNG and refrigerant. This is 7% lower for the same shaft work, but the actual numbers will depend heavily on several factors such as feed pressure, feed temperature, feed composition and actual compressor performance.

6.5 Conclusion

An objective function for design optimization has been derived for a PRICO process. The process is optimized for several different constraints and compared with the commercial process and other publications. Using compressor specifications found online we are able to increase the LNG production compared to the commercial process. Important constraints, especially concerning the compressor feasibility, are discussed. Finally, we found that the PRICO process has about 7% less production than the AP-X process with the same available shaft power.

Bibliography

Barclay, M. A. and Yang, C. C. (2006), Offshore LNG: The perfect starting point for the 2-phase expander?, *in* 'Offshore Technology Conference, Houston, Texas, USA'.

Del Nogal, F., Kim, J., Smith, R. and Perry, S. J. (2005), 'Improved design of mixed refrigerant cycles using mathematical programming', *Gas Processors Association (GPA) Europe Meeting, Amsterdam* .

General Electric Oil and Gas (January 2007), 'Liquefied natural gas: Enhanced solutions for LNG plants'. `www.gepower.com/businesses/ge_oilandgas/en/downloads/liquified_natural_gas.pdf`.

Jensen, J. B. and Skogestad, S. (2007), 'Optimal operation of simple refrigeration cycles. Part I: Degrees of freedom and optimality of sub-cooling', *Comput. Chem. Eng.* **31**, 712–721.

Lee, G. C., Smith, R. and Zhu, X. X. (2002), 'Optimal synthesis of mixed-refrigerant systems for low-temperature processes', *Ind. Eng. Chem. Res.* **41**(20), 5016–5028.

Lüdtke, K. H. (2004), *Process centrifugal compressors*, Springer-Verlag, Berlin Heidelberg.

Price, B. C. and Mortko, R. A. (1996), PRICO - a simple, flexible proven approach to natural gas liquefaction, *in* 'GASTECH, LNG, Natural Gas, LPG international conference , Vienna'.

Roberts, M. J., Liu, Y., Bronfenbrenner, J. C. and Petrowski, J. M. (2004), Reducing LNG capital cost in today's competitive environment, *in* 'LNG 14 conference, Doha, Quatar'.

Stebbing, R. and O'Brien, J. (1975), An updated report on the PRICO (TM) process for LNG plants, *in* 'GASTECH, LNG, Natural Gas, LPG international conference , Paris'.

Chapter 7

Optimal operation of a simple LNG process

Considering the large amount of work that goes into the design of LNG processes, there is surprisingly little attention to their subsequent operation. This partly comes from the assumption that optimal design and optimal operation are the same, but this is not generally true. In this paper we study the optimal operation of a relatively simple LNG process, namely the PRICO process. We find that the process has four operational degrees of freedom (neglecting the degrees of freedom related to refrigerant composition). We then study the two modes of operation; i) given production and ii) maximum production.

7.1 Introduction

The process considered in this paper is a single mixed refrigerant process, namely the PRICO process (Stebbing and O'Brien, 1975; Price and Mortko, 1996). This is the simplest configuration used commercially for liquefaction of natural gas and it has been optimized in several publications (Lee et al., 2002; Del Nogal et al., 2005, Chapter 6), but only with respect to design. Singh and Hovd (2006) study the controllability of the process but they do not consider optimal operation which is the theme in this paper.

An important issue in plantwide control is to find the degrees of freedom that may be used for online optimization (Skogestad, 2002). In our case these are the same as the steady-state operational degrees of freedom and this number is important for several reasons. First, it determines the degrees of freedom available for solving

the optimization problem. However, more importantly in terms of operation it determines the number of steady-state controlled variables that need to be selected. Optimal operation is normally implemented by keeping the selected variables at constant setpoints. Note that the selection of controlled variables is equally important if we use a model-based control structure such as model predictive control (MPC).

There are two main modes of operation for a LNG process:

1. With a given LNG production (load), minimize the compressor shaft work, W_s, (optimize efficiency).

2. Maximize the LNG production rate subject to given constraint (maximum shaft work W_s^{max}).

In general, to implement optimal operation, we first need to control active constraints. Second, we need to find controlled variables for the unconstrained degrees of freedom. We here use the self-optimizing control approach. "Self-optimizing control is when we can achieve acceptable loss with constant setpoint values for the controlled variables (without the need to re-optimize when disturbances occur)" (Skogestad, 2000).

7.2 Process description

Figure 7.1 shows a simplified flowsheet of the PRICO process. The PRICO process works as follows: After compression to pressure P_h, the mixed refrigerant is cooled to 30 °C in a sea water (SW) cooler before it is further cooled together with the natural gas in the main heat exchanger. The high pressure sub-cooled liquid is then sent through a liquid turbine and a choke valve to give a low-temperature saturated liquid at pressure P_m in the receiver. The liquid is further expanded to low pressure P_l to give a two-phase mixture which is vaporized in the main heat exchanger to provide the necessary cooling duty. The vapour is slightly super-heated before it is compressed back to the high pressure. The PRICO process is discussed in more detail in Chapter 6. We here consider Case 6.9 from Chapter 6, where a liquid turbine is included both in the expansion of natural gas and expansion of the refrigerant.

Note that the refrigerant is only partially condensed at pressure P_h in the sea water (SW) cooler so both liquid and vapour are fed to the main heat exchanger. We have placed the liquid receiver at an intermediate pressure (P_m) before the choke valve.

The extra choke valve between the liquid turbine and receiver is to give a safety margin to saturation at the liquid turbine outlet.

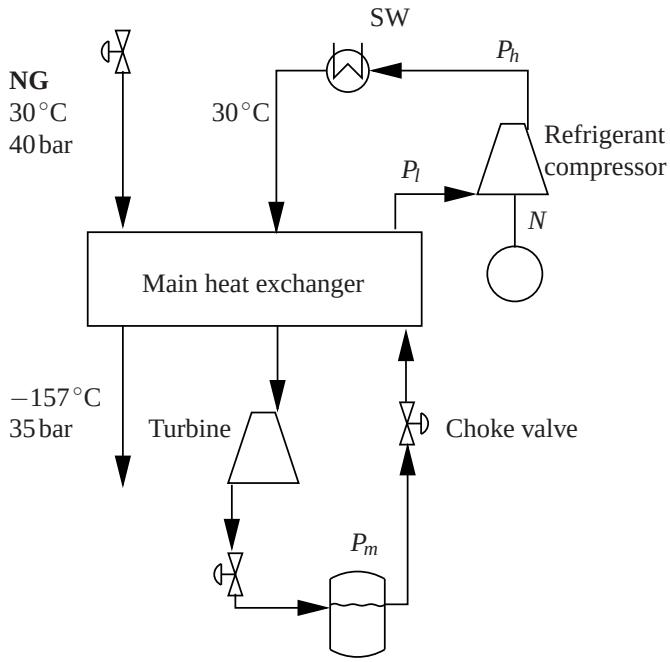

Figure 7.1: A simplified flowsheet of the PRICO process

Note that we have not included any extraction of heavy components from the natural gas feed.

7.2.1 Nominal conditions

- The natural gas enters, after pretreatment, with a pressure of 40 bar and a temperature of 30 °C
- Composition of natural gas (mole-%): 89.7% methane, 5.5% ethane, 1.8% propane, 0.1% n-butane and 2.8% nitrogen
- Pressure drops:
  - 5 bar in natural gas stream
  - 0.1 bar in SW cooler
  - 4 bar for hot refrigerant in main heat exchanger

  - 1 bar for cold refrigerant in main heat exchanger
  - 0.3 bar for the compressor suction
- Constant heat transfer coefficients (UA)
- The refrigerant is a mix of nitrogen (N_2), methane (C_1), ethane (C_2), propane (C_3) and n-butane (nC_4) and the composition is used as a degree of freedom in the optimization
- Cooling of refrigerant to 30 °C in SW cooler
- Maximum shaft work in the compressor $W_s^{max} = 120\,\text{MW}$
- We have not considered the turbine characteristic and we have assumed a constant pressure drop of 2.0 bar across the valve after the turbine. This valve is necessary to guarantee that no vapour is formed in the liquid turbine.

7.2.2 Manipulated inputs

There are 9 manipulated inputs with a steady-state effect (potential control degrees of freedom for control, u_0):

1 Compressor: rotational speed N

2 Choke valve: valve opening z

3 Turbine: rotational speed

4 Cooler: flow of sea water (SW) in cooler

5 Load: Feed flow of natural gas (can also be considered a disturbance)

6-9 Composition of refrigerant (5 components give 4 independent compositions). These degrees of freedom are not considered for control, but need to be optimized at the design stage.

Assuming maximum cooling of refrigerant in the SW cooler, or rather fixing $T = 30\,^{\circ}\text{C}$ after the SW cooling, which consumes 1 degree of freedom this leaves 8 degrees of freedom. To find the nominal optimal steady-state operating point we will use all 8 degrees of freedom, but during operation we will assume constant refrigerant composition so there are only 4 steady-state control degrees of freedom.

7.2.3 Operational constraints

In general there are many constraints (represented by the equation $c \leq 0$ in the optimization problems) that must be satisfied during operation.

- Super-heating (ΔT_{sup}): The stream entering the compressor must not contain liquid (but note that this is not necessary an active constraint in this case, because there is internal heat exchange, so it is actually optimal with some super-heating, see Chapter 6).

- T_{LNG}^{out}: Natural gas temperature out of the main heat exchanger should be within certain bounds. This temperature sets the amount of flash gas and affects the composition of flash gas and LNG.

- Refrigerant pressure: Maximum bound (not considered in this paper)

- Compressor outlet temperature: Maximum bound (not considered in this paper)

- Compressor power (W_s): We assume maximum at 120 MW, see Chapter 6.

- Compressor rotational speed (N): We assume maximum at 100 %.

- Compressor surge: The compressor may in theory be operated in the surge region using active surge control (Gravdahl and Egeland, 1999), but normally one would like to operate with a certain margin to surge. In this paper, we use the peak of the compressor characteristic curve as the limit (see Figure 7.3). We define the variable $\Delta \dot{m}_{\text{surge}}$ to be the distance from the peak of the characteristic curve, and use the value $\Delta \dot{m}_{\text{surge}} \geq 0.0\,\text{kg}\,\text{s}^{-1}$ (i.e. no back-off).

- All flows must be non-negative and also have upper bounds.

In particular, the cooling water flow has a maximum value, and it is clear from physical insight that maximum cooling is optimal (active constraint). Assuming that we have a large area in this heat exchanger, we will in the following replace this constraint by the following:

- Maximum cooling: Assume refrigerant has $T = 30\,^{\circ}\text{C}$ after SW cooler

With the assumption of $T = 30\,^{\circ}\text{C}$ after the SW cooler (flow of sea water at maximum), we are left with 8 steady-state degrees of freedom (4 for control).

7.3 Model

When switching from design simulations to operation it is necessary to reformulate parts of the models, because the equipment is fixed. Our goal is to have simple models that capture the most important operational effects. We will here discuss the features that we have included in the operational models and also briefly mention the effects that we have not considered.

The process is modelled using the gPROMS software with the accompanying Multiflash package for thermodynamic calculations. The SRK equation of state is used for thermodynamic calculations both for the natural gas and the refrigerant. The main heat exchanger is a distributed system, which for modelling purposes has been discretized into 100 cells using forward and backward finite difference method, for the cold and hot streams respectively.

The pressure drop at the compressor inlet (suction) is modelled as:

$$\Delta P_{\text{suc}} = \Delta P_{\text{suc},0} \left(\frac{V_{\text{suc}}}{V_{\text{suc},0}} \right)^2 \tag{7.1}$$

The remaining pressure drops are assumed constant. The structure of the model equations are summarized in Table 7.3.

7.3.1 Compressor characteristic

In operation, one normally uses compressor characteristic curves to model the compressor behaviour. These curves, relating flow, efficiency, pressure increase and rotational speed, are normally supplied by the compressor vendor of the installed compressor, but since we do not have a specific design and vendor we need a more general approach.

Non-dimensional groups

Compressor characteristics are easiest represented using non-dimensional groups. For example, Saravanamuttoo et al. (2001) assume the following functional dependence*:

$$f(D, N, \dot{m}, P_1, P_2, T_1, T_2, \hat{R}) = 0 \tag{7.2}$$

*They actually use the two groups $\hat{R}T_1$ and $\hat{R}T_2$ instead of our three terms, T_1, T_2 and $\hat{R}$

where the characteristic length $D\,[\mathrm{m}]$ is usually taken as the compressor wheel diameter, $N\,[\mathrm{s^{-1}}]$ is the rotational speed, $\dot{m}\,[\mathrm{kg\,s^{-1}}]$ is the mass flowrate, $P\,[\mathrm{kg\,m\,s^{-2}}]$ is the pressure, $\hat{R} = R/MW\,[\mathrm{J\,kg^{-1}\,K^{-1}}]$ is the specific gas constant and $T\,[\mathrm{K}]$ is the temperature. Subscripts 1 and 2 represent the compressor inlet and outlet, respectively. Using the Pi theorem of dimensional analysis, Saravanamuttoo et al. (2001) reduce these 7 function dependencies to 4 independent non-dimensional groups:

$$Pr = \frac{P_2}{P_1}, \quad Tr = \frac{T_2}{T_1}, \quad \dot{m}r = \frac{\dot{m}\sqrt{\hat{R}T_1}}{D^2 P_1} \quad \text{and} \quad Nr = \frac{ND}{\sqrt{\hat{R}T_1}} \tag{7.3}$$

(pressure ratio, temperature ratio, reduced flow and reduced speed). From these four groups it is possible to express one group in terms of the remaining three, but Saravanamuttoo et al. (2001) claims that the groups $\frac{P_2}{P_1}$ and $\frac{T_2}{T_1}$ may be plotted against the last two groups. The justification for this (which we could not find in Saravanamuttoo et al. (2001)) is probably that the outlet conditions of the compressor (T_2 and P_2) should depend on the inlet conditions only, which are expressed by $\dot{m}r$ and Nr.

It is common to report the isentropic efficiency η instead of the temperature rise $\frac{T_2}{T_1}$ so the following dependencies are used to quantify the steady-state operation of the compressor:

$$Pr = f(\dot{m}r, Nr) \tag{7.4}$$

$$\eta = f(\dot{m}r, Nr) \tag{7.5}$$

Characteristic compressor curves

The dependencies in 7.4 and 7.5 are normally given graphically as "curves", but we are here looking for simple algebraic relationships.

We use the method of Moore and Greitzer (1986) cited in Gravdahl and Egeland (1999) with some adjustments. Moore and Greitzer (1986) proposed to use a cubic equation to predict the characteristic curve of a compressor. The equation for the pressure ratio is (using our own nomenclature):

$$Pr = Pr_0 + H\left(1 + \frac{3}{2}\left(\frac{\dot{m}r}{W} - 1\right) - \frac{1}{2}\left(\frac{\dot{m}r}{W} - 1\right)^3\right) \tag{7.6}$$

where $Pr = \frac{P_2}{P_1}$ is the pressure ratio over the compressor (the first non-dimensional group in Equation 7.3), Pr_0 is the shut-off value for the compressor (the pressure

ratio delivered at zero flow), H and W are called the semi-height and semi-width of the characteristic curve, respectively, and $\dot{m}_r$ is the reduced mass flowrate (the second non-dimensional group in Equation 7.3).

The cubic equation has three parameters (Pr_0, H and W) which physical significance are indicated in Figure 7.2. The curve is for a given reduced rotational speed N_r (the third non-dimensional group in Equation 7.3).

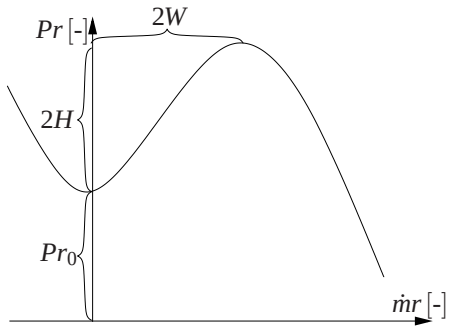

Figure 7.2: A cubic compressor characteristic curve for a constant reduced compressor speed

The surge point where dynamic instability occurs is somewhere near the peak value of the pressure ratio in Figure 7.2. Operation to the left of this point is unstable without active (feedback) control. This is discussed extensively by Gravdahl and Egeland (1999). Note that the surge point is normally close to the "optimal" operating point with peak pressure ratio and peak efficiency.

To get the entire compressor map, for all values of the reduced speed N_r, we propose the following dependency on Nr for the parameter H and W.:

$$H = H_0 - 1.2\left(H_0 + \frac{Pr_0}{2} - 1\right)\cdot(1 - Nr) \tag{7.7}$$

$$W = W_0\,(Nr)^{\frac{1}{3}} \tag{7.8}$$

This is by no means an exact approach, but we get compressor characteristic curves that are similar to typical example curves shown in textbooks (e.g. Saravanamuttoo et al., 2001).

For the isentropic efficiency we propose to use the following function:

$$\eta = \eta_0\left(\left(1 - \left(\frac{H - H_0}{H_0}\right)^2\right) - 1000\,(\dot{m}r - 2W)^2\right) \tag{7.9}$$

This captures the two most important effects; the efficiency has a peak value for a given reduced rotational speed and the peak value is slightly affected by the rotational speed.

A sample compressor map is shown in Figure 7.3. To compute $\dot{m}r$ we have used a compressor with wheel diameter $D = 1.7\,\text{m}$ and a working fluid with molecular weight $MW = 0.032\,\text{kg}\,\text{mol}^{-1}$ and the following values for the parameters in Equation 7.6 to Equation 7.9:

- $Pr_0 = -29$. Note that we have used a negative value for the pressure ratio at zero flowrate. Gravdahl and Egeland (1999) state that $Pr_0 > 0$, but we are only interested in the operating regime to the right of the peak value so this parameter does not have any physical meaning in our model. We have used a high negative value to get a steeper characteristic curve.
- $H_0 = 18.125$
- $W_0 = 0.0698$
- $\eta_0 = 82.2\,\%$

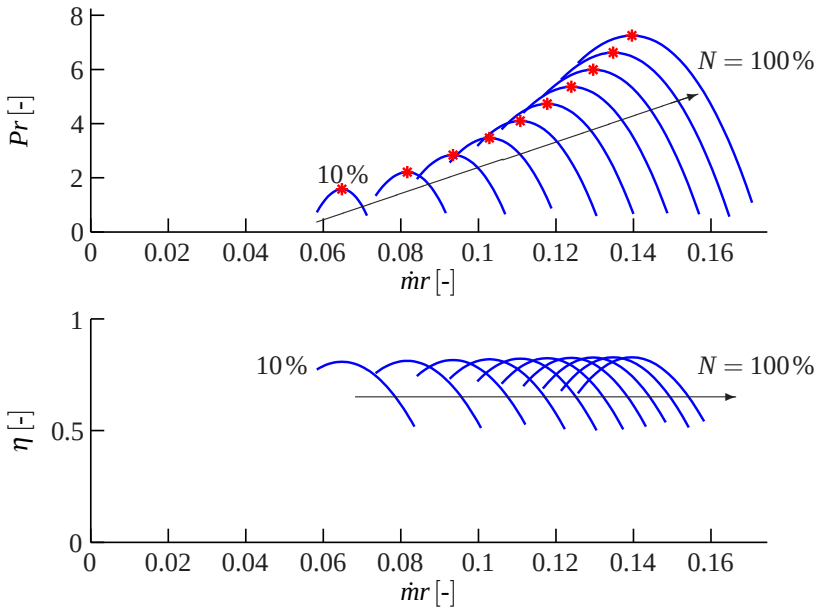

Figure 7.3: Compressor map for the refrigerant compressor using Equations 7.6-7.9 with N in the range 10 % to 100 % and nominal inlet temperature. The red dots indicates the peak for the pressure ratio curve

7.4 Objective function

The objective function for optimal operation is simpler than for optimal design, discussed in Chapter 6, because the investments are already made and the capital cost does not need to be considered. The cost function to be minimized then becomes:

$$\begin{aligned} J_{\text{operation}} = & p_{W_s} \cdot W_s - p_{W_{s,\text{turbine}}} \cdot W_{s,\text{turbine}} + p_{SW} \cdot Q_C \\ & - p_{\text{LNG}} \cdot \dot{m}_{\text{LNG}} + p_{\text{feed}} \cdot \dot{m}_{\text{feed}} - p_{\text{fuel}} \cdot \dot{m}_{\text{fuel}} \end{aligned} \tag{7.10}$$

We make the following assumptions:

- Same price for fuel and feed. Then, $p_{\text{feed}} \cdot \dot{m}_{\text{feed}} - p_{\text{fuel}} \cdot \dot{m}_{\text{fuel}} - p_{\text{LNG}} \cdot \dot{m}_{\text{LNG}} = (p_{\text{feed}} - p_{\text{LNG}}) \cdot \dot{m}_{\text{LNG}} = \hat{p}_{\text{LNG}} \cdot \dot{m}_{\text{LNG}}$
- Neglect income from turbine work, $p_{W_{s,\text{turbine}}} = 0$.
- Neglect cost of cooling, $p_{SW} = 0$

The optimization problem then becomes:

$$\begin{aligned} \min_u \quad & W_s - \hat{p}_{\text{LNG}} \cdot \dot{m}_{\text{LNG}} \\ \text{subject to} \quad & c \leq 0 \end{aligned} \tag{7.11}$$

Here, $c \leq 0$ represent the mathematical formulation of the operational constraints and the model equations.

Depending on product prize and other external factors there are two main operating modes:

Mode I Given throughput: With a given feed flowrate or given LNG production, the optimization problem simplifies to:

$$\begin{aligned} \min_u \quad & W_s \\ \text{subject to} \quad & \dot{m}_{\text{feed}} = \text{given} \quad (\text{or } \dot{m}_{\text{LNG}} = \text{given}) \\ & c \leq 0 \end{aligned} \tag{7.12}$$

Mode I will result in the same optimal operation as the nominal optimal design, provided the optimal design is done correctly (e.g using the simplified TAC method in Chapter 6) and m_{feed} is kept at the nominal feedrate.

Mode II Maximum throughput: If the LNG prize ($\hat{p}_{\text{LNG}}$) is sufficiently high and there is no active constraint related to available feed or product distribution

Table 7.1: The nominal operating point for: Mode I - Given production. Mode II - Maximum production

		Mode I	Mode II
W_s [kW]	Compressor work	106	**120**
P_h [bar]	Cycle high pressure	26.8	30.0
P_l [bar]	Cycle low pressure	3.67	4.14
N [%]	Compressor rotational speed	**100**	**100**
η [%]	Compressor efficiency	82.8	82.8
$\dot{m}_{\text{LNG}}$ [kg s^{-1}]	LNG flowrate	**69.8**	76.7
$\dot{m}_{\text{REF}}$ [kg s^{-1}]	Refrigerant flowrate	549	614
$\Delta\dot{m}_{\text{surge}}$ [kg s^{-1}]	Surge margin	**0.000**	**0.000**
ΔT_{sup} [°C]	Super-heating before compressor	12.9	11.3
T_{out} [°C]	NG temperature after cooling	**-157**	**-157**
x_{CH_4} [mole-%]	Methane in refrigerant	31.9	32.7
$x_{C_2H_6}$ [mole-%]	Ethane in refrigerant	35.2	34.3
$x_{C_3H_8}$ [mole-%]	Propane in refrigerant	**0.0**	**0.0**
$x_{n-C_4H_10}$ [mole-%]	nButane in refrigerant	24.7	23.3
x_{N_2} [mole-%]	Nitrogen in refrigerant	8.2	9.7

Boldface: Specifications and active constraints

(so $\dot{m}_{\text{LNG}}^{\max}$ is not an active constraint), then it will be optimal to maximize the production of LNG and the objective function may be simplified:

$$\begin{aligned} \min_{u} \quad & -\dot{m}_{\text{LNG}} \\ \text{subject to} \quad & c \leq 0 \end{aligned} \tag{7.13}$$

Note that the operation in this mode may be quite different from the "nominal" optimum found for mode I.

7.5 Nominal optimum; given production case (Mode I)

Since the production rate (or feed rate) is fixed there are 7 steady-state degrees of freedom including the 4 refrigerant compositions.

With a given production rate $\dot{m}_{\text{LNG}} = 69.8\,\text{kg s}^{-1}$, the nominal optimum is found by solving the optimization problem in Equation 7.12. The results are summarized in the left column of Table 7.1. The work in 7.12 was minimized with respect to the 7 degrees of freedom, including the 4 refrigerant compositions. Note that we have

assumed that the refrigerant is 30 °C after the SW cooling. The optimal operation of the compressor was found subject to compressor maps (Figure 7.3). We find that the following constraints are active at the nominal optimum:

1. Temperature of natural gas after cooling at maximum ($T_{\text{out}} = -157\,^{\circ}\text{C}$)
2. Surge margin at minimum ($\Delta\dot{m}_{\text{surge}} = 0$)
3. Compressor speed at maximum ($N = 100\,\%$)

Thus, at the nominal optimum, the only unconstrained degrees of freedom are the refrigerant compositions.

7.6 Nominal optimum; maximum production case (Mode II)

Here, we consider mode II where maximum production is the objective, see Equation 7.13. Since the production rate (or feed rate) is free there are 8 steady-state degrees of freedom (with 30 °C after SW cooling). For numerical reasons, optimal operation in mode II was found by solving mode I for increasing values of $\dot{m}_{\text{LNG}} =$ given, until no feasible solution was found.

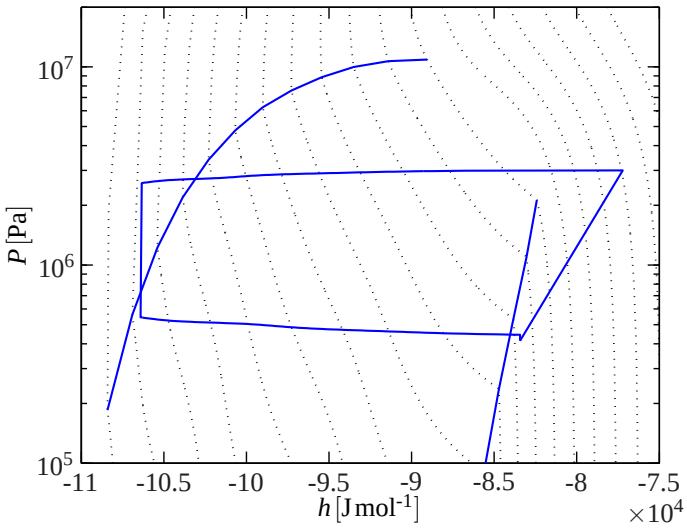

Figure 7.4: Optimal (nominal) pressure enthalpy diagram for the maximum production case (mode II)

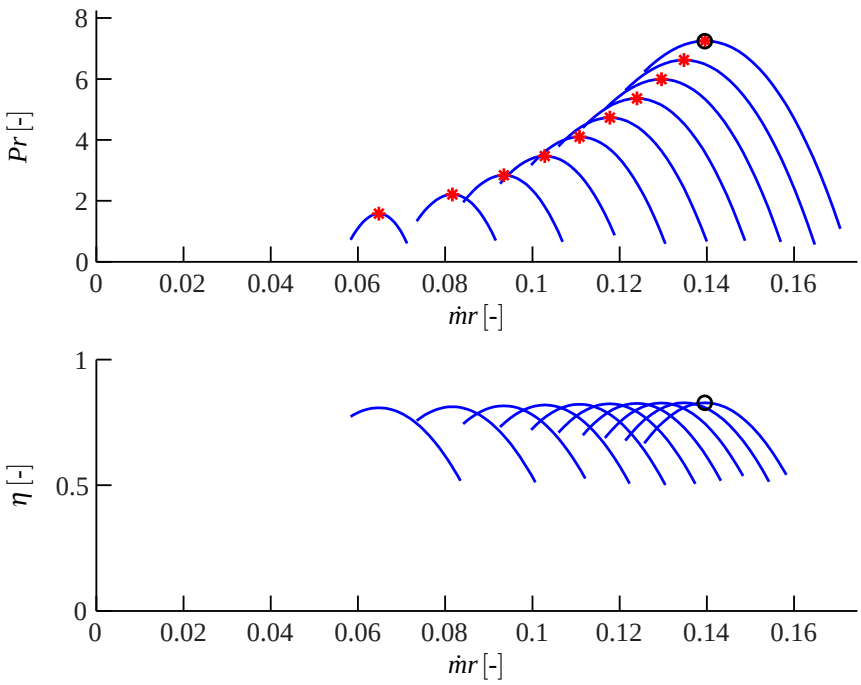

Figure 7.5: The circle shows the optimal (nominal) compressor operating point for the maximum production case (mode II)

The nominal optimum, including the optimal composition of the refrigerant, is summarized in the right column of Table 7.1. The cycle is illustrated in a pressure enthalpy diagram in Figure 7.4 and the optimal temperature and temperature difference profiles in the main heat exchanger are shown in Figure 7.6(a) and 7.6(b) respectively.

We find that the following constraints are active at the nominal optimum:

1. Compressor work at maximum ($W_s = 120\,\text{MW}$)
2. Surge margin at minimum ($\Delta\dot{m}_{\text{surge}} = 0$)
3. Temperature of natural gas after cooling at maximum ($T_{\text{out}} = -157\,^{\circ}\text{C}$)
4. Compressor rotational speed at maximum ($N = 100\,\%$)

Note that there are two “capacity” constraints that are active (1 and 4). Again, the only unconstrained degrees of freedom are related to the refrigerant composition.

We have now identified the nominal optimum for the two cases, but how should

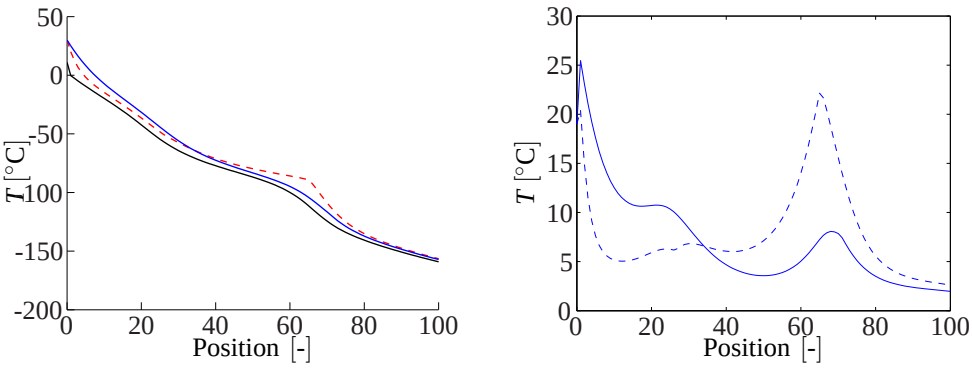

(a) Temperature profile

(b) Temperature difference profile

Figure 7.6: Optimal temperatures in the heat exchanger for the maximum production case (mode II)

we control the process to maintain close to optimal operation when the process is exposed to disturbances? This is discussed next.

7.7 Optimum with disturbances

Table 7.2: Nominal, minimum and maximum values for the disturbances. The numbers in parentheses are for mode I.

	Nominal	Min	Max	Name
W_s^{max} [MW]	120	110	130	d_1*
P_{feed} [bar]	40	35	45	d_2
T_{in} [°C]†	30	25	35	d_3
x_{CH_4} [%]	32.7 (31.9)	29.4 (28.7)	36.0 (35.1)	d_4
$x_{C_2H_6}$ [%]	34.3 (35.2)	30.9 (31.7)	37.7 (38.7)	d_5
$x_{C_4H_{10}}$ [%]	23.3 (24.7)	21.0 (22.2)	25.6 (27.2)	d_6
x_{N_2} [%]	9.7 (8.2)	8.7 (7.4)	10.7 (9.0)	d_7
$\dot{m}_{\text{LNG}}$ [kg s^{-1}]	69.8	66.5	73.1	d_8‡

*Only used for mode II
†The temperature of natural gas and refrigerant at the inlet to the main heat exchanger
‡Only used for mode I

The next step is to consider optimal operation with disturbances, and we consider the eight disturbance variables given in Table 7.2. We here fix the refrigerant com-

position, because it is assumed to be unavailable as a degree of freedom during normal operation (instead, the composition is treated as a disturbance, see Table 7.2). With a fixed temperature (30 °C) after the SW cooler, there are then 4 remaining degrees of freedom. During operation, it is always optimal to cool the natural gas to −157 °C (to avoid product give-away), and, one degree of freedom is spent to set the load:

Mode I The production rate is given

Mode II In the maximum production case, it is always optimal (for all disturbances) to operate the compressor at its maximum ($W_s = W_s^{\max}$)

Thus, two constraints are always active and this leaves for both modes only 2 steady-state operational degrees of freedom, and the resulting optimal operation conditions for various disturbances are summarized in Table 7.5. The results are also shown graphically as dots in Figure 7.7 and Figure 7.8 for mode I and mode II respectively.

Recall that the surge margin constraint ($\Delta\dot{m}_{\text{surge}} = 0$) and compressor maximum speed constraint ($N = N^{\max}$) were active in the nominal point, and we find, as one would expect, that these remain active for most of the disturbances, but not all. Also note that some disturbances are not feasible in mode I, probably because of the fixed refrigerant composition.

To obtain optimal operation, we should always implement the active constraints, and then find "self-optimizing" variables for the remaining unconstrained degrees of freedom in each region. Strictly speaking, to be truly optimal, we then need to consider four regions:

1. $N = N^{\max}$ and $\Delta\dot{m}_{\text{surge}} = 0$ is optimal (two active constraints, implementation is obvious)
2. $\Delta\dot{m}_{\text{surge}} = 0$ and $N < N^{\max}$ is optimal (unconstrained optimum, i.e. need to find an associated controlled variable for N)
3. $N = N^{\max}$ and $\Delta\dot{m}_{\text{surge}} > 0$ is optimal (unconstrained optimum, i.e. need to find an associated controlled variable for $\Delta\dot{m}_{\text{surge}}$)
4. $N < N^{\max}$ and $\Delta\dot{m}_{\text{surge}} > 0$ is optimal (unconstrained optimum, i.e. need to find an associated controlled variable for N and $\Delta\dot{m}_{\text{surge}}$)

All this cases can occur as seen in Table 7.5. This becomes rather complicated. First, a large effort is required to find the best self-optimizing variables in each of the three last regions. Second, even if we can find the self-optimizing variables in each region, it is not clear when to switch between the regions (that it, it is easy to

identify when to switch when we encounter a constraint, e.g. going from region 2 to 1, but it is more difficult to determine when to leave a constraint region).

For practical implementation, we would therefore prefer to have the same controlled variables in all regions, and in our case the obvious policy is to consider keeping the variables at constraint ($\Delta\dot{m}_{\text{surge}} = 0$ and $N = 100\,\%$) in all regions. Obviously, this is not optimal, but the loss is rather small as discussed next, except for some cases in mode I, where it seems operation is not feasible (without changing the composition or feed rate).

7.7.1 Selection of controlled variables

A preliminary screening was performed by using the maximum scaled gain method (Halvorsen et al., 2003). Some variables where discarded based on these results (e.g. the degree of sub-cooling, cycle high pressure). Also, we found that the surge margin ($\Delta\dot{m}_{\text{surge}}$) is a much more promising controlled variable than any of the alternatives we tested. Thus, we choose to fix $\Delta\dot{m}_{\text{surge}} = 0$ and this gives only minor losses as seen below.

Figure 7.7 shows compressor shaft work as a function of 6 of the 7 disturbances ($d_3 - d_8$) considered for mode I. $\Delta\dot{m}_{\text{surge}} = 0$ and the following controlled variables are tested for the remaining degree of freedom; $N = 100\,\%$, $\Delta T_{\text{sup}} = 12.9\,^{\circ}\text{C}$, $P_l = 3.67\,\text{bar}$, $T_{\text{com}}^{out} = 126\,^{\circ}\text{C}$ and $\dot{m}_{\text{ref}} = 549\,\text{kg}\,\text{s}^{-1}$. The dots shows re-optimized operation, where both N and $\Delta\dot{m}_{\text{surge}}$ has been optimized. Note that the composition of the refrigerant is still the same as for the nominal operating point. The plots are obtained by "bruteforce evaluation" which involves fixing the variables and computing the resulting operating point for varying disturbances. The disturbance is plotted on the X-axis with the nominal value at the center and the Y-axis shows the corresponding compressor shaft work in MW.

For the four last disturbances ($d_5 - d_8$) we are not able to find a feasible solution for some values of the disturbances. This means that we are not able to satisfy the specified production rate with the given refrigerant composition. The best controlled variable to maintain constant is the compressor rotational speed N. For some disturbances is it the only feasible controlled variable and it remains close to optimal for all operating points.

Figure 7.8 shows LNG production as a function of 6 of the 7 disturbances ($d_1, d_2, d_4 - d_6$) considered for mode II. $\Delta\dot{m}_{\text{surge}} = 0$ and the following alternative controlled variables are tested for the remaining degree of freedom; $N = 100\,\%$, $\Delta T_{\text{sup}} = 11.3\,^{\circ}\text{C}$, $P_l = 4.14\,\text{bar}$, $T_{\text{com}}^{out} = 124\,^{\circ}\text{C}$ and $\dot{m}_{\text{ref}} = 614\,\text{kg}\,\text{s}^{-1}$. The dots shows re-

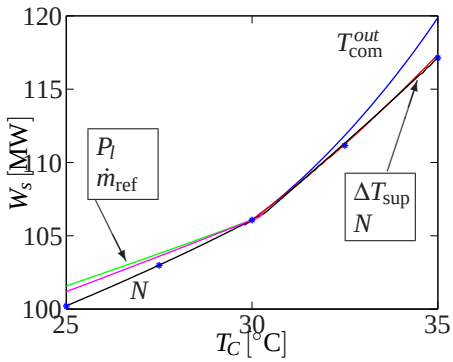

(a) Disturbance $d_3 = T_{in}$

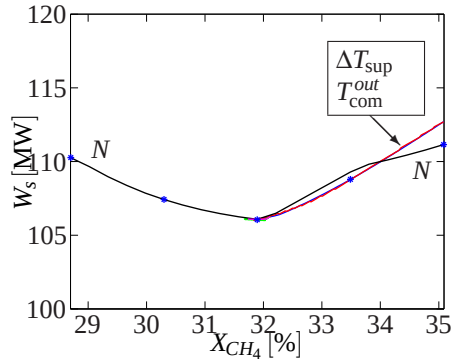

(b) Disturbance $d_4 = x_{CH_4}$

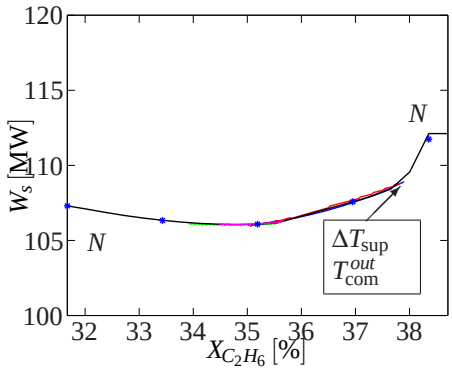

(c) Disturbance $d_5 = x_{C_2H_6}$

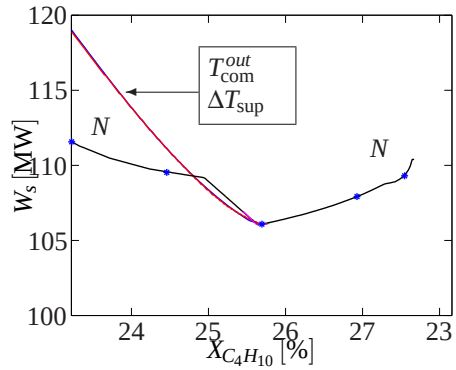

(d) Disturbance $d_6 = x_{C_4H_{10}}$

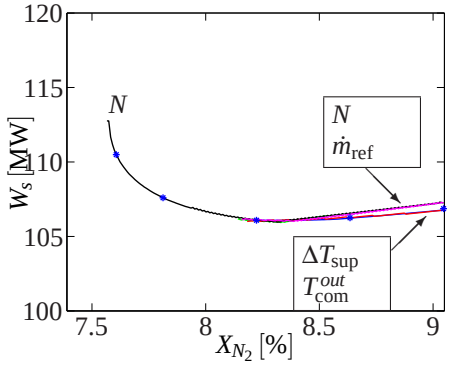

(e) Disturbance $d_7 = x_{N_2}$

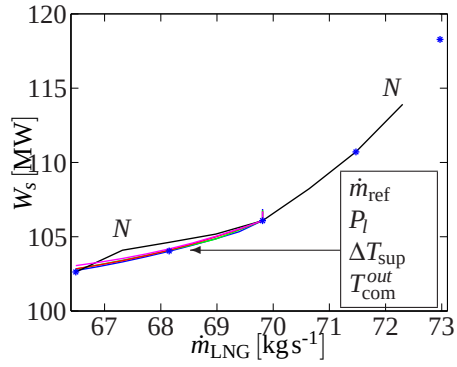

(f) Disturbance $d_8 = \dot{m}_{LNG}$

Figure 7.7: Shaft work for different control structures as function of disturbances for mode I. Dots are re-optimized operation with constant composition.

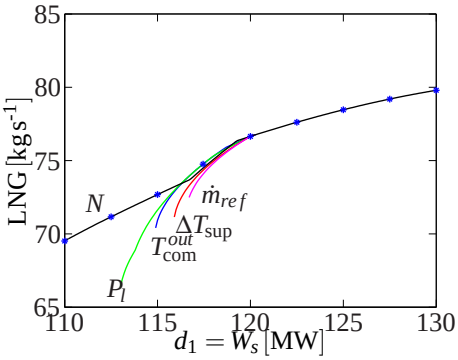

(a) Disturbance $d_1 = W_{s,\max}$

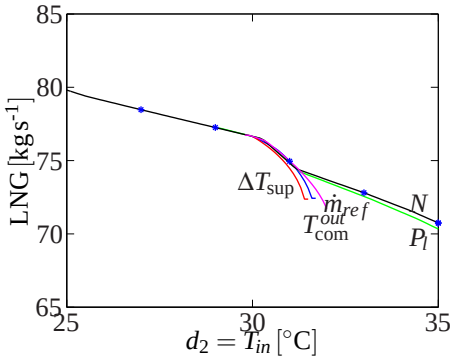

(b) Disturbance $d_3 = T_{in}$

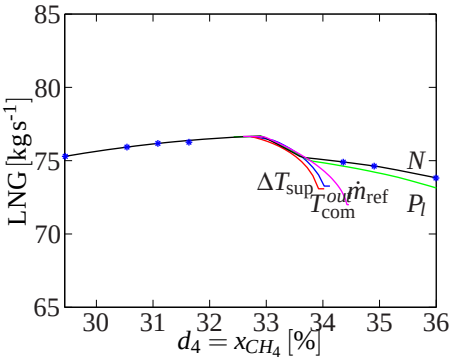

(c) Disturbance $d_4 = X_{CH_4}$

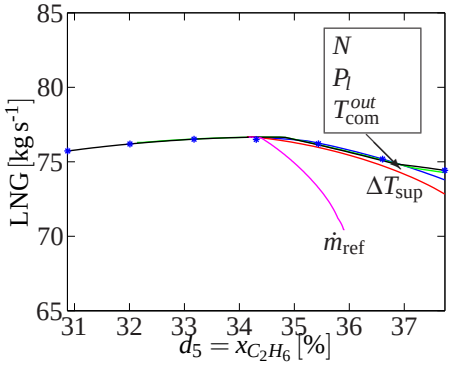

(d) Disturbance $d_5 = X_{C_2H_6}$

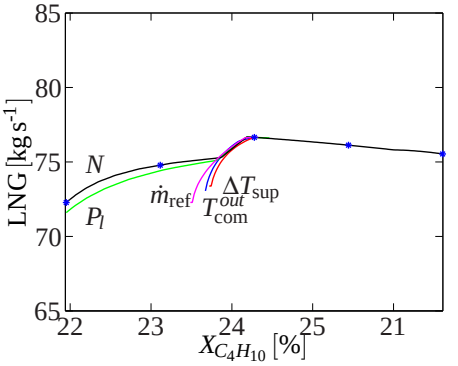

(e) Disturbance $d_6 = X_{C_4H_{10}}$

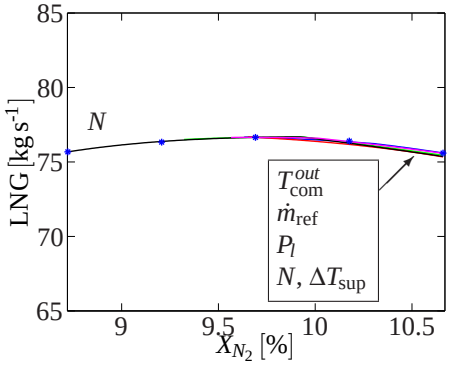

(f) Disturbance $d_7 = X_{N_2}$

Figure 7.8: LNG production for different control structures as function of disturbances for mode II. Dots are re-optimized operation with constant composition.

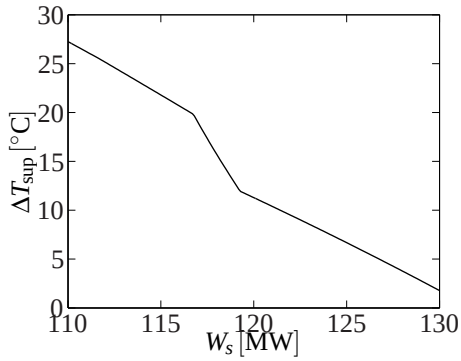

Figure 7.9: ΔT_{sup} as function of disturbance in $W_s^{\max}$ for the constant N control strategy

optimized operation, where both N and $\Delta\dot{m}_{\text{surge}}$ has been optimized. The disturbance is plotted on the X-axis with the nominal value at the center and the Y-axis shows the corresponding production rate in $\text{kg}\,\text{s}^{-1}$. Note that the composition of the refrigerant is still the same as for the nominal operating point.

N is actually the only feasible control structure for some disturbance directions. This may be seen from Figure 7.8(a), where all lines except the constant N line ends at the nominal point (from left to right). The reason for this is that the other control structures would require a non-feasible rotational speed (higher than the maximum of 100 %) to maintain the controlled variable constant.

From Figure 7.8 we see that controlling N seems to be a good self-optimizing control strategy that gives close to optimal operation over the entire disturbance range. This means that the implementation is quite simple, since $N = N^{\max}$ is optimal in one region and close to optimal in the other regions.

Note that we have <u>not</u> considered the constraint on ΔT_{sup} in Figure 7.7 and in Figure 7.8. The nominal value for ΔT_{sup} is 12.9 °C (mode I) and 11.3 °C (mode II) which should be more than sufficient for normal operation. For disturbances that leads the process into operation in the region where $N = N^{\max}$ is optimal (e.g. to the right in Figure 7.8(a)) the super-heating is gradually reduced, see Figure 7.9, but still remains positive. At some point it will be necessary to discard one of the optimally active constraints (e.g. maximum shaft work $W_s = W_s^{\max}$) to satisfy a minimum degree of super-heating. One solution to this could be to select a refrigerant composition that would assure sufficient super-heating for all operating points. Another solution is to implement some logic that will switch controlled variables depending on the operating point.

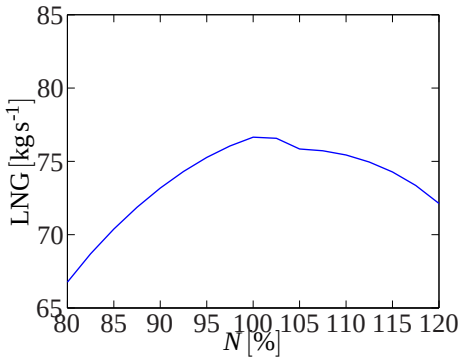

Figure 7.10: LNG production as function of N

In summary: For both mode I and mode II, fixing $\Delta\dot{m}_{\text{surge}} = 0$ and $N = 100\,\%$ is optimal for the nominal operating point and in some of the disturbance regions. Since maintaining constant N and $\Delta\dot{m}_{\text{surge}}$ is also close to optimal for the remaining disturbance regions we propose to use this control structure.

7.8 Discussion

7.8.1 Moving temperature profile

An interesting result to note from Figure 7.7 and Figure 7.8 is the "kink" that seems to be at the nominal point for all disturbances. This was at first puzzling to us since we are not changing the set of constraints that are active.

Let us consider the nominal point with N as degree of freedom (not worrying about the constraint $N^{\max}$, which can be exceeded for a short time). Looking at the resulting graphs, see Figure 7.10, we note that $\dot{m}_{\text{LNG}}$ as a function of N has a discontinuity at the nominal point (100 %) and one at approximately 105 %. We found that the reason behind this rather strange behaviour is the shape of the obtained temperature profile in the heat exchanger. Figure 7.6(b) shows that the temperature difference profile in the heat exchanger has two clear peaks, one at the heat exchanger inlet and one about 70 % through the heat exchanger. The "kink" that we observe in the objective function ($\dot{m}_{\text{LNG}}$) occurs when the peak at the heat exchanger inlet leaves the heat exchanger, which causes an abrupt change in the heat transfer at the inlet to the heat exchanger. Figure 7.9 shows the effect in superheating out of the heat exchanger.

7.8.2 Compressor characteristic

The compressor characteristics used to link the flowrate, pressure ratio, efficiency and the rotational speed of the compressor is not fitted to the data of a real compressor so it is uncertain if an installed compressor has the behaviour our model predicts. An issue for further research could be to investigate if our conclusion on the proposed control structure ($\Delta\dot{m}_{\text{surge}} = 0\,\text{kg}\,\text{s}^{-1}$ and $N = 100\,\%$) is affected by the compressor characteristic.

7.8.3 Refrigerant composition

The refrigerant composition has been optimized for the nominal operating point only. Since it is not adjusted in operation it would have been better to optimize it with respect to the expected range of operating points (given by the disturbances). This strategy, "robust optimum", is discussed in Govatsmark and Skogestad (2005).

7.8.4 Additional considerations

The optimization problems for mode I and mode II presented above are simplified, for example;

- There might be a given schedule of ships arriving to transport the LNG to markets elsewhere. Because of boil-off from the storage tanks it may be desirable to minimize the storage, but on the other hand there should be sufficient storage to minimize the loading time of the ships. This kind of thinking is discussed by Zaim (2002).

- If there are more parallel production trains, one needs to decide on how many trains that should operate and how large production each train should have. This is also discussed by Zaim (2002).

- If the ambient temperature is changing (for example from night to day or seasonal changes) it may be optimal to produce more LNG during night (or in colder periods) when the gas turbine has higher efficiency and the condenser temperature is lower. Related topics are discussed for simpler refrigeration systems in Cai et al. (2007) (also included as Appendix B).

Bibliography

Cai, J., Jensen, J., Skogestad, S. and Stoustrup, J. (2007), Balancing energy consumption and food quality loss in supermarket refrigeration system, *in* 'IEEE'.

Del Nogal, F., Kim, J., Smith, R. and Perry, S. J. (2005), 'Improved design of mixed refrigerant cycles using mathematical programming', *Gas Processors Association (GPA) Europe Meeting, Amsterdam* .

Govatsmark, M. and Skogestad, S. (2005), 'Selection of controlled variables and robust setpoints', *Ind.Eng.Chem.Res* **44**(7), 2207–2217.

Gravdahl, J. T. and Egeland, O. (1999), *Compressor Surge and Rotating Stall: Modeling and Control*, London: Springer Verlag.

Halvorsen, I. J., Skogestad, S., Morud, J. C. and Alstad, V. (2003), 'Optimal selection of controlled variables', *Ind. Eng. Chem. Res.* **42**, 3273–3284.

Lee, G. C., Smith, R. and Zhu, X. X. (2002), 'Optimal synthesis of mixed-refrigerant systems for low-temperature processes', *Ind. Eng. Chem. Res.* **41**(20), 5016–5028.

Moore, F. K. and Greitzer, E. M. (1986), 'A theory of post-stall transients in a axial compressor systems: Part I - Development of equations', *Journal of Engineering for Gas Turbines and Power* **108**, 68–76.

Price, B. C. and Mortko, R. A. (1996), PRICO - a simple, flexible proven approach to natural gas liquefaction, *in* 'GASTECH, LNG, Natural Gas, LPG international conference , Vienna'.

Saravanamuttoo, H. I. H., Rogers, G. F. C. and Cohen, H. (2001), *Gas turbine theory*, 5th edn, Pearson Education Limited, Harlow, England.

Singh, A. and Hovd, M. (2006), Dynamic modeling and control of the PRICO LNG process, *in* 'American Institute of Chemical Engineers (AIChE) annual meeting'.

Skogestad, S. (2000), 'Plantwide control: the search for the self-optimizing control structure', *J. Process Contr.* **10**(5), 487–507.

Skogestad, S. (2002), Plantwide control: towards a systematic procedure, *in* 'European Symposium on Computer Aided Process Engineering (ESCAPE)- 12, The Hague, The Netherlands'.

Stebbing, R. and O'Brien, J. (1975), An updated report on the PRICO (TM) pro-

cess for LNG plants, *in* 'GASTECH, LNG, Natural Gas, LPG international conference , Paris'.

Zaim, A. (2002), Dynamic optimization of an LNG plant, Case study: GL2Z LNG plant in Arzew, Algeria, PhD thesis, RWTH Aachen.

Table 7.3: Structure of model equations

Unit	**Equations**	
Compressor	$W_s = \dot{m} \cdot (h_{out} - h_{in})$	$W_s = \dot{m}(h_s - h_{in})/\eta$
	$\frac{P_{out}}{P_{in}} = f(\dot{m}_r, N_r)$	$\eta = f(\dot{m}_r, N_r)^*$
Turbines	$W_s = \dot{m} \cdot (h_{out} - h_{in})$	$W_s = \dot{m}(h_s - h_{in})/\eta$
Valves	$h_{out} = h_{in}$	$\dot{m} = z \cdot C_v \cdot \sqrt{\Delta P \cdot \rho}$
SW cooler	$Q = \dot{m} \cdot (h_{out} - h_{in})$	
Heat exchanger	$Q_i(z) = U_i \cdot \Delta T_i(z) \delta A_i$	$\dot{m} \cdot \frac{\partial h_i(z)}{\partial z} = Q_i(z)^\dagger$
	$\frac{\partial P_i(z)}{\partial z} = \text{constant}$	

*Consult Section 7.8.2 for details regarding the compressor characteristic
†i is the stream, either natural gas, hot refrigerant or cold refrigerant

Table 7.4: Data for the PRICO process

UA for natural gas in main heat exchanger	8.45 MW °C^{-1}
UA for warm refrigerant in main heat exchanger	53.2 MW °C^{-1}
UA for cold refrigerant in main heat exchanger	61.6 MW °C^{-1}
Nominal compressor isentropic efficiency	82.2 % *
Isentropic efficiency for the liquid turbines	80.0 %

*At nominal conditions and $N = 100\,\%$, see Section 7.8.2 for further details

Table 7.5: Optimal operation with disturbances (nominal refrigerant composition)

	Mode I					**Mode II**				
	W_s [MW]	P_h [bar]	P_l [bar]	N [%]	$\Delta\dot{m}_{\text{surge}}$ [kg s^{-1}]	$\dot{m}_{\text{LNG}}$ [kg s^{-1}]	P_h [bar]	P_l [bar]	N [%]	$\Delta\dot{m}_{\text{surge}}$ [kg s^{-1}]
$d_1(-1)$						69.5	26.6	3.75	99.9	0.489
$d_1(-0.5)$						72.7	28.1	3.94	100	0.00
$d_1(0)$		Not relevant for mode I				76.7	30.0	4.14	100	0.00
$d_1(0.5)$						78.5	31.6	4.34	100	0.00
$d_1(1)$						79.8	33.2	4.53	100	0.00
$d_2(-1)$	115	29.7	4.02	100	0.000	73.6	30.1	4.15	100	0.000
$d_2(-0.5)$	110	28.0	3.82	100	0.000	75.2	30.1	4.15	99.9	0.000
$d_2(0)$	106	26.8	3.67	100	0.000	76.7	30.0	4.14	100	0.000
$d_2(0.5)$	105	26.3	3.75	96.0	1.125	77.8	29.9	4.16	99.4	0.000
$d_2(1)$	104	25.8	3.59	100	0.000	78.6	29.8	4.21	98.0	0.000
$d_3(-1)$	100	25.6	3.47	100	0.000	79.8	30.9	4.18	100	0.000
$d_3(-0.5)$	103	26.1	3.57	100	0.000	78.2	30.4	4.16	99.9	0.000
$d_3(0)$	106	26.8	3.67	100	0.000	76.7	30.0	4.14	100	0.000
$d_3(0.5)$	111	27.9	3.88	100	0.024	73.3	29.2	4.11	100	0.000
$d_3(1)$	117	29.4	4.10	99.1	0.000	70.8	28.7	4.09	100	0.602
$d_4(-1)$	110	29.3	3.91	100	0.000	75.3	31.1	4.20	100	0.000
$d_4(-0.5)$	107	27.7	3.75	100	0.000	76.2	30.6	4.17	100	0.000
$d_4(0)$	106	26.8	3.67	100	0.000	76.7	30.0	4.14	100	0.000
$d_4(0.5)$	109	27.0	3.88	95.6	1.832	74.9	29.0	4.09	100	1.002
$d_4(1)$	111	27.0	3.80	100	0	73.8	28.5	4.07	100	0.471
$d_5(-0.5)$	106	27.0	3.69	100	0.000	75.8	29.8	4.21	97.9	0.000
$d_5(0)$	106	26.8	3.67	100	0.000	76.7	30.0	4.14	100	0.000
$d_5(0.5)$	108	27.1	3.72	100	0.000	76.4	30.1	4.15	100	0.000
$d_5(1)$			Infeasible			75.7	30.3	4.15	100	0.000
$d_6(-1)$	112	26.7	3.79	100	0.000	72.0	28.0	4.10	98.0	0.000
$d_6(-0.5)$	110	26.8	3.76	100	0.000	74.3	28.8	4.16	97.6	0.000
$d_6(0)$	106	26.8	3.67	100	0.000	76.7	30.0	4.14	100	0.000
$d_6(0.5)$	108	28.0	3.77	100	0.000	75.7	30.8	4.26	97.9	0.000
$d_6(1)$			Infeasible			75.5	32.0	4.31	100	0.000
$d_7(-1)$			Infeasible			75.7	30.2	4.16	100	0.503
$d_7(-0.5)$	108	27.3	3.74	100	0.000	76.3	30.0	4.14	100	1.971
$d_7(0)$	106	26.8	3.67	100	0.000	76.7	30.0	4.14	100	0.000
$d_7(0.5)$	106	26.7	3.72	98.6	0.367	76.4	29.9	4.18	98.7	0.000
$d_7(1)$	107	26.8	3.76	97.8	0.657	75.6	29.7	4.25	96.3	0.000
$d_8(-1)$	103	25.4	3.53	100	0.000					
$d_8(-0.5)$	104	26.0	3.70	96.2	2.493					
$d_8(0)$	106	26.8	3.67	100	0.000		Not relevant for mode II			
$d_8(0.5)$	111	28.2	3.85	100	0.000					
$d_8(1)$			Infeasible							

$d_i(j)$; i is the disturbance number (see below) and j is the fraction of the full disturbance (e.g. $j=-1$ is the minimum value of the disturbance and $j=0.5$ is in the middle of the nominal value and the maximum value of the disturbance)

$$d_1 = W_s^{\max} \qquad d_5 = x_{C_2H_6}$$
$$d_2 = P_{\text{feed}} \qquad d_6 = x_{C_4H_10}$$
$$d_3 = T_{\text{in}} \qquad d_7 = x_{N_2}$$
$$d_4 = x_{CH_4} \qquad d_8 = \dot{m}_{\text{LNG}}$$

Chapter 8

Degrees of freedom for refrigeration cycles

Submitted for publication in Industrial & Engineering Chemistry Research

An important issue for optimal operation and plantwide control is to find the degrees of freedom available for optimization. A previously published systematic approach to determine the steady state degrees of freedom is expanded to take into account the active charge as a possible degree of freedom in cyclic processes. Additional degrees of freedom related to composition of the circulating refrigerant are also discussed. Two LNG processes of current interest, the C3MR LNG process from Air Products and the MFC process developed by Statoil-Linde LNG Technology Alliance are studied with respect to operational degrees of freedom.

8.1 Introduction

This paper considers degrees of freedom for available for optimization of refrigeration processes. Skogestad (2000) points out that it is normally steady-state that effects the plant economics, so we will consider only steady-state operation. We are then interested in the steady-state degrees of freedom that affects the plant economics (objective function J), $N_{\text{opt}} = N_{\text{MV}} - N_0$, where N_{MV} is the manipulated variables (valves etc.) and N_0 is the variables that does not affect the economics (e.g. liquid level in an open process) Skogestad (2002, 2004). The number of manipulated variables are usually quite easily obtain by counting the valves, pumps and other inputs to the process. The N_0 variables that does not affect the plant

economics however, requires detailed process overview and understanding. A list of the potential degrees of freedom for some typical process units is given in Skogestad (2002) with an updated version in Araujo et al. (2007). We wish to extend this list to also include degrees of freedom that are special for closed cycles.

Glemmestad et al. (1999) discuss degrees of freedom for heat exchanger networks (HEN). The review paper on plantwide control by Larsson and Skogestad (2000) discuss degrees of freedom as this is an important step in plantwide control. A more recent study on degrees of freedom is that of Konda et al. (2006).

Processes for liquefaction of natural gas are very cost intensive and requires large amounts of energy in operation. It is therefore important that the plants are both well designed and later operated close to optimum, also for changing conditions. The optimal design of LNG processes has been studied extensively by several companies such as Air Products, Shell, Phillips and Statoil-Linde LNG Technology Alliance. It seems, however, that the subsequent operation of LNG plants has been less studied, at least in the open literature. This is a bit surprising considering the large throughputs which makes even small improvements economically attractive. There are some publications regarding control of LNG plants (Mandler, 2000; Singh and Hovd, 2006), but they consider the dynamic performance and controllability rather than the optimal steady-state operation. Zaim (2002) looked into dynamic optimization of a plant with several trains in parallel.

Degrees of freedom for refrigeration processes are covered in the next section and in Section 8.3 we apply the findings on some case studies, including the two LNG processes;

- The propane pre-cooled mixed refrigerant (C3MR) process from Air Products
- The mixed fluid cascade (MFC) process from Statoil-Linde LNG Technology Alliance

8.2 Degrees of freedom

An important issue in plantwide control is to find the degrees of freedom that may be used for optimization (Skogestad, 2000) which in our case is equal to the number of steady-state degrees of freedom N_{ss}. This is an important number for several reasons. First, it determines the degrees of freedom available for solving the optimization problem. However, more importantly in terms of operation it determines the number of steady-state controlled variables (N_{ss}) that need to be

Table 8.1: Potential operational degrees of freedom (N_{ss}^{max}) for some typical process units

Process unit	**Potential DOF**
Feed	1 (feedrate)
Splitter	number of exit streams - 1
Mixer	0
Compressor, turbine, pump	1 (work)
Adiabatic flash tank	0*
Liquid phase reactor	1
Gas phase reactor	0*
Heat exchanger	1 (bypass or flow)
Column (excluding heat exchangers)	0* + number of side streams
.....	
Valve	0*
Choke valve	1
Each closed cycle:	
Active charge (holdup fluid)	1†
Composition of fluid	$N_C - 1$‡

*Pressure is normally assumed to be given by the surrounding process and is then not a degree of freedom. However, on must add one degree of freedom for each extra pressure that is independently set, and which has a steady-effect (need a manipulated input not already counted, e.g. a valve)

†The active charge in the equipment is a potential degree of freedom, but it may not be available in some designs.

‡*NC* is the number of components in the working fluid (refrigerant)

selected. Optimal operation is normally implemented by keeping those variables at constant setpoints.

Rule (actual degrees of freedom): The number N_{ss} of steady-state degrees of freedom may be obtained by counting the number of manipulated variables N_{MV} and subtracting the following N_0 variables (Skogestad, 2002, 2004);

- manipulated variables with no effect on the cost J, e.g. extra bypasses of heat exchangers (only used to improve dynamic performance)
- variables with no steady state effect that need to be controlled, e.g. liquid holdups with no steady state effect

Thus, $N_{ss} = N_{MV} - N_0$.

Potential (maximum) degrees of freedom

Based on this rule, Skogestad (2002) derived the potential number of degrees of freedom N_{ss}^{max} for some typical process units and an updated version was published by Araujo et al. (2007). In Table 8.1 the list is further updated to include also the potential degrees of freedom for cyclic processes. The additions are shown below the dotted line in the table. First, a valve should normally not be counted, unless it affects a pressure that has a steady-state effect. An example is a choke valve which is installed to lower the pressure, and it has therefore been added explicitly as a degree of freedom in the table. In addition, we potentially have $N_C - 1$ degrees of freedom related to the fluid composition in the cycle. Finally, the active charge in the cycle is a potential degree of freedom. For example, it may change the pressure level. This is explained in more detail below.

Many designs will have fewer actual degrees of freedom than given in Table 8.1. For example, a heat exchanger will not have any degrees of freedom if all flows are given and there is no bypass or other means of affecting the heat transfer, e.g. the main exchanger in a LNG process. Similarly, one may not be able to adjust the total active charge or fluid composition in practice.

Potential degrees of freedom	
	1 Compressor
	2 Heat exchangers
	1 Choke valve
+	1 "Active charge"
$N_{ss}^{max} =$	5 degrees of freedom

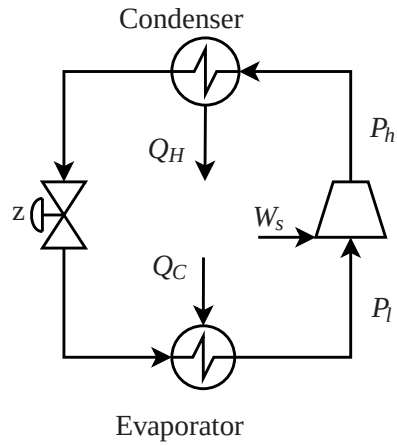

Figure 8.1: A simple refrigeration cycle with $N_{ss}^{max} = 5$ potential degrees of freedom. However, if the drawing shows the actual process there will only be $N_{ss} = 4$ degrees of freedom, because there is no means of changing the active charge by filling or removing refrigerant.

Example: From Table 8.1 the simple cooling cycle shown in Figure 8.1 with pure fluid ($N_C = 1$) has five potential degrees of freedom (N_{ss}^{max}) related to; one compressor, two heat exchangers, one choke valve and the active charge. Exactly how

these degrees of freedom may be changed depends on the case. For example, for a compressor the actual manipulated variable (MV) may be the rotational speed or the fraction of time the compressor is on (home or automotive installations). The active charge in Figure 8.1 may be changed by filling or removing refrigerant to the cycle, but since this is not included, the actual process does not have a degree of freedom related to the active charge and thus has only 4 degrees of freedom (N_{ss}).

Table 8.2: Actual degrees of freedom for refrigeration cycles, $N_{\text{ss}} = N_{\text{MV}} - N_0$

Process unit	**Actual DOF**
Each MV (Valve, heat exchanger, compressor, turbine etc.)	1
For each cycle subtract variables with no steady-state effect (N_0):	
Pure fluid:	
Liquid receivers exceeding the first*	-1
Multi component:	
Liquid receiver exceeding the $\underline{NC}$ first†	-1

*The first receiver is not subtracted in a closed cycle as this has a steady state effect

†Assumes composition different in each of the *NC* first receivers, otherwise the number of degrees of freedom is less

8.2.1 Remark on active charge or “feed” for closed cycles

The degree of freedom related to the total active charge is not obvious so we here discuss this “extra” degree of freedom that may occur in closed cycles. Consider the process shown in Figure 8.2 where we have included an external tank with a valve for filling refrigerant into the closed cycle. A temperature controller adjusts the compressor speed to assure that the cooling load is constant. The choke valve is a thermostatic expansion valve (TEV) that controls the degree of super-heating at the evaporator outlet. With the fan speeds for the two heat exchangers fixed (e.g. at maximum), there are then one potential remaining degree of freedom related to the active charge.

First, assume that the process is operated with just enough charge (refrigerant in the closed cycle) to obtain saturation out of the condenser, see Figure 8.2(a). We then open the external valve for some time and then close it again to fill more refrigerant into the cycle. We then get to the operating point shown in Figure 8.2(b) where the added amount of refrigerant has accumulated in the condenser. This follows since the evaporator will not change its holdup (significantly) due to the thermostatic expansion valve that indirectly sets the area available for super-heating so the only

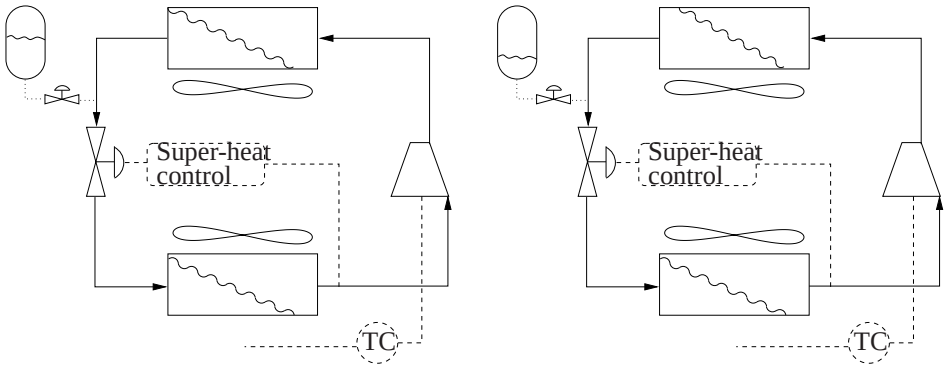

(a) Saturation at condenser outlet (b) Sub-cooling at condenser outlet

Figure 8.2: A simple (not closed) refrigeration cycle. The external filling/emptying system illustrates the degree of freedom related to the active charge.

place the extra refrigerant can go is to the condenser. The increased charge in the condenser will lead to a higher pressure P_h, which again leads to larger mean temperature difference and thus more heat transfer and the liquid at the outlet from the condenser will be sub-cooled, as indicated in Figure 8.2(b). It has been shown that this may reduce the necessary compressor power in some cases (Jensen and Skogestad, 2007*b*), but the main point here is to note that the charge in the system has an effect on the steady state operation.

Remark 1 Note that Table 8.2 discussed below does not apply because the cycle in Figure 8.2 is not closed.

Remark 2 If we add a liquid receiver to the cycle in Figure 8.2 then we loose one degree of freedom (as we have a level with no steady-state effect that needs to be controlled). To regain this degree of freedom we (at least) would need to add another valve.

8.2.2 Actual degrees of freedom for refrigerant cycles

For a closed cycle, in order to adjust the active charge during operation we need a liquid receiver (variable holdup) in the cycle. However, for a pure refrigerant adding additional (two or more) receivers will not increase the number of degrees of freedom, as the holdup has no steady-state effect and needs to be controlled (actually, it may reduce the number unless we also add a valve for this purpose). In general, for a multicomponent (mixed) refrigerant, the holdup of the *NC* first tanks do have a steady-state effect provided the tanks have different compositions,

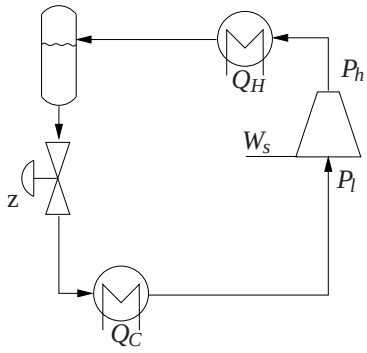

(a) No extra choke valve, $N_{\mathrm{MV}} = 4$ and $N_{\mathrm{ss}} = 4$

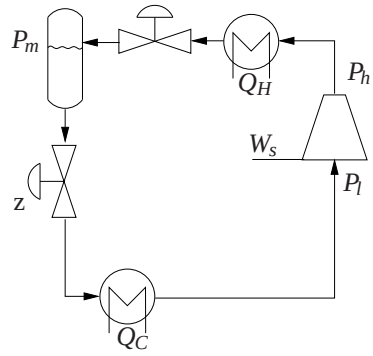

(b) An extra choke valve, $N_{\mathrm{MV}} = 5$ and $N_{\mathrm{ss}} = 5$

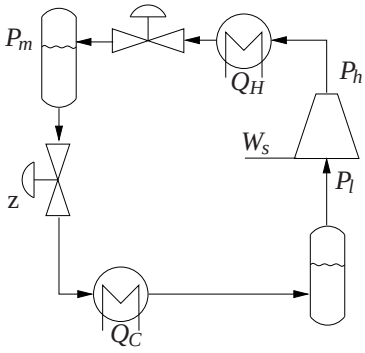

(c) Extra choke valve and liquid receiver on low pressure side, $N_{\mathrm{MV}} = 5$, but $N_{\mathrm{ss}} = 4$

Figure 8.3: Simple cycle with liquid receiver on the high pressure side

as they provide an indirect means of adjusting the fluid composition. Only liquid receivers exceeding the *NC* first will have no steady-state effect. These arguments are the basis for Table 8.2 which gives the actual (rather than the potential in Table 8.1) degrees of freedom for vapour compression cycles.

Let us apply Table 8.2 to the process in Figure 8.1 which has $N_{\text{MV}} = 4$ (two heat exchangers, one valve and one compressor). Since there are no liquid receivers, there is no variables that need to be subtracted($N_0 = 0$). Thus, $N_{ss} = 4$ degrees of freedom, which confirms our earlier findings.

Note that adding a liquid receiver somewhere in this cycle will not change the number of steady-state degrees of freedom. In order to do this we also need to add a valve, for example upstream of the receiver. The addition of a liquid receiver to the cycle is shown in Figure 8.3. We have from Table 8.2 the following degrees of freedom for the three cases in Figure 8.3:

Figure 8.3(a)	**Figure 8.3(b)**	**Figure 8.3(c)**
$N_{\text{MV}} = 4$	$N_{\text{MV}} = 5$	$N_{\text{MV}} = 5$
$-N_0 = 0$	$-N_0 = 0$	$-N_0 = 1$
$N_{\text{ss}} = 4$	$N_{\text{ss}} = 5$	$N_{\text{ss}} = 4$

For the two first cases, the liquid level does not need to be subtracted as it has a steady-state effect (see Figure 8.2) and also does not need to be controlled in a closed cycle.

The design in Figure 8.3(a) with no extra valve does not allow for adjusting the active charge. The design in Figure 8.3(b) with an extra choke valve has an additional degree of freedom. This may be more optimal (Jensen and Skogestad, 2007*b*) since it allows for the condenser outlet to be sub-cooled. This is because the pressure in the receiver is equal to the saturation pressure and the extra valve gives $P > P_{\text{sat}}$ (sub-cooling) at the condenser outlet.

In Figure 8.3(c) we have added also a liquid receiver on the low pressure side. Thus, we have lost one degree of freedom compared to Figure 8.3(b), because one of the liquid levels need to be controlled. Another way of understanding why there is one less degree of freedom, is that we now always have saturated vapour at the inlet to the compressor, whereas it before could be super-heated.

Remark. Note that a loss of a degree of freedom does not mean that the process is less optimal. In fact, in this case it is opposite, because for a simple cycle (without internal heat exchange) it is optimal to have saturation (no super-heating) before the compressor. Thus Figure 8.3(c) is optimal by design, whereas in Figure 8.3(b) one needs to adjust one of the degrees of freedom to get optimality, and this may be difficult to achieve in practice.

8.3 Case studies

We will here present some more complex case studies. First we will look at two processes not directly related to LNG plants; a two-pressure level refrigeration cycle cooling a process stream and a heat integrated distillation column (two different configurations). Then we will look at three LNG case studies; a small scale LNG process with a single mixed refrigerant, the propane pre-cooled mixed refrigerant (C3MR) process from Air Products and the mixed fluid cascade (MFC) process from Statoil-Linde LNG Technology Alliance.

8.3.1 Two-pressure level refrigeration

Figure 8.4(a) shows a refrigeration system with two-stage expansion using a pure refrigerant ($NC = 1$). The process stream is first cooled by the intermediate-pressure refrigerant (Evaporator 1) and then by the low-pressure refrigerant (Evaporator 2). The evaporators are kettle type boilers so there is no super-heating of the vapour. The temperature profile in the evaporators is illustrated in Figure 8.4(b). Control of such cycles is discussed by Wilson and Jones (1994). The two compressors are usually driven with a common driver, so there is only one manipulated variable for the two compressors ①. There are three valves, ②, ③ and ④, shown in Figure 8.4(a). The valve between Evaporator 1 and the second compressor, ④, is present to limit the amount of cooling in Evaporator 1 if necessary. In addition we may manipulate the flow of coolant in the condenser ⑤ and the process stream ⑥. Thus, this two-pressure level cycle has $N_{\mathrm{MV}} = 6$ manipulated variables.

The two evaporators in Figure 8.4(a) will function as liquid receivers so there are in total three variable liquid levels. Two of the liquid levels, typically the evaporators, need to be controlled for stabilization, and since the refrigerant is pure the setpoints for these (levels) has no steady-state effect (see also Table 8.2). Thus, we end up with $N_{\mathrm{ss}} = N_{\mathrm{MV}} - N_0 = 6 - 2 = 4$ degrees of freedom. To operate the system we need to decide on four controlled variables. In general, these should be selected as the possible active constraints (e.g. max cooling, ⑤ fully open) plus "self-optimizing" variables.

It is interesting to compare the actual degrees of freedom with the potential degrees of freedom according to Table 8.1. We have for Figure 8.4(a):

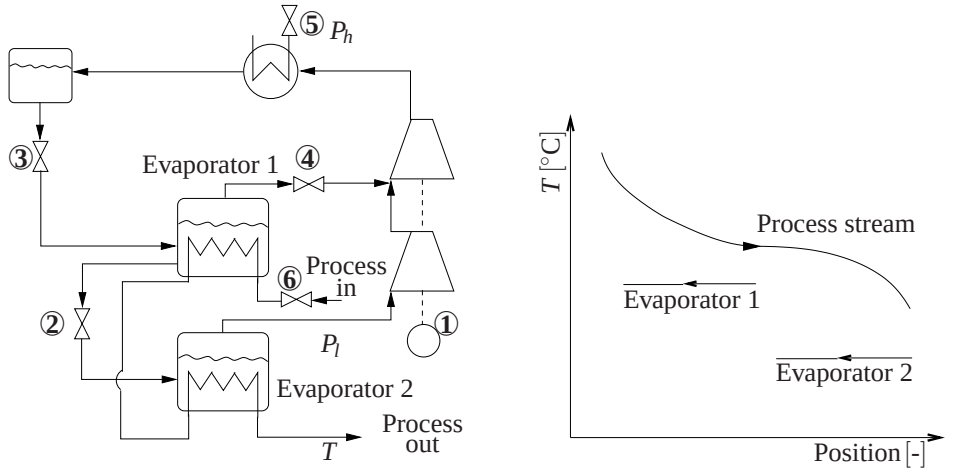

(a) Flowsheet (b) Temperature profile

Figure 8.4: Cooling at two pressure levels, $N_{ss} = 4$

Actual DOF		**Potential DOF**
N_{MV} = 6		1 Feed
$-N_0$ = 2		1 Compressors
		3 Heat exchangers
		3 Valve
	+	1 Active charge
N_{ss} = 4	N_{ss}^{max} =	9 degrees of freedom

The 5 "lost" degrees of freedom are related to:

1 No sub-cooling in the condenser (not optimal)

2,3 No super-heating in the two evaporators (optimal)

4,5 No bypass for the two evaporators (optimal)

Thus, four of the five lost degrees of freedom are "optimal by design" in this case. The only possible loss is related to not allowing for sub-cooling of the stream leaving the condenser. To fix this would require an additional valve between the condenser and the liquid receiver.

8.3.2 Heat integrated distillation

To reduce the energy consumption in distillation, one may use a heat pump between the condenser and reboiler (Salim et al., 1991). Two possible designs are

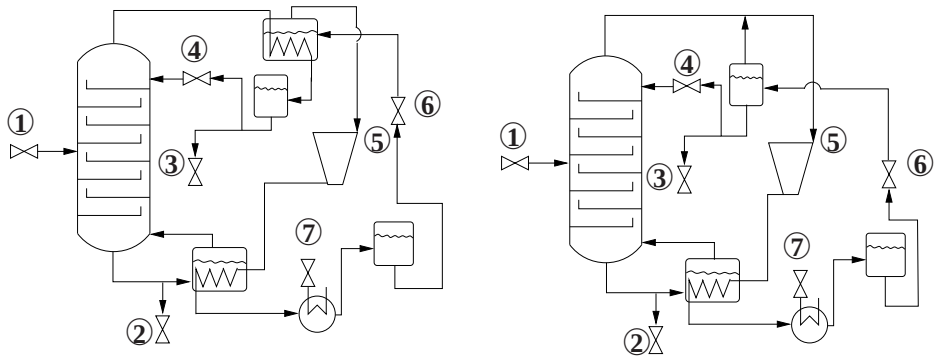

(a) External working fluid (b) Vapour overhead as working fluid

Figure 8.5: Two ways of using a heat pump to integrate the reboiler with the condenser in a distillation column

shown in Figure 8.5.

a) With external working fluid. Control of such columns have been studied by Jørgenses and coworkers (Hallager et al., 1990; Nielsen et al., 1987, 1988; Li et al., 2003) who also have an experimental setup.

b) With the vapour overhead as working fluid (not a closed cycle)

There are in total 7 manipulated variables for both systems (see Figure 8.5): Feed flowrate ①, Bottom product flowrate ②, Top product flowrate ③, Reflux flowrate ④, Compressor ⑤, Choke valve ⑥, Cooling water flowrate ⑦.

On the column side, there are two liquid levels with no steady-state effect that must be controlled:

- Condenser liquid level (e.g. may be controlled by the reflux flowrate ④)
- Reboiler liquid level (e.g. may be controlled by the bottom product flowrate ②)

Using the method in Table 8.2 combined with the general rule we get the actual degrees of freedom:

Figure 8.5(a)

N_{MV}	= 7
$-N_0$	= 3*
N_{ss}	= 4

*One of the two levels in the heat pump cycle must be controlled and has no steady-state effect

Figure 8.5(b)

N_{MV}	= 7
$-N_0$	= 3*
N_{ss}	= 4

*The heat pump cycle is no longer closed so the single liquid level (receiver) must be controlled

Thus, in both cases there are 4 steady-state degrees of freedom when the feedrate and column pressure are included. This is the same as for an "ordinary" distillation column.

Govatsmark (2003) studied the process with external working fluid (Figure 8.5(a)) and found that the top composition and the column pressure are at their constraints for the case where the top product is the valuable product. Assuming a given feed flowrate there is then one unconstrained degree of freedom left. This unconstrained degree of freedom could then be used to control a temperature in the bottom section of the column, which is found to be a good self-optimizing controlled variable (Govatsmark, 2003).

It is interesting to compare the actual degrees of freedom with the potential (maximum) degrees of freedom according to Table 8.1:

	Figure 8.5(a)		**Figure 8.5(b)**
	1 Feed		1 Feed
	0 Column		0 Column
	1 Pressure (in column)		1 Pressure (in column)
	1 Compressor		1 Compressor
	3 Heat exchanger		2 Heat exchanger
	1 Choke valve		1 Choke valve
+	1 Active charge	+	1 Pressure (in condenser)
N_{ss}^{max}=	8 degrees of freedom	N_{ss}^{max}=	7 degrees of freedom

In Figure 8.5(a) the four "lost" degrees of freedom are related to:

1,2 No bypass of two heat exchangers* (optimal)

3 Saturation before compressor (optimal)

4 Saturation at condenser outlet (not optimal)

For Figure 8.5(b) there are three "lost" degree of freedom related to:

1 No bypass of the column reboiler (optimal)

*Not the cooler because the flow of coolant is an actual degree of freedom

2 Saturation before compressor (optimal)

3 Saturation at condenser outlet (not optimal)

The only non-optimal "lost" degree of freedom is for both cases related to saturation out of the condenser in the heat pump cycle. This may be close to optimal (Jensen and Skogestad, 2007*a*). However, to gain this degree of freedom it is necessary to have a valve between the cooler and the liquid receiver. This valve will then give sub-cooling out of the cooler.

8.3.3 Small scale LNG process

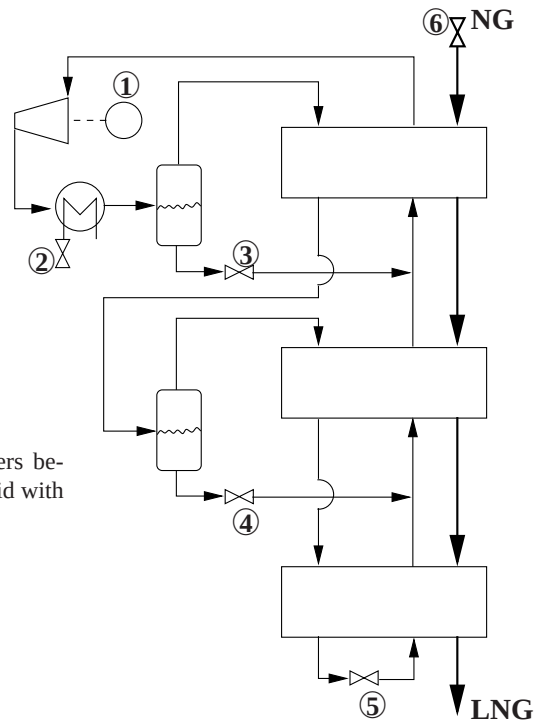

From Table 8.2

N_{MV}	= 6
$-N_0$	= 0*
N_{ss}	= 6

*No subtraction of liquid receivers because of multicomponent working fluid with $NC \geq 2$

Figure 8.6: A small scale LNG concept to illustrate the degrees of freedom related to changing the composition via liquid levels

Consider the small-scale LNG process in Figure 8.6 with a mixed refrigerant $NC \geq 2$ (Neeraas and Brendeng, 2001). Note that the original process design has additional degrees of freedom related to individual heat exchangers for refrigerant cooling and natural gas cooling. Our simplified flowsheet assumes that it is

optimal to cool the refrigerant and the natural gas to the same temperature. We find (using Table 8.2) that the process has six manipulated variables, $N_{\text{MV}} = 6$, see Figure 8.6. Since there are two liquid levels, we need to control at least one for stabilization. Thus, it is tempting to remove one degree of freedom. However, the level setpoint has a steady-state effect, because the composition in the two tanks are different and we may change the composition of the circulating refrigerant by shifting mass from one tank to the other. Thus, $N_{\text{ss}} = N_{\text{MV}} = 6$.

Using Table 8.1 we get the potential degrees of freedom if we assume $N_C = 3$:

	Figure 8.6
	1 Feed
	1 Compressor
	3 Choke valve
	4 Heat exchanger
	1 Active charge
	2 Compositions
$N_{\text{ss}}^{\text{max}} =$	12 degrees of freedom

We have the following 6 lost degrees of freedom:

1-3 No bypass of process heat exchangers (optimal)

4,5 Pressure in the two flash drums (optimal, discussed below)

6 Composition of the refrigerant (not optimal)

The "lost" degree of freedom related to the pressure in the two flash drums are not obvious. Adding a valve before the second flash drum will give a lower temperature in the flash drum and thus also of the vapour that is sent through the second heat exchanger. This is not optimal since the vapour will then be colder than the natural gas which it is cooled together with. The same is true for the first flash drum if the natural gas feed is cooled with the same coolant as the refrigerant after compression.

8.3.4 Propane pre-cooled mixed refrigerant (C3MR)

The C3MR process developed by the Air Products company has a large market share of the existing liquefaction plants worldwide. A flowsheet of the C3MR process is given in Figure 8.7. The first cycle is with a pure refrigerant, usually propane. The second cycle is with a mixed refrigerant. We identify the following manipulated variables:

- Natural gas feed ①

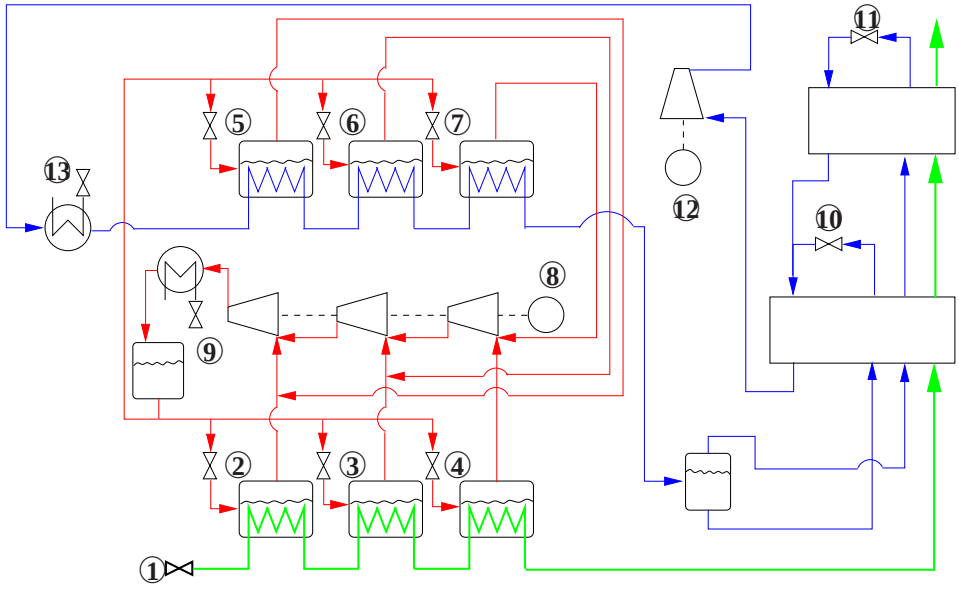

Figure 8.7: Flowsheet of the C3MR process. Propane (C3), Mixed refrigerant (MR), Natural gas (NG)

- 6 choke valves for propane pre-cooling (one for each pressure level for natural gas cooling and one for each pressure level for mixed refrigerant cooling) ②, ③, ④, ⑤, ⑥ and ⑦
- Propane compressor, one speed ⑧
- Flow of cooling water or air in propane condenser ⑨
- Two choke valves for mixed refrigerant cycle, ⑩ and ⑪
- Mixed refrigerant compressor ⑫
- Flow of cooling water or air in mixed refrigerant cooler ⑬

For the propane cycle we need to control 6 of the 7 liquid levels (e.g. the heat exchanger levels) and since $N_C = 1$ none of these level setpoints will have a steady-state effect. Assuming $N_C = 3$ for the mixed refrigerant cycle we get the following actual and potential degrees of freedom:

Actual DOF		Potential DOF
$N_{MV} = 13$		1 Feed
$-N_0 = -6$		2 Compressor
		10 Heat exchanger
		8 Choke valve
		2 Active charge
	+	2 Compositions (MR)
$N_{ss} = 7$	$N_{ss}^{max} =$	25 degrees of freedom

The 18 "lost" degrees of freedom are related to:

1-8 No bypass of process heat exchangers (optimal)

9-14 Saturation at propane compressor inlet (no super-heating, optimal)

15 Saturation out of propane condenser (no sub-cooling, not optimal)

16 Pressure in the flash drum in the MR cycle (optimal)

17,18 Composition of the mixed refrigerant (not optimal)

The only loss in efficiency due to the "lost" degrees of freedom are caused by having no sub-cooling in the propane condenser and by not being able to change the composition in the mixed refrigerant cycle. To get sub-cooling in the condenser it is necessary to have a valve between the condenser and the liquid receiver. Adjusting the composition is discussed further in Section 8.4.

It is optimal to have the flash drum in the mixed refrigerant cycle at the same pressure as the outlet from the last propane cooler. Otherwise the warm refrigerant would be colder than the natural gas in the first mixed refrigerant heat exchanger, causing a non-optimal temperature profile.

Optimal operation:
Let us consider two different operating strategies:

Case 8.1 *Maximum production given available shaft work.*

Case 8.2 *Minimum shaft work given feed flowrate.*

For both cases the following is true:

It is not economical to cool more than necessary so the natural gas outlet temperature is at its maximum constraint*, this may be controlled by the last choke valve

*This temperature will implicitly set the amount of flash gas, see Chapter 6 and the composition of both the flash gas and the LNG.

in the mixed refrigerant cycle*, removing one degree of freedom. Cooling water is usually cheap so it is usually wise to maximize the flow of cooling water which removes two additional degrees of freedom. We are then left with 4 degrees of freedom to optimize the operation.

For Case 8.1. Two degrees of freedom are used to maximize compressor shaft work, one for each cycle (active constraints). This leaves us with two unconstrained degrees of freedom, so two setpoints must be specified for this case (e.g. P_h in the mixed refrigerant cycle and P_l in the propane cycle)

For Case 8.2. The feed flowrate is given so we loose one degree of freedom. This leaves us with three unconstrained degrees of freedom, so three setpoints must be specified for this case (e.g. P_l and P_h in the mixed refrigerant cycle and P_l in the propane cycle).

Remark. If the cooling water is too cold it may be necessary to limit the flow of cooling water to avoid violating constraints on the compressor suction pressure (minimum constraint). This, however, does not change the analysis since the number of active constraints are the same since we exchange the maximum cooling constraint with the minimum pressure constraint.

8.3.5 Mixed fluid cascade (MFC)

The Statoil-Linde LNG Technology Alliance has developed a mixed fluid cascade (MFC) process (Bach, 2002; Forg et al., 1999). A flowsheet of the process is given in Figure 8.8. It consists of three refrigeration cycles i) Pre-cooling cycle (PR), ii) liquefaction cycle (LC) and iii) sub-cooling cycle (SC). All three refrigerant cycles use mixed refrigerants.

There are in total 13 manipulated variables ($N_{\text{MV}} = 13$):

- Natural gas feed ①
- Flow of cooling water/air in PC cycle ②
- Choke valve intermediate pressure level PC cycle ③
- Choke valve low pressure level PC cycle ④
- Compressor PC cycle ⑤
- Flow of cooling water/air in LC cycle ⑥

*Another solution is to use the natural gas feed flowrate by adjusting the LNG expansion. This expansion device (valve or turbine) is not shown here, as we have indicated the feed manipulator at the inlet of the stream instead.

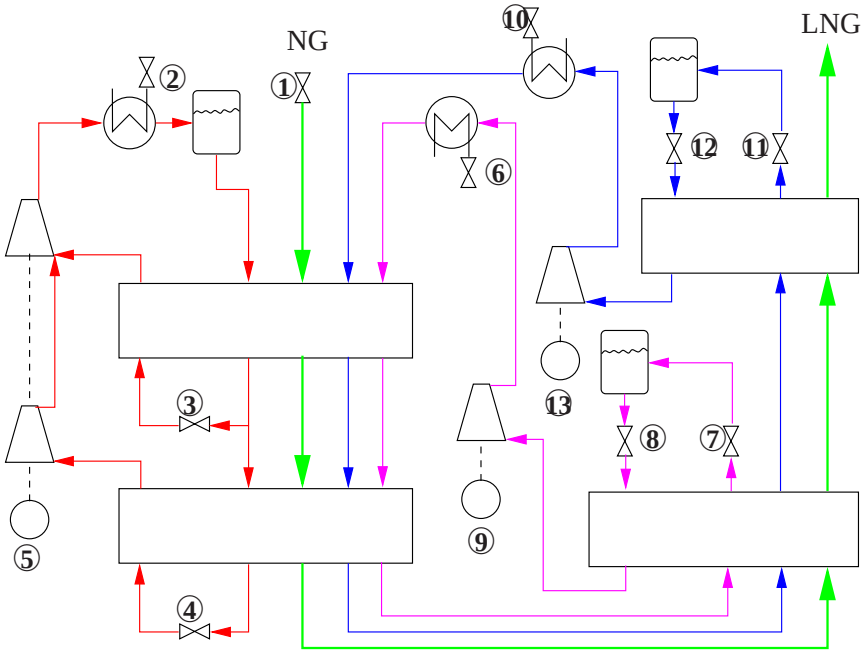

Figure 8.8: Flowsheet of the MFC process. Pre-cooling cycle (PC), Liquefaction cycle (LC), Sub-cooling cycle (SC) and Natural gas (NG)

- Extra valve LC cycle ⑦
- Choke valve LC cycle ⑧
- Compressor LC cycle ⑨
- Flow of cooling water/air in SC cycle ⑩
- Extra valve SC cycle ⑪
- Choke valve SC cycle ⑫
- Compressor SC cycle ⑬

There are no liquid levels that must be controlled ($N_0 = 0$). Assuming $N_C = 3$ for each cycle we get the following actual and potential degrees of freedom:

Actual DOF		Potential DOF
$N_{MV} = 13$		1 Feed
$-N_0 = 0$		3 Compressor
		7 Heat exchangers
		4 Choke valve
		3 Active charge
	+	6 Composition
$N_{ss} = 13$	$N_{ss}^{max} =$	24 degrees of freedom

The 11 "lost" degrees of freedom are related to:

1-4 No bypass of process heat exchangers (optimal)

5 Saturation at PC condenser outlet (not optimal)

6-11 Two compositions for each of the three cycles (not optimal)

Also for this process it is the saturation specification out of the condenser for the first cycle and the fixed compositions that will give the losses.

Optimal operation: Let us again consider optimal operation for two cases. The LNG outlet temperature must be controlled and the amount of cooling water in three sea water coolers are maximized, giving 9 unconstrained degrees of freedom.

For Case 8.1 (maximum feed). We use three degrees of freedom to maximize the compressor shaft work in each cycle. We are then left with 6 unconstrained degrees of freedom so 6 setpoints must be specified.

For Case 8.2 (given feed). The feed is given so there are then 8 unconstrained degrees of freedom. For this case we need 8 setpoints.

Note that there may be active constraints on the temperature after PCHX1 and/or the temperature after PCHX2 if the NGL extraction is integrated. For each active constraint we will have one less unconstrained degree of freedom, that we have to find a controlled variable for.

8.4 Discussion

8.4.1 Degrees of freedom

Table 8.1 is not straightforward to use in practice. This is mainly because an intermediate pressure may or may not have a steady-state effect. This is not easily captured by simply counting the degrees of freedom for each unit operation, but

requires a process understanding. The method shown in Table 8.1 is only one of several alternatives that will lead to the same result.

8.4.2 Refrigerant composition

For mixed refrigerants there are $N_C - 1$ potential degrees of freedom related to the composition of the refrigerant. However, all of these are usually not realized as actual degrees of freedom. We have claimed above that liquid level setpoints (provided different composition) may be used to effectively utilize the degrees of freedom related to refrigerant composition, see the small scale LNG process presented above. This is not a practical solution with several compositions as it is necessary with equally many liquid tanks (with sufficiently different compositions) and control elements (valves). So in practice one will instead rely on a constant composition that may be changed on a larger timescale by utilizing the make-up system.

8.4.3 Saturation in condenser

Another potential degree of freedom that is sometimes "lost" is related to the condenser pressure. By having a liquid receiver after the condenser it will not be possible to have a condenser pressure different from the saturation pressure ($P_{\text{con}} = P_{\text{sat}}$). By having a valve in between the condenser and the liquid receiver it is possible to have sub-cooling in the condenser ($P_{\text{con}} \geq P_{\text{sat}}$). This is discussed in more detail in Jensen and Skogestad (2007*b*). However, it may also be necessary with a different condenser design if the design does not allow for sub-cooling. This is the case if the liquid formed in the condenser leaves the heat transfer zone (e.g. due to gravity).

8.5 Conclusion

The degrees of freedom available for optimization (N_{ss}) is an important number for several reasons. It determines the number of free variables available to solve the optimization problem. However, more importantly it determines how many steady-state controlled variables that must be selected to operate the process.

This paper extends an earlier published simple approach to determine the potential degrees of freedom ($N_{\text{ss}}^{\text{max}}$) based on unit operations to also cover vapour compression cycles. A simple method to determine the actual degrees of freedom (N_{ss})

for vapour compression cycles is also presented. Both methods are illustrated on four case studies where the difference between the potential and actual degrees of freedom are explained and related to the process layout.

For the two LNG case studies (C3MR and MFC) we also illustrate the effect of operating strategy (maximum production and given production) on the number of unconstrained degrees of freedom.

Bibliography

Araujo, A., Govatsmark, M. and Skogestad, S. (2007), 'Application of plantwide control to the HDA process. I - steady-state optimization and self-optimizing control', *Control engineering practice* **15**, 1222–1237.

Bach, W. A. (2002), 'Developments in the mixed fluid cascade process (MFCP) for LNG baseload plants', *Reports on science and technology Linde* **63**.

Forg, W., Bach, W., Stockmann, R., Heiersted, R. S., Paurola, P. and Fredheim, A. O. (1999), 'A new LNG baseload process and manufacturing of the main heat exchanger', *Reports on science and technology Linde* **61**.

Glemmestad, B., Skogestad, S. and Gundersen, T. (1999), 'Optimal operation of heat exchanger networks', *Comput. Chem Eng.* **23**, 509–522.

Govatsmark, M. S. (2003), Integrated Optimization and Control, PhD thesis, Norwegian University of Science and Technology (NTNU), Trondheim, Norway.

Hallager, L., Jensen, N. and Jø rgensen, S. B. (1990), Control system configuration for a heat pump operating as energy source for a distillation column, *in* 'Presented at Nordic CACE symposium, Lynby, Denmark'.

Jensen, J. B. and Skogestad, S. (2007*a*), 'Optimal operation of a simple refrigeration cycles. Part II: Selection of controlled variables', *Comput. Chem Eng.* **31**, 1590–1601.

Jensen, J. B. and Skogestad, S. (2007*b*), 'Optimal operation of simple refrigeration cycles. Part I: Degrees of freedom and optimality of sub-cooling', *Comput. Chem. Eng.* **31**, 712–721.

Konda, N., Rangaiah, G. and Krishnaswamy, P. (2006), 'A simple and effective procedure for control degrees of freedom', *Chem. Engng. Sci.* **61**, 1184–1194.

Larsson, T. and Skogestad, S. (2000), 'Plantwide control - a review and a new design procedure', *Modeling, Identification and Control* **21**, 209–240.

Li, H., Gani, R. and Jø rgensen, S. B. (2003), Integration of design and control for energy integrated distillation, *in* 'European Symposium on Computer Aided Process Engineering (ESCAPE) 13, Lappeenranta, Finland'.

Mandler, J. A. (2000), 'Modelling for control analysis and design in complex industrial separation and liquefaction processes', *Journal of Process Control* **10**, 167–175.

Neeraas, B. O. and Brendeng, E. (2001), 'Method and device for small scale liquefaction of a product gas', U.S. Patent number: 6751984.

Nielsen, C. S., Andersen, H. W., Brabrand, H. and Jørgensen, S. B. (1988), Adaptive dual composition control of a binary distillation column with a heat pump, *in* 'Preprints IFAC Symp. on Adaptive Control of Chem. Processes'.

Nielsen, C. S., Andersen, H. W., Brabrand, H., Toftegård, B. and Jørgensen, S. B. (1987), Dynamics and identification of distillation pilot plant with heat pump, *in* 'Presented at CHISA'87, Prague', pp. 1–10.

Salim, M. A., Sadasivam, M. and Balakrishnan, A. R. (1991), 'Transient analysis of heat pump assisted distillation system. 1. the heat pump', *Int. J. of Energy Research* **15**, 123–135.

Singh, A. and Hovd, M. (2006), Dynamic modeling and control of the PRICO LNG process, *in* 'American Institute of Chemical Engineers (AIChE) annual meeting'.

Skogestad, S. (2000), 'Plantwide control: the search for the self-optimizing control structure', *J. Process Contr.* **10**(5), 487–507.

Skogestad, S. (2002), Plantwide control: towards a systematic procedure, *in* 'European Symposium on Computer Aided Process Engineering (ESCAPE)- 12, The Hague, The Netherlands'.

Skogestad, S. (2004), 'Near-optimal operation by self-optimizing control: From process control to marathon running and business systems', *Comput. Chem Eng.* **29**, 127–137.

Wilson, J. A. and Jones, W. E. (1994), 'The influence of plant design on refrigeration circuit control and operation', *European Symposium on Computer Aided Process Engineering (ESCAPE) 4, Dublin* pp. 215–221.

Zaim, A. (2002), Dynamic optimization of an LNG plant, Case study: GL2Z LNG plant in Arzew, Algeria, PhD thesis, RWTH Aachen.

Chapter 9

Conclusion

The charge (holdup) does not affect the steady-state for an *open* process (e.g. liquid level in a buffer tank), because of the boundary conditions on pressure. It has been shown that "active charge" in *closed* cycles has a steady-state effect. One way of affecting the "active charge" is by having a liquid receiver in the cycle. This degree of freedom is often lost by designing the cycle without sub-cooling in the condenser. We find that some sub-cooling is desirable and for the ammonia case study the compressor shaft work is reduced by about 2% by allowing for sub-cooling. The savings are not very large, but more importantly, the results show that the active charge is a degree of freedom and that the sub-cooling gives some decoupling between the high pressure P_h and the hot source temperature T_H. This shows that there are no fundamental differences between the typical sub-critical cycles and the trans-critical CO_2 cycles.

In terms of practical operation there are differences between the sub-critical ammonia cycle and the trans-critical CO_2 cycle. For the ammonia cycle several simple control structures gives acceptable performance. The best control structure found is to control the temperature approach at the condenser exit. For the CO_2 cycle we had to use a linear combination of measurements to get acceptable performance.

It is common to do the early design of refrigeration cycles by specifying a minimum approach temperature in the heat exchangers ($\min J$ subject to $\Delta T \geq \Delta T_{\min}$). This method fails to give the optimal operating point and also fails to find that sub-cooling is optimal. As a simple alternative we propose the simplified TAC method ($\min(J + C_0 \sum A_i^n)$), where C_0 replaces $\Delta T_{\min}$ as the adjustable parameter.

A PRICO LNG process has been designed by using realistic compressor specifications found online. We are able to increase the LNG production compared with

the commercial PRICO process. Compared with the AP-X LNG process we find that the PRICO process has about 7% less production for the same available shaft power.

Operation of the PRICO process is studied for two modes of operation; i) minimum shaft work (for given production) and ii) maximum production. Both modes has 2 controlled variables that must be selected (after controlling constraints that are always optimally). We find that maintaining a minimum distance to surge ($\Delta\dot{m}_{\text{surge}} = 0.0\,\text{kg}\,\text{s}^{-1}$) and maximum rotational speed of the compressor ($N = 100\,\%$) gives optimal operation for the nominal operating point and for some of the disturbances (for both modes). Since this control structure also gives close to optimal operation for the remaining disturbances, we propose to control $\Delta\dot{m}_{\text{surge}} = 0.0\,\text{kg}\,\text{s}^{-1}$ and $N = 100\,\%$.

The degrees of freedom available for optimization is an important number for several reasons. First, it determines the number of free variables to solve the optimization problem. Second, it determines how many steady-state controlled variables that must be selected to operate the process. Finding the degrees of freedom is not straightforward and requires a detailed process understanding. An earlier published simple approach to determine the potential degrees of freedom based on unit operations is extended to also cover vapour compression cycles. A simple method to determine the actual degrees of freedom for vapour compression cycles is also presented. Both the methods are illustrated on four case studies where the difference between potential and actual degrees of freedom are explained and related to the process layout.

Appendix A

Optimal operation of a mixed fluid cascade LNG plant

Studies on the operation of complex vapour compression cycles, like the one used for the production of liquefied natural gas (LNG), are not widely reported in the open literature. This is a bit surprising, considering the large amount of work that has been put into optimizing the design of such processes. It is important that the process is operated close to optimum to fully achieve the maximum performance in practice. There are possibilities for savings, both due to (a) identifying the optimal point of operation, and (b) selecting the controlled variables such that the optimal operation depends weakly on disturbances.
In this paper we study the mixed fluid cascade (MFC) LNG process developed by *The Statoil Linde Technology Alliance*. We study the degrees of freedom and how to adjust these to achieve optimal steady-state operation.

A.1 Introduction

Large amounts of natural gas (NG) are found at locations that makes it infeasible or not economical to transport it in gaseous state (in pipelines or as compressed NG) to the customers. The most economic way of transporting NG over long distances is to first produce liquefied natural gas (LNG) and then transport the LNG by ships. At atmospheric pressure LNG has approximately 600 times the density of gaseous NG.

At atmospheric pressure LNG has a temperature of approximately $-162\,^{\circ}\mathrm{C}$, so

the process of cooling and condensing the NG requires large amounts of energy. Several different process designs are used and they can be grouped roughly as follows:

- Mixed refrigerant: The refrigerant composition is adjusted to match the cooling curve of NG. Some are designed with a separate pre-cooling cycle
- Cascade process (pure fluid): Several refrigerant cycles are used to limit the mean temperature difference in the heat exchange
- Mixed fluid cascade process: Energy efficiency is further improved by using several mixed refrigerant cycles

The process considered in this paper is the Mixed Fluid Cascade (MFC) process developed by *The Statoil Linde Technology Alliance* (Bach, 2002). The MFC process has three different cycles, all with mixed refrigerant and the first cycle with two pressure levels.

The steady-state model for this plant is implemented in gPROMS (, n.d.) resulting in approximately 14000 equations. Optimizing the plant takes in the order of 2 hours on a Pentium 4 computer with 2.8 GHz and 512 MB RAM running GNU/Linux.

A.2 Process description

A simplified flowsheet is given in Figure A.1. For more details about the process consult Bach (2002) and Forg et al. (1999).

Nominal conditions:

- Feed: NG enters with $P = 61.5\,\text{bar}$ and $T = 11\,^{\circ}\text{C}$ after pretreatment. The composition is: 88.8% methane, 5.7% ethane, 2.75% propane and 2.75% nitrogen. Nominal flow rate is $1\,\text{kmol}\,\text{s}^{-1}$
- Product: LNG is at $P = 55.1\,\text{bar}$ and $T = -155\,^{\circ}\text{C}$
- The refrigerants are a mix of nitrogen (N_2), methane (C_1), ethane (C_2) and propane (C_3) and the compositions are used in optimization.
- The refrigerant vapour to the compressors are super-heated $10\,^{\circ}\text{C}$
- The refrigerants are cooled to $11\,^{\circ}\text{C}$ in all sea water (SW) coolers (assumed maximum cooling)

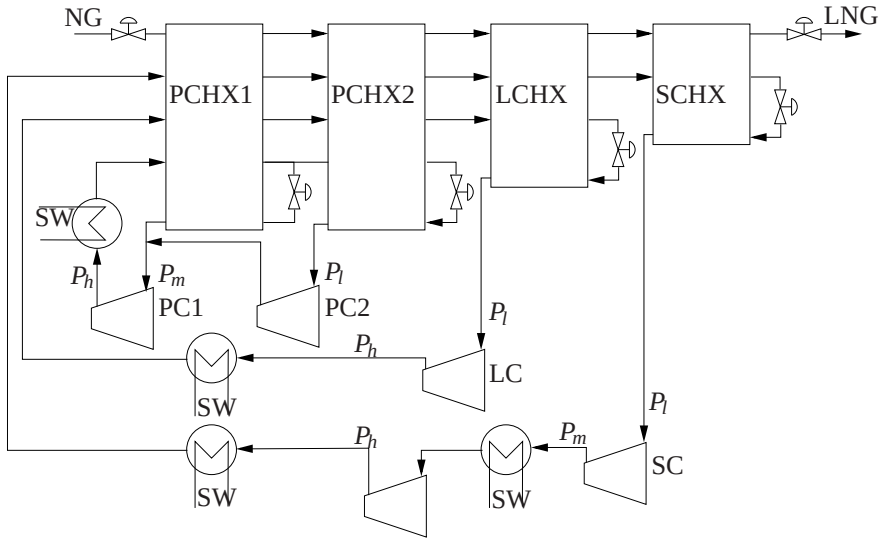

Figure A.1: Simplified flowsheet of the MFC process. SC - sub-cooling cycle, LC - liquefaction cycle, PC - pre-cooling cycle (two stages 1 and 2). Degrees of freedom associated with variable active charge in each cycle are not shown

- Pressure drops are 0.5 bar in SW coolers, 0.5 bar for hot flows in main heat exchangers and 0.2 bar for cold refrigerant in main heat exchangers

The SRK equation of state is used both for NG and the refrigerants. The heat exchangers are distributed models with constant heat transfer coefficients. The compressors are isentropic with 90 % constant efficiencies.

A.3 Degree of freedom analysis

In this section we present a detailed degree of freedom analysis which is an important result of this work.

In a single simple vapour compression cycle (e.g. a home refrigerator) there are two obvious manipulated inputs, namely the compressor and the valve*. In addition, there is a less obvious manipulated variable. This is the "active charge" in the cycle, which may be modified by introducing a unit (tank) with variable holdup (Jensen and Skogestad, 2007). The active charge may be changed by placing tanks

*In addition one might control flow of hot and cold fluid, but this is outside the cycle, so let us overlook that for now

at many different locations, but from a simple mass balance it may be verified that for each cycle one may have only one independent variable (tank) associated with the active charge. Thus for the cycles the number of manipulated variables are the number of compressors and valves plus one active charge for each cycle.

Let us now look at the MFC process.

A.3.1 Manipulated variables (MV's)

From the discussion above we find that there are in total 26 manipulated variables (degrees of freedom):

- 5 Compressor powers $W_{s,i}$
- 4 Choke valve openings z_i
- 4 SW flows in coolers
- 1 NG flow (can also be considered a disturbance)
- 9 Composition of three refrigerants
- 3 active charges (one for each cycle)

A.3.2 Constraints during operation

There are some constraints that must be satisfied during operation.

- Super-heating: The vapour entering the compressors must be $\geq 10\,^{\circ}\mathrm{C}$ super-heated
- T_{LNG}^{out}: NG Temperature out of SCHX must be $\leq -155\,^{\circ}\mathrm{C}$ or colder
- Pressure: $2\,\mathrm{bar} \geq P \leq 60\,\mathrm{bar}$
- NG temperature after PCHX1 and PCHX2 (not considered in this paper)
- Compressor outlet temperature (not considered in this paper)

A.3.3 Active constraints

We are able to identify some constraints that will be active at optimum. In total there are 11 active constraints:

- Excess cooling is costly so $T_{LNG}^{out} = -155\,^{\circ}\mathrm{C}$
- Optimal with low pressure in cycles so $P_l = 2\,\mathrm{bar}$ (for all 3 cycles)
- Maximum cooling: Assume $T = 11\,^{\circ}\mathrm{C}$ at 4 locations

A.3.4 Unconstrained degrees of freedom

After using 11 of the 26 manipulated inputs to satisfy active constraints, we are left with 15 unconstrained degrees of freedom. In this work we consider the NG flow given from elsewhere (disturbance to the process). In addition we assume that the degree of super-heating is controlled at $\Delta T_{\mathrm{sup}} = 10\,^{\circ}\mathrm{C}$, so we are left with 13 degrees of freedom in optimization. For a steady state analysis the pairing of inputs and outputs is insignificant, so say we are left with the following subset of the MV's:

- 3 NG temperatures (after PCHX1, PCHX2 and LCHX)
- P_m in SC
- 9 Refrigerant compositions

In this paper we will not consider manipulating refrigerant composition in operation (only in the optimization), so of the 13 unconstrained degrees of freedom we are left with 4 during operation.

A.4 Optimization results

In this section we are optimizing on the 13 degrees of freedom given above to locate the optimal operation of a given MFC LNG plant. The resulting temperature profiles for the four main heat exchangers are given in Figure A.2. Some key values of the refrigerant cycles are given in Table A.1 where the nomenclature is given in Figure A.1.

Some remarks:

- The total shaft work is 10.896 MW
- The optimal NG temperature out of PCHX1, PCHX2 and LCHX is $-17.3\,^{\circ}\mathrm{C}$, $-51.5\,^{\circ}\mathrm{C}$ and $-77.1\,^{\circ}\mathrm{C}$, respectively

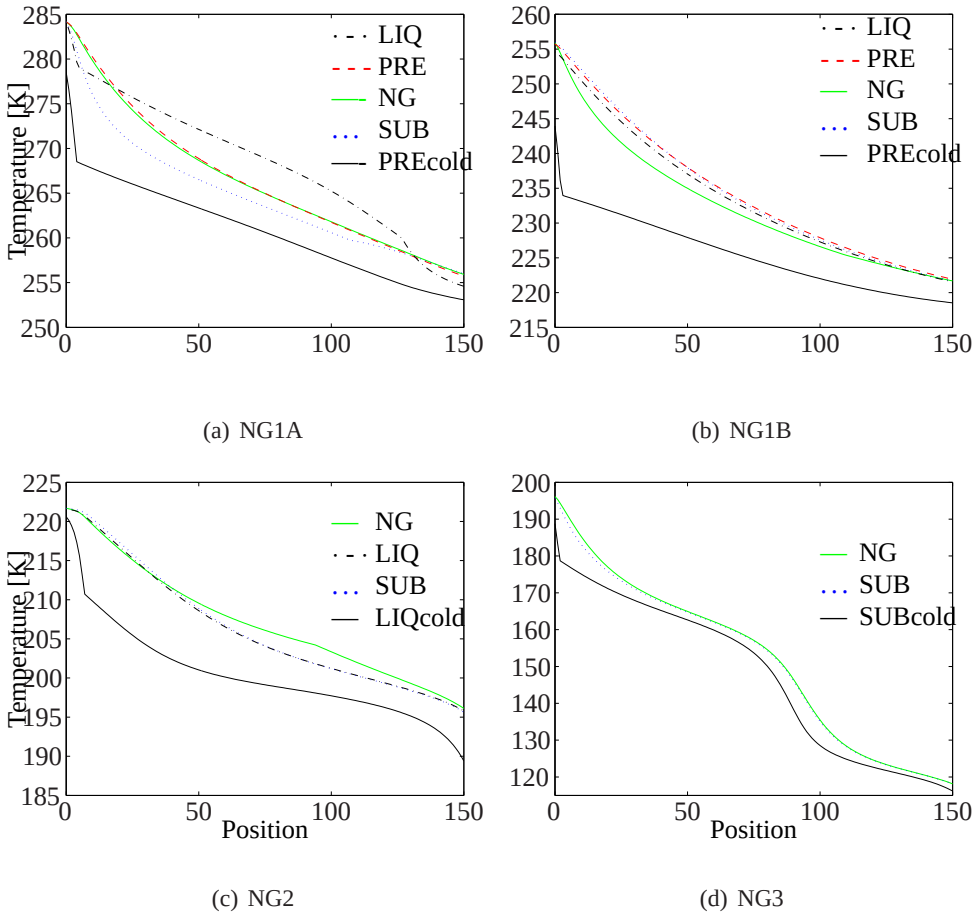

(a) NG1A

(b) NG1B

(c) NG2

(d) NG3

Figure A.2: Temperature profiles

- In the true design there will separators at the high pressure side of the cycles, which has not been considered here. Further work will include an analysis of the effect of this sub-optimal design

- In the SC cycle the pressure ratios over the two compressor stages are far from equal (which is a rule of thumb for compression ratios). This is because the inlet temperature to the first stage (approximately $-80\,^{\circ}\mathrm{C}$) is much lower than inlet temperature to the second stage ($11\,^{\circ}\mathrm{C}$)

- Nitrogen is present in SC only to satisfy the minimum pressure of 2 bar

Table A.1: Optimal operation of a MFC process

	PC1	PC2	LC	SC
P_l [bar]	6.45	2.00	2.00	2.00
P_m [bar]		6.45	-	28.38
P_h [bar]	15.03	15.03	20.58	56.99
C_1 [%]	0.00	0.00	4.02	52.99
C_2 [%]	37.70	37.70	82.96	42.45
C_3 [%]	62.30	62.30	13.02	0.00
N_2 [%]	0.00	0.00	0.00	4.55
$\dot{n}$ [mol s^{-1}]	464	685	390	627
W_s [MW]	1.2565 + 2.644		2.128	3.780+1.086

A.5 Control structure design

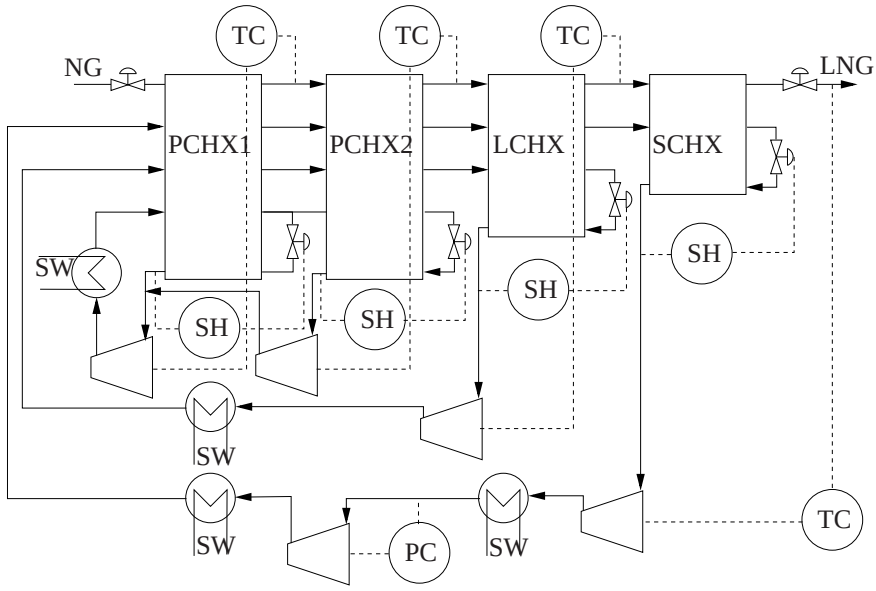

Figure A.3: Suggested control structure for the MFC process. SH is degree of super-heating controllers, PC and TC are pressure and temperature controllers respectively. Not shown: Three pressure controllers on the low pressure side using the active charge in each cycle

In the section above we where able to identify the optimum for the process, but how should this optimum be implemented in practice? First we need to control the active constraints:

- P_l is for each of the 3 cycles: For this we may use "active charge" (see discussion above)
- Maximum cooling in 4 SW coolers: SW flow at maximum
- LNG outlet temperature at $-155\,^{\circ}$C: May use first compressor stage in SUB

In addition, we choose to control:

- Degree of super-heating (4 locations): For this we may use the corresponding choke valve opening

The four remaining degrees of freedom should be used to control variables which have good self optimizing properties:

"Self optimizing control is when we can achieve acceptable loss with constant setpoint values for the controlled variables (without the need to re-optimize when disturbances occur)" (Skogestad, 2000).

To evaluate the loss one needs to consider the effect of disturbances and implementation errors. A steady-state analysis is usually sufficient because the economics are primarily determined by the steady-state.

Based on physical insight the following four variables may been suggested

- T_{NG1A}^{out}
- T_{NG1B}^{out}
- T_{NG2}^{out}
- P_m

A possible control structure with these four variables and the active constraints controlled is shown in Figure A.3. However, note that the "pairings" of controlled and manipulated inputs are included primarily to illustrate that we have available degrees of freedom, as this does not matter for evaluating self-optimizing control at steady-state. It will be the subject of future work to compare this choice of controlled variables with one that follows from a systematic procedure.

A.6 Conclusion

We have shown that the degrees of freedom in vapour compression cycles are equal to the number of compressors and valves plus one. The extra degree of freedom is

related to the "active charge" in the system, and a tank with variable holdup should be included to gain this degree of freedom.

A detailed degree of freedom analysis for the MFC process reveals that there are four unconstrained degrees of freedom in operation (not considering manipulating refrigerant compositions). To fully achieve the potentially high thermodynamic efficiency of the MFC process it is important that these four unconstrained degrees of freedom are utilized optimally.

Bibliography

(n.d.). `http://www.psenterprise.com/products_gproms.html`.

Bach, W. A. (2002), 'Developments in the mixed fluid cascade process (MFCP) for LNG baseload plants', *Reports on science and technology Linde* **63**.

Forg, W., Bach, W., Stockmann, R., Heiersted, R. S., Paurola, P. and Fredheim, A. O. (1999), 'A new LNG baseload process and manufacturing of the main heat exchanger', *Reports on science and technology Linde* **61**.

Jensen, J. B. and Skogestad, S. (2007), 'Optimal operation of simple refrigeration cycles. Part I: Degrees of freedom and optimality of sub-cooling', *Comput. Chem. Eng.* **31**, 712–721.

Skogestad, S. (2000), 'Plantwide control: the search for the self-optimizing control structure', *J. Process Contr.* **10**(5), 487–507.

Appendix B

On the Trade-off between Energy Consumption and Food Quality Loss in Supermarket Refrigeration Systems

J. Cai*, J. B. Jensen†, S. Skogestad†, J. Stoustrup*

Submitted for publication in the proceedings of the 2008 American Control Conference, Seattle, USA

This paper studies the trade-off between energy consumption and food quality loss, at varying ambient conditions, in supermarket refrigeration systems. Compared with the traditional operation with pressure control, a large potential for energy savings without extra loss of food quality is demonstrated. We also show that by utilizing the relatively slow dynamics of the food temperature, compared with the air temperature, we are able to further lower both the energy consumption and the peak value of power requirement. The Pareto optimal curve is found by off-line optimization.

*Automation and Control, Department of Electronic Systems, Aalborg University (AAU), 9220 Aalborg, Denmark. (e-mail: jc@es.aau.dk, jakob@es.aau.dk)

†Department of Chemical Engineering, Norwegian University of Science and Technology (NTNU), 7491 Trondheim, Norway. (e-mail: jorgenba@chemeng.ntnu.no, skoge@chemeng.ntnu.no)

B.1 Introduction

Increasing energy costs and consumer awareness on food products safety and quality aspects impose a big challenge to food industries, and especially to supermarkets, which have direct contacts with consumers. A well-designed optimal control scheme, continuously maintaining a commercial refrigeration system at its optimum operation condition, despite changing environmental conditions, will achieve an important performance improvement, both on energy efficiency and food quality reliability.

Many efforts on optimization of cooling systems have been focused on optimizing objective functions such as overall energy consumption, system efficiency, capacity, or wear of the individual components, see Jakobsen and Rasmussen (1998), Jakobsen et al. (2001), Larsen and Thybo (2004), Leducqa et al. (2006), Swensson (1994). They have proved significant improvements of system performance under disturbances, while there has been little emphasis on the quality aspect of foodstuffs inside display cabinets.

This paper discusses a dynamic optimization of commercial refrigeration systems, featuring a balanced system energy consumption and food quality loss. A former developed quality model of food provides a tool for monitoring and controlling the quality loss during the whole process, see Cai et al. (2006).

The paper is organized as follows: Operation and modelling of a refrigeration systems is presented in Section B.2. In Section B.3 we introduce the problem formulation used for optimization. Different optimization schemes and results are presented in Section B.4. Finally some discussions and conclusions follow in Section B.5 and Section B.6.

B.2 Process description

A simplified sketch of the process is shown in Figure B.1. In the evaporator there is heat exchange between the air inside the display cabinet and the cold refrigerant, giving a slightly super-heated vapor to the compressor. After compression the hot vapor is cooled, condensed and slightly sub-cooled in the condenser. This slightly sub-cooled liquid is then expanded through the expansion valve giving a cold two-phase mixture.

The display cabinet is located inside a store and we assume that the store has a constant temperature. This is relative true for stores with air-conditioning. The

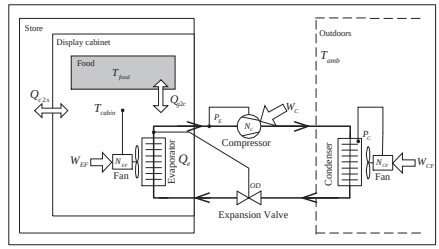

Figure B.1: Sketch of a simplified supermarket refrigeration system studied in this paper.

condenser and fans are located at the roof of the store. Condensation is achieved by heat exchange with ambient air.

B.2.1 Degree of freedom analysis

There are 5 degrees of freedom (input) in a general simple refrigeration system, see Jensen and Skogestad (2007). Four of these can be recognized in Figure B.1 as the compressor speed (N_C), condenser fan speed (N_{CF}), evaporator fan speed (N_{EF}) and opening degree of the expansion valve (OD). The fifth one is related to the active charge in the system.

Two of the inputs are already used for control or are otherwise constrained:

- Constant super-heating ($\Delta T_{sup} = 3\,^{\circ}\mathrm{C}$): This is controlled by adjusting the opening degree (OD) of the expansion valve.
- Constant sub-cooling ($\Delta T_{sub} = 2\,^{\circ}\mathrm{C}$): We assume that the condenser is designed to give a constant degree of sub-cooling, which by design consumes the degree of freedom related to active charge, see Jensen and Skogestad (2007).

So we are left with three unconstrained degrees of freedom that should be used to optimize the operation. These are:

1. Compressor speed N_C
2. Condenser fan speed N_{CF}
3. Evaporator fan speed N_{EF}

These inputs are controlling three variables:

1. Evaporating pressure P_E

2. Condensing pressure P_C
3. Cabinet temperature T_{cabin}

However, the setpoints for these three variables may be used as manipulated inputs in our study so the number of degrees of freedom is still three.

B.2.2 Mathematical model

The model equations are given in Table B.1; please see Larsen (2005) for the modelling of refrigeration systems. We assume that the refrigerator has fast dynamics compared with the display cabinet and food, so for the condenser, evaporator, valve and compressor we have assumed steady-state. For the display cabinet and food we use a dynamic model, as this is where the slow and important (for economics) dynamics will be. The food is lumped into one mass, and the air inside the cabinet together with walls are lumped into one mass. The main point is that there are two heat capacities in series. For the case with constant display cabinet temperature we will also have constant food temperature. There are then no dynamics and we may use steady-state optimization.

Some data for the simulations are given in Table B.2; please see Larsen (2005) for further data.

B.2.3 Influence of setpoints on energy consumption

As stated above, this system has three setpoints that may be manipulated: P_C, P_E and T_{cabin}. In Figure B.2, surface shows that under 2 different cabinet temperatures, the variation of energy consumption with varying P_C and P_E. Point A is the optimum for cabinet temperature T_{cabin1} and point B is the optimum for T_{cabin2}. T_{cabin1} is lower than T_{cabin2}, so the energy consumption is higher in point A than in point B.

B.2.4 Influence of setpoint on food quality

Food quality decay is determined by its composition factors and many environmental factors, such as temperature, relative humidity, light etc. Of all the environmental factors, temperature is the most important, since it not only strongly affects reaction rates but is also directly imposed to the food externally. The other factors are at least to some extent controlled by food packaging.

Table B.1: Model equations

Compressor

$\dot{W}_C = \frac{\dot{m}_{ref} \cdot (h_{is}(P_e,P_c) - h_{oe}(P_e))}{\eta_{is}}$

$h_{ic} = \frac{1-f_q}{\eta_{is}} \cdot (h_{is}(P_e,P_c) - h_{oe}(P_e)) + h_{oe}(P_e)$

$\dot{m}_{ref} = N_C \cdot V_d \cdot \eta_{vol} \cdot \rho_{ref}(P_e)$

Condenser

$\dot{W}_{CF} = K_{1,CF} \cdot (N_{CF})^3$

$\dot{m}_{air,C} = K_{2,CF} \cdot N_{CF}$

$T_{aoc} = T_c + (T_{amb} - T_c) \cdot \exp\left(-(\alpha_C \cdot \dot{m}_{air,C}^{m_C})/(\dot{m}_{air,C} \cdot Cp_{air})\right)$

$0 = \dot{m}_{ref} \cdot (h_{ic}(P_e,P_c) - h_{oc}(P_c)) - \dot{m}_{air,C} \cdot Cp_{air} \cdot (T_{aoc} - T_{amb})$

Evaporator

$\dot{W}_{EF} = K_{1,EF} \cdot (N_{EF})^3$

$\dot{m}_{air,E} = K_{2,EF} \cdot N_{EF}$

$T_{aoe} = T_e + (T_{cabin} - T_e) \cdot \exp\left(-(\alpha_E \cdot \dot{m}_{air,E}^{m_E})/(\dot{m}_{air,E} \cdot Cp_{air})\right)$

$0 = \dot{Q}_e - \dot{m}_{air,E} \cdot Cp_{air} \cdot (T_{cabin} - T_{aoe})$

Display cabinet

$\dot{Q}_{c2f} = UA_{c2f} \cdot (T_{cabin} - T_{food})$

$\dot{Q}_{s2c} = UA_{s2c} \cdot (T_{store} - T_{cabin})$

$\frac{dT_{food}}{dt} = (mCp_{food})^{-1} \cdot \dot{Q}_{c2f}$

$\frac{dT_{cabin}}{dt} = (mCp_{cabin})^{-1} \cdot (-\dot{Q}_{c2f} - \dot{Q}_E + \dot{Q}_{s2c})$

$Q_{food,loss} = \int_{t_0}^{t_f} 100 \cdot D_{T,ref} \exp(\frac{T_{food} - T_{ref}}{z}) dt$

Table B.2: Some data used in the simulation

Display cabinet*
heat transfer area $UA_{s2c} = 160\,\mathrm{W\,K^{-1}}$
heat capacity: $mCp_{cabin} = 10\,\mathrm{kJ\,K^{-1}}$
Food
heat transfer area: $UA_{c2f} = 20.0\,\mathrm{W}K^{-1}$
heat capacity: $mCp_{food} = 756\,\mathrm{kJ\,K^{-1}}$
quality parameter: $D_{T,ref} = 0.2\,\mathrm{day^{-1}}$;
quality parameter: $T_{ref} = 0\,^\circ\mathrm{C}$
quality parameter: $Z = 10\,^\circ\mathrm{C}$

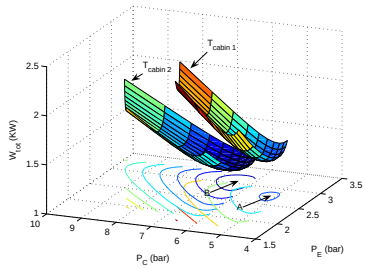

Figure B.2: Energy consumption under different setpoints.

Here we focus on the temperature influence to food quality Q_{food}. The only setpoint directly influencing food temperature (and thus food quality) is T_{cabin}. Fig. B.3 shows the daily quality loss for chilled cod product under 4 cases: T_{food} of 2, 1 °C and T_{sin}. $T_{\text{sin},1}$ and $T_{\text{sin},2}$ are the sinusoidal function with mean value of 1 °C, amplitude of 1 °C and 3 °C respectively, period is 24 h. Note that the quality loss is higher with higher temperature, but there is only minor extra loss over 24 h by using a sinusoidal temperature with small amplitude. A sinusoidal with large amplitude has a larger influence on quality due to the non-linearity of the quality function, it will not be considered here.

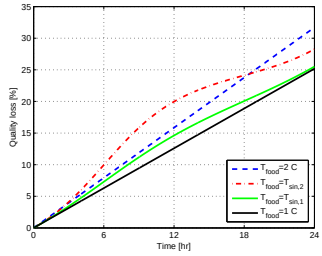

Figure B.3: Fresh fish quality loss when stored at different temperatures.

B.3 Problem formulation

We here consider at a time horizon of three days, ambient temperature (T_{amb}) follows a sinusoidal function with a mean value of 20 °C, period of 24 hours and amplitude of 6 °C. This is a normal temperature profile in Denmark during summer, see *Danmarks Meteorologiske Institut* (2007).

The objective is to minimize the energy consumption, subject to maintaining a fixed quality loss, by using those 3 DOF. This can be formulated mathematically as:

$$\min_{(N_C(t),N_{CF}(t),N_{EF}(t))} J \tag{B.1}$$

$$\text{where} \qquad J = \int_{t_0}^{t_f} \underbrace{(W_C(t) + W_{CF}(t) + W_{EF}(t))}_{W_{tot}(t)} \mathrm{d}t \tag{B.2}$$

The quality loss of the food could be included in the objective function directly, but we choose to limit it by using constraints. The optimization is also subjected to other constraints, such as maximum speed of fans and compressor, minimum and maximum value of evaporator and condenser pressure etc.

In this paper, the food is a fresh cod product. Danish food authorities require it to be kept at a maximum of 2°C. The control engineer will normally set the temperature setpoint a little lower, for example at 1°C.

> **Case 1** Traditional operation with constant pressures (P_E), (P_C) and constant temperatures ($T_\mathrm{cabin} = T_\mathrm{food} = 1\,^\circ\mathrm{C}$)

There are usually large variations in the ambient temperature during the year so in traditional operation it is necessary to be conservative when choosing the setpoint for condenser pressure. To reduce this conservativeness it is common to use one value for summer and one for winter. We will here assume that the summer setting is used.

To get a fair comparison with traditional control, which operates at 1°C, we will illustrate our optimization by considering the following cases:

> **Case 2** T_cabin and T_food constant at $1\,^\circ\mathrm{C}$.
> Two remaining unconstrained degrees of freedom as functions of time are used for minimizing the energy consumption in B.1.

> **Case 3** $\overline{T_\mathrm{food}} = \frac{1}{t_f - t_0} \int_{t_0}^{t_f} T_\mathrm{food}(t)\,\mathrm{d}t = 1\,^\circ\mathrm{C}$.
> Three remaining unconstrained degrees of freedom as functions of time are used for minimizing the energy consumption in B.1.

> **Case 4** $Q_{\text{food, loss}}(t_f) \leq 75.5\%$.
> Three remaining unconstrained degrees of freedom as functions of time are used for minimizing the energy consumption in B.1. 75.5% is the quality loss at constant temperature of $1\,^\circ\mathrm{C}$ obtained in cases 1 and 2.

B.4 Optimization

B.4.1 Optimization

The model is implemented in *gPROMS*® and the optimization is done by dynamic optimization (except for Case 1). For the Case 2, we have used piecewise linear manipulated variables with a discretisation every hour. For the cases with varying cabinet temperature (Case 3 and 4), we have used sinusoidal functions $u = u_0 + A \cdot \sin(\pi \cdot t/24 + \phi)$, where u_0 is the nominal input, A is the amplitude of the input, t is the time and ϕ is the phase shift of the input.

Using a sinusoidal function has several advantages:

- There are much fewer variables to optimize on, only 3 for each input, compared with 3 parameters for each time interval for discrete dynamic optimization
- There are no end-effects.

In all cases we find that the phase shift is very small.

B.4.2 Optimization results

Table B.3 compares the four cases in terms of the overall cost J, end quality loss, maximum total power ($W_{\text{tot,max}}$) and maximum compressor power ($W_{C,\text{max}}$). The two latter variables might be important if there are restrictions on the maximum compressor power or on the total electric power consumption.

Some key variables, including speed and energy consumption for compressor and fans as well as temperatures, are plotted for each case in Figure B.5 through Figure B.8.

Table B.3: Traditional operation and optimal operation for three different constraints

	Case 1*	Case 2†	Case 3‡	Case 4§
J [MJ]	273.7	242.8	240.7	241.4
$Q_{food,loss}(t_f)$ [%]	75.5	75.5	76.1	75.5
$W_{C,\text{max}}$ [W]	955	1022	836	879
$W_{\text{tot,max}}$ [W]	1233	1136	946	981

For Case 1 (traditional operation) the total energy consumption over three days is 273.7 MJ. Note that the condenser temperature (and pressure) is not changing with time.

If we keep $T_{\text{cabin}} = T_{\text{food}}$ constant at 1 °C, but allow the pressures (and temperatures) in the condenser and evaporator to change with time (Case 2), we may reduce the total energy consumption by 11.3 % to 242.8 MJ. Fig. B.6 shows that the evaporator temperature is constant, because we still control the cabinet temperature, while the condenser temperature varies with ambient temperature. The quality is the same as in Case 1 because of the constant cabinet temperature. The power variations are larger, but nevertheless, the maximum total power ($W_{\text{tot,max}}$) is reduced by 7.9 % to 1136 W.

Next, we also allow the cabinet temperature to vary, but add a constraint on the average food temperatures $\overline{T}_{\text{food}} = 1.0\,^{\circ}\text{C}$ (Case 3). This reduces the total energy consumption with another 0.9 %, while the food quality loss is slightly higher. Note from Figure B.7 that the evaporator, cabinet and food temperature is varying a lot.

Finally, in Case 4 we do not care about the average food temperature, but instead restrict the quality loss. With $Q_{\text{food,loss}}(t_f) \leq 75.5\,\%$, which is the same end quality we obtained for Case 1, we save 11.8 % energy compared with Case 1, but use slightly more than for Case 3 (0.29 %). Note from Figure B.8 that the amplitude for food, cabinet and evaporator temperature are slightly reduced compared to Case 3.

An important conclusion is that most of the benefit in terms of energy savings is obtained by letting the setpoint for P_E and P_C vary (Case 2). The extra savings by changing also the cabinet temperature T_{cabin} (Case 3 and 4) are small. However, the peak value for compressor power and total system power is significantly decreased for Case 3 and 4. This is also very important, because a lower compressor capacity means a lower investment cost, and a lower peak value of total power consumption will further reduce the bill for supermarket owner, according to the following formula:

$$C_{op} = \int_{month}^{year} (P_{el}(t) \cdot E_{el}(t) + \max(P_{el}(t)) \cdot E_{el,dem}(t))\,\mathrm{d}t \tag{B.3}$$

where C_{op} is the operating cost, E_{el} is the electricity rate, P_{el} is the electric power, $E_{el,dem}$ is the electricity demand charge, $\max(P_{el}(t))$ is the maximum electric power during one month.

B.4.3 Trade-off between energy consumption and food quality loss

Fig. B.4 plots the Pareto optimal curve between food quality loss and energy consumption. It shows that reducing quality loss and saving energy is a conflicting

objective to a system. An acceptable tradeoff between these two goals can be selected by picking a point somewhere along the line. It also shows that Case 1 is far away from optimization; Case 4 is one optimal point, while Case 2 and 3 are near optimal solutions.

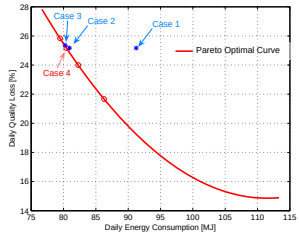

Figure B.4: Optimization between food quality loss and energy consumption

B.5 Discussion

Having oscillations in the pressures will impose stress and cause wear on the equipment. This might not be desirable in many cases, but in this study the oscillations are with a period of one day, so this should not be an issue.

Experiments on the influence of fluctuating temperatures on food quality were reviewed by Ulrich (1981), where marginal reduction in final quality due to fluctuations was reported. In our case, food temperature is only slowly varying, and with an amplitude of less than 1 °C. Thus, this will not pose any negative influence on food quality.

B.6 Conclusion

We have shown that traditional operation where the pressures are constant gives excessive energy consumption. Allowing for varying pressure in the evaporator and condenser reduces the total energy consumption by about 11 %. Varying food temperature gives only minor extra improvements in terms of energy consumption, but the peak value of the total power consumption is reduced with an additional 14 % for the same food quality loss.

Reducing quality loss and saving energy is a conflicting objective. Our optimization result will help the engineer to select an acceptable tradeoff between these two

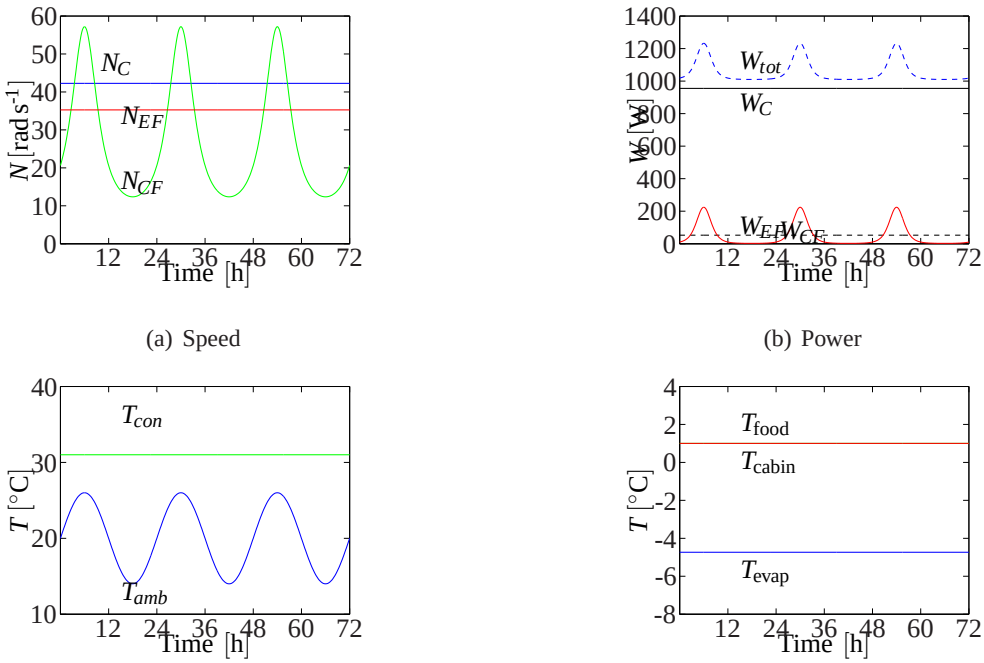

(a) Speed

(b) Power

(c) High temperatures

(d) Low temperatures

Figure B.5: Traditional operation with $T_{\text{cabin}} = 1\,^{\circ}\text{C}$, $P_E = 2.4\,\text{bar}$ and $P_C = 8.0\,\text{bar}$ (Case 1)

goals by picking a point somewhere along the Pareto front line.

This paper investigates the potential of finding a balancing point between quality and energy consumption, by open-loop dynamic optimizations. It uses the sinusoid ambience temperature as one example. In real life, weather patterns are not exactly a sinusoidal function, but real weather conditions can be easily obtained in advance from forecast. Practical implementation, including selecting controlled variables and using closed-loop feedback control, will be the theme of future research.

Bibliography

Cai, J., Risum, J. and Thybo, C. (2006), Quality model of foodstuff in a refrigerated display cabinet, In proc.: International refrigeration conference, Purdue, USA.

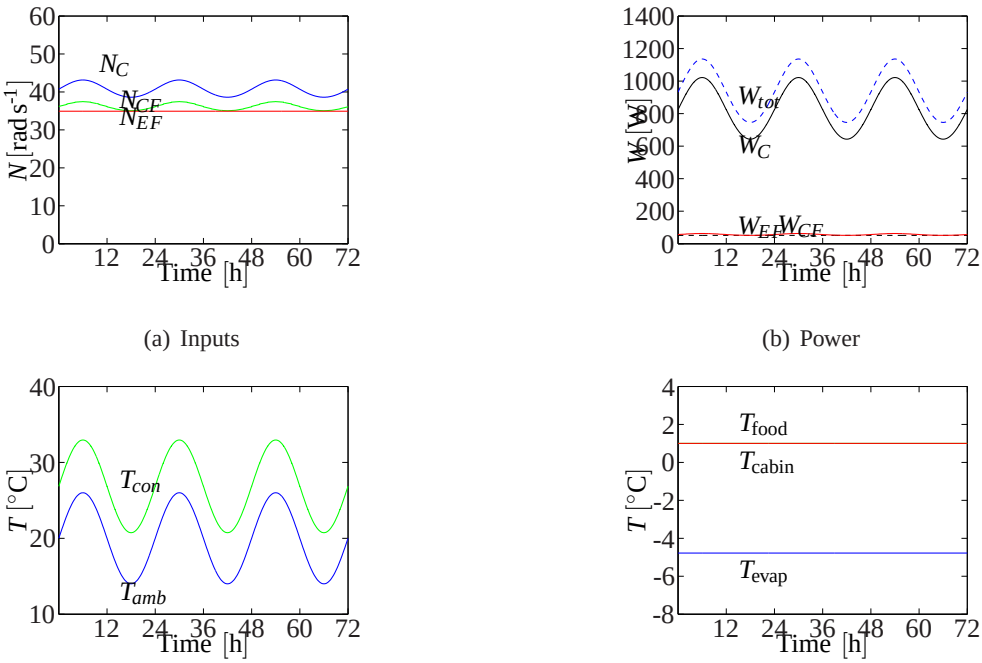

(a) Inputs

(b) Power

(c) High temperatures

(d) Low temperatures

Figure B.6: Optimal operation for $T_{\text{cabin}} = 1\,^{\circ}\text{C}$ (Case 2)

Danmarks Meteorologiske Institut (2007).
URL: `www.dmi.dk`

Jakobsen, A. and Rasmussen, B. (1998), Energy-optimal speed control of fans and compressors in a refrigeration system, Eurotherm 62, Nancy, France, pp. pp 317–323.

Jakobsen, A., Rasmussen, B., Skovrup, M. J. and Fredsted, J. (2001), Developement of energy optimal capacity control in refrigeration systems, In proc.: International refrigeration conference, Purdue, USA.

Jensen, J. B. and Skogestad, S. (2007), 'Optimal operation of simple refrigeration cycles. Part I: Degrees of freedom and optimality of sub-cooling', *Comput. Chem. Eng.* **31**, 712–721.

Larsen, L. F. S. (2005), Model based control of refrigeration system, PhD thesis, Department of Control Engineering, Aalborg University, Fredrik Bajers Vej 7C, DK 9220 Aalborg, Denmark.

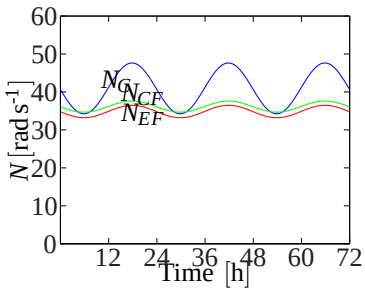

(a) Speed

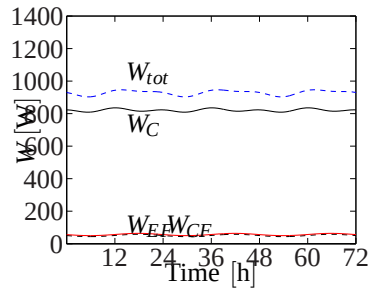

(b) Power

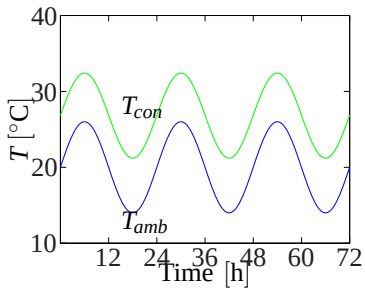

(c) High temperatures

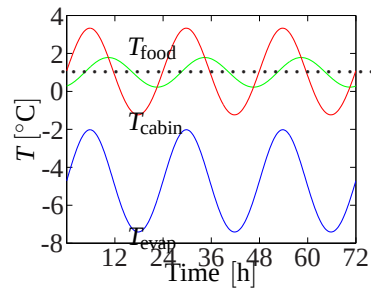

(d) Low temperatures

Figure B.7: Optimal operation for $\overline{T}_{\text{food}} = 1\,^{\circ}\text{C}$ (Case 3)

Larsen, L. F. S. and Thybo, C. (2004), Potential energy saving in refrigeration system using optimal setpoint, In proc.: Conference on control applications, Taipei, Taiwan.

Leducqa, D., Guilparta, J. and Trystramb, G. (2006), 'Non-linear predictive control of a vapour compression cycle', *International Journal of Refrigeration* **29**, 761–772.

Swensson, M. C. (1994), studies on on-line optimizing control, with application to a heat pump, PhD thesis, Department of refrigeration Engineering, NTNU.

Ulrich, R. (1981), 'Variations de temperature et qualite des produits surgeles', *Review Generale due Froid* **71**, 371 V389.

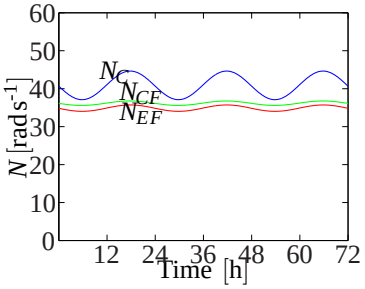

(a) Speed

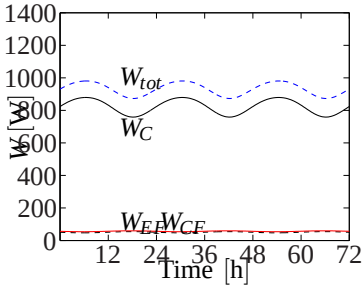

(b) Power

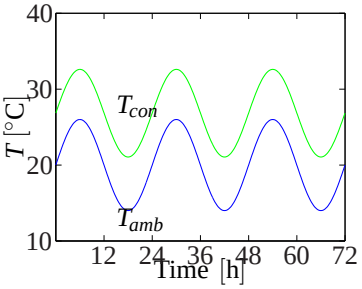

(c) High temperatures

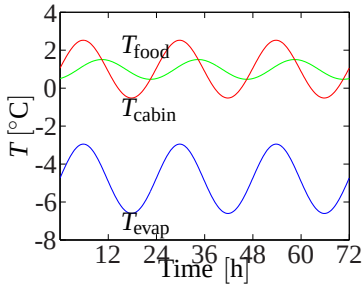

(d) Low temperatures

Figure B.8: Optimal operation for $Q_{\text{food}} \leq 75.5\,\%$ (Case 4)